Charles University in Prague
Third Faculty of Medicine

DOCTORAL THESIS

Effect of selected drugs on mitochondrial metabolism in an *in vitro* model of human skeletal muscle

MUDr. Adéla Krajčová

Supervisor: prof. MUDr. Michal Anděl, CSc.

Consultant: doc. MUDr. František Duška, Ph.D.

Study programme: Human Physiology and Pathophysiology

IDENTIFICATION RECORD (identifikační záznam)

Krajčová, Adéla. *Effect of selected drugs on mitochondrial metabolism in an in vitro model of human skeletal muscle. [Vliv vybraných farmak na mitochondriální metabolismus v in vitro modelu lidského kosterního svalu].* Praha, 2018. 99 stran; 5 příloh. Dizertační práce. Univerzita Karlova v Praze, 3. lékařská fakulta, Ústav biochemie, buněčné a molekulární biologie 3. LF UK, Laboratoř metabolismu a bioenergetiky. Školitel: Anděl, Michal. Konzultant: Duška, František.

DECLARATION

My doctoral thesis is based on the experimental work which I performed in the Laboratory of Metabolism and Bioenergetics, Third Faculty of Medicine, during my PhD programme.

I declare that I worked out this doctoral thesis independently with my own and original results and used only the cited sources and literature. I also did not use any sources figures than those stated in the bibliography.

This work has never been submitted by me or by anyone else at Charles or any other university and has not been used to obtain Ph.D. or any other academic degree.

The article "Krajčová, A., Ziak, J., Jiroutková, K., Patková, J., Elkalaf, M., Džupa, V., Trnka, J. and Duška, F.: Normalizing glutamine concentration causes mitochondrial uncoupling in an in vitro model of human skeletal muscle. JPEN. 2015;39(2):180-189" was used as a part of doctoral thesis by MUDr. Kateřina Jiroutková, Ph.D., Mgr. Jana Tůmová, Ph.D. and MUDr. Moustafa Elkalaf, Ph.D.

The article "Ziak J, Krajcova A, Jiroutkova K, Nemcova V, Dzupa V, Duska F. Assessing the function of mitochondria in cytosolic context in human skeletal muscle: adopting high-resolution respirometry to homogenate of needle biopsy tissue samples. Mitochondrion. 2015 Mar;21:106-12" was used as a part of doctoral thesis of MUDr. Kateřina Jiroutková, Ph.D.

I agree that an electronic version of this work will be permanently saved in the database system of the inter-university project Theses.cz for the systematic control of the similarity of theses.

Prague, 20th April 2018 ……..

Signature

CONFLICT OF INTEREST STATEMENT

I have no competing financial or other relationships with any organization that might have an interest in the submitted work in the previous five years.

This study was financially supported by grants GAUK 270915, AZV 16-28663A, PRVOUK P31/P33 and UNCE 204015/2012.

ACKNOWLEDGEMENT

I would like to thank my supervisor professor Michal Anděl for his valuable comments and advices during my PhD study. Firstly, I am very grateful that he gave me an opportunity to combine my clinical work with research and persistently supported me in both fields. He also strongly encouraged me to continue in the research of metabolism. Discussions with him were always very inspiring and persuaded me to pursue this research area in future.

I am very thankful to my consultant doc. František Duška, who started to help me already during my pregradual studies at medical faculty and introduced me to the basics of scientific principles and methods. Later he brought me to the experimental work in laboratory and involved me in very interesting projects. I was always looking forward for his comments and discussions. I am very grateful for his ideas and enthusiasm for science, particularly energy metabolism.

I would like to thank also my colleagues in laboratory – doc. Jan Trnka, Mgr. Jana Tůmová, Dr. Kateřina Jiroutková, Dr. Jakub Žiak and Dr. Moustafa Elkalaf for the friendly atmosphere in lab and for their advices with methods and cell cultures, and particularly Dr. Moustafa Elkalaf for the help with spectrophotometric analysis. I am thankful to the team from Laboratory of prof. Arild Rustan from Oslo, particularly Dr. Hege Thoresen and Nils Løvsletten for analysis of acid soluble metabolites. I am also very grateful to Dr. Petr Waldauf who helped me with statistics and graphs. I would like to thank also doc. Valér Džupa and his team from Department of Orthopaedic Surgery who provided me muscle biopsies during their surgeries and helped me with inform consents. I am also thankful for all the patients who decided to agree with the biopsy and enabled me to perform my study on human muscle samples.

CONTENTS

List of abbreviations:

ACAD	Acyl-CoA Dehydrogenase
ACS	Acyl-CoA Synthetase
ADP	Adenosine Diphosphate
ASMs	Acid-soluble Metabolites
ATPase	ATP Synthase
ATP	Adenosine Triphosphate
AA	Antimycin A
BMI	Body Mass Index
BSA	Bovine Serum Albumin
CACT	Carnitine Acyl-CoA Transferase
CI	Complex I
CII	Complex II
CIII	Complex III
CIV	Complex IV
CPT	Carnitine-Palmitoyl Transferase
CoA	Coenzyme A
CS	Citrate Synthase
CoQ	Coenzyme Q
Cyt C	Cytochrome C
DCIP	2,6-dichloroindophenol
DMEM	Dulbecco's Modified Eagle's Medium
DMF	Dimethylformamide
DMSO	Dimethylsulfoxide
ECAR	Extracellular Acidification Rate
ECG	Electrocardiogram
ETH	Ethanol
EGTA	Ethylene glycol-bis(2-aminoethylether)-*N,N,N',N'*-tetraacetic acid
ETC	Electron Transfer Chain
ETF	Electron Transfer Flavoprotein

FAD	Flavin adenine dinucleotide
FAO	Fatty Acid Oxidation
FBS	Foetal Bovine Serum
FCCP	Cyanide-4-[trifluoromethoxy]phenylhydrazone
FDA	Food and Drug Administration
HEPES	4-(2-Hydroxyethyl)piperazine-1-ethanesulfonic acid
ICU	Intensive Care Unit
IL	Intralipid
KHB	Krebs-Henseleit Buffer
MAS	Mitochondrial Assay Solution
Mito	Mitochondrial
MTS	3-(4,5-dimethylthiazol-2-yl)-2,5-diphenyltetrazolium bromide
NAD	Nicotinamide adenine dinucleotide
NEFA	Non-esterified Fatty Acids
NOF#	Neck of Femur Fracture
OA	Osteoarthritis of the Hip
OCR	Oxygen Consumption Rate
P/S	Penicilin/Streptomycin Solution
PBS	Phosphate Buffer Saline
PRIS	Propofol Infusion Syndrome
TBI	Trauma Brain Injury
TCA cycle	Tricarboxylic Acid (Krebs) Cycle
TMPD	N,N,N',N'-tetramethyl-p-phenylenediamine

SOUHRN

Úvod: Rostoucí počet studií ukazuje, že mitochondriální dysfunkce mohou být způsobeny některými běžně užívanými léky a sehrávat klíčovou roli v rozvoji jejich nežádoucích účinků. Jedním z příkladů je derivát fenolu propofol. Propofol je intravenózní, rychle a krátkodobě působící hypnotikum, které se rutinně užívá jak k anestezii v průběhu operačních zákroků, tak i k sedaci na jednotkách intenzivní péče. Syndrom propofolové infuze (PRIS) je vzácnou, avšak závažnou komplikací podávání léku s velmi vysokou mortalitou. Mezi jeho typické známky patří metabolická acidóza, nově vzniklé arytmie, změny na EKG podobné známkám pozorovaným u Brugada syndromu, hypertriglyceridémie, horečka, hepatomegalie, rhabdomyolýza, srdeční a/nebo renální selhání. Riziko vzniku syndromu se zvyšuje se stoupající dávkou a dobou podávání (>48 hod). Mechanismus vzniku syndromu není dosud znám: pilotní studie provedené na animálních modelech naznačují poškození mitochondriálního metabolismu. V úvodní části práce byla provedena rešerše všech 153 publikovaných kazuistik popisujících PRIS a všech dosud provedených experimentálních prací. Dalším cílem studie bylo potvrdit hypotézu mitochondriálního poškození pomocí prolongované *in vitro* expozice lidských svalových buněk různým koncentracím propofolu a poté měřením jejich mitochondriálních funkcí metodou extracelulárního fluxu.

Metody: Vyhledány byly všechny kazuistiky popisující syndrom propofolové infuze (v období let 1990-2014) a provedena byla analýza jak vztahu mezi jednotlivými známkami PRIS a dávkou a dobou podávání propofolové infuze, tak i rizikových faktorů zvyšujících pravděpodobnost mortality. V *in vitro* studii byly použity svalové buňky, izolované z kosterního svalu (m. vastus lateralis) získaného biopsií pacientů (n=30) v průběhu elektivních operací kyčelního kloubu. Buňky byly vydiferencovány v myotuby a poté exponovány 4 koncentracím propofolu odpovídajících jeho hladině v plazmě při podávání propofolové infuze při sedaci či anestezii (1, 2.5, 5 a 10 μg/ml). Po 96 hodinách expozice byl měřen jejich energetický metabolismus pomocí XF-24 extracelulárního flux analyzátoru. V průběhu experimentu byla měřena spotřeba kyslíku jak bazální, tak po přidání dalších 3 látek: inhibitoru ATPasy, odpřahovače a inhibitoru dýchacího řetězce. Z naměřených dat jsme následně určili bazální spotřebu kyslíku (OCR), obrat ATP, leak protonů přes vnitřní mitochondriální membránu a kapacitu dýchacího řetězce. Kapacita β-oxidace mastných kyselin byla měřena jak metodou extracelulárního fluxu (jako

etomoxirem inhibovatelná OCR po přidání odpřahovače a palmitátu), tak pomocí radioaktivně značeného palmitátu. Pro detailnější otestování funkce dýchacího řetězce byla měřena respirace po přidání specifických substrátů a inhibitorů pro jednotlivé komplexy (I, II, III a IV). Aktivity jednotlivých komplexů byly navíc měřeny spektrofotometricky.

Výsledky: Meta-analýza dat získaných ze 153 publikovaných kazuistik PRIS ukázala více než >51% mortalitu. Faktory spojenými s vyšší mortalitou byly dávka a délka podávání propofolové infuze, horečka a kraniotrauma. Srdeční selhání a metabolická acidóza se objevily časně po začátku podávání propofolu a byly závislé na dávce, zatímco výskyt arytmií, změn na EKG a rhabdomyolýzy se zvýšil s dobou podávání propofolové infuze, nezávisle na dávce. V *in vitro* studii byl porovnáván efekt propofolu s kontrolními buňkami rostoucími v čistém mediu i s buňkami exponovanými buď pouze lipidovému nosiči propofolu (Intralipidu) anebo směsi mastných kyselin odpovídajících složení Intralipidu (55% kyselina linoleová, 27% kyselina olejová a 10.5% kyselina palmitová). Viabilita buněk a bazální spotřeba kyslíku byla ovlivněna pouze nejvyššími koncentracemi propofolu (10 μg/ml), zatímco již nejnižší testované koncentrace snížily maximální kapacitu dýchacího řetězce. Expozice propofolem způsobila mírné odpřažení vnitřní mitochondriální membrány, nezávislé na dávce propofolu. Jednotlivé komplexy dýchacího řetězce nebyly inhibovány. Nejvýznamnější abnormitou, navozenou propofolem, byla inhibice oxidace mastných kyselin na 36%, resp. 33% bazálních hodnot (expozice 2.5, resp. 10 μg/ml propofolu).

Závěr: Diagnóza PRIS může být obtížná, protože některé z typických příznaků PRIS mohou často (>95%) chybět (hypertriglyceridémie, horečka, hepatomegalie, srdeční selhání) a jiné (např. arytmie) se objevují později. Klinické projevy PRIS naznačují poškození mitochondriálního metabolismu. Provedená *in vitro* studie prokázala, že propofol snižuje maximální respirační kapacitu dýchacího řetězce a způsobuje výraznou inhibici β-oxidace mastných kyselin v lidském kosterním svalu.

SUMMARY

Introduction: Increasing number of reports reflect that mitochondrial dysfunction can be induced by some of the commonly used drugs and can play a key role in the development of their adverse effects. One of these drugs is a phenol derivative propofol. Propofol is an intravenous, fast and short-acting hypnotic agent, routinely used either for induction and maintenance of anaesthesia during surgery, or for sedation in intensive care units. Propofol infusion syndrome (PRIS) is a rare, but serious adverse effect of the drug with a very high mortality. Typical features of the syndrome include metabolic acidosis, arrhythmias, ECG changes that are similar to those of Brugada syndrome, hypertriglyceridemia, fever, hepatomegaly, rhabdomyolysis, cardiac and/or renal failure. The risk of the syndrome increases with raising dose and duration of propofol administration (>48 hours). The mechanism of the syndrome is still unknown: pilot studies performed on animal models are suggestive of its mitochondrial origin. In the first part of the study, we performed the analysis of 153 published case reports and all experimental studies related to PRIS. Another aim of the study was to test hypothesis of propofol-induced mitochondrial damage by *in vitro* exposure of human skeletal muscle-derived cells to a range of propofol concentrations and then assessment of mitochondrial functions by Extracellular Flux Analysis.

Methods: We searched for all case reports describing PRIS (published between 1990 and 2014) and we analysed both the relationship between signs of PRIS and the rate and duration of propofol infusion, and risk factors for mortality. In the *in vitro* study, we used human skeletal muscle cells that were isolated from skeletal muscle (m. vastus lateralis) obtained from patients (n=30) undergoing hip replacement surgery. Cells were differentiated into myotubes and exposed to a range of 4 propofol concentrations resembling its levels in human plasma during propofol infusion at sedation or anaesthesia (1, 2.5, 5 a 10 μg/mL). After 96 hours of exposure, energy metabolism was assessed using XF-24 Extracellular Flux Analyzer. During experiment, we measured oxygen consumption rate (OCR) at baseline and after addition of three agents: inhibitor of ATPase, uncoupler and inhibitor of respiratory chain. The measurement enabled us to determine basal OCR, ATP production, proton leak and maximal respiratory capacity of the respiratory chain. The capacity of fatty acid oxidation was measured using both Extracellular Flux Analyzer (by etomoxir-induced inhibition of OCR after addition of palmitate and uncoupler) and radioactively labelled [1-^{14}C] palmitate. In addition, we measured respiration after addition of specific substrates and

inhibitors for individual complexes of the respiratory chain (complex I, II, III and IV). Activities of individual complexes were also measured spectrophotometrically.

Results: Meta-analysis of 153 case reports about PRIS showed more than >51% mortality. Risk factors associated with high mortality were dose and duration of propofol infusion, fever and craniotrauma. Cardiac failure and metabolic acidosis occurred early after initiation of propofol infusion and are dose-dependent, whilst arrhythmias, ECG changes and rhabdomyolysis appeared more frequently after prolonged propofol infusion, irrespective of dose. In the *in vitro* study, we compared effect of propofol on myotubes with control cells incubated in fresh medium or exposed to either lipid vehicle (Intralipid) or non-esterified fatty acids (NEFA) mixture resembling Intralipid composition (55% of linoleic acid, 27% of oleic acid and 10.5% of palmitic acid). Cell viability and basal oxygen consumption were influenced by only the highest propofol concentration (10 μg/mL), whilst the lowest concentration already caused decrease of maximal respiratory capacity. Exposure to propofol caused a mild uncoupling of inner mitochondrial membrane, irrespective of propofol dose. Individual complexes of the respiratory chain were not inhibited. The most significant propofol-induced abnormality was inhibition of fatty acid oxidation to 36% and 33% of baseline values (exposure to 2.5 and 10 μg/mL of propofol, respectively).

Conclusion: Diagnosis of PRIS may be challenging as some of its typical features are often (>95%) missing (hypertriglyceridemia, fever, hepatomegaly, cardiac failure) and others (e.g. arrhythmias) appear later. Clinical features of PRIS are suggestive of its mitochondrial origin. Our *in vitro* study showed that propofol decreases maximal respiratory capacity and causes profound inhibition of fatty acid oxidation in human skeletal muscle.

1. Introduction: mitochondria

Mitochondria are cellular organelles generating energy in the form of ATP molecules, essential to maintain homeostasis and survival of cells[1], sometimes signed as “powerhouse of the cell”. Mitochondria have also another important functions including calcium and iron homeostasis, synthesis of pyrimidines and steroids, calcium signalling or thermogenesis and fever response[2].

Term of mitochondria. In 1886, Richard Altmann firstly observed the organelles under microscope and described them as granula inside the cell[3]. He called them *“bioblasts”* because he believed that these “blasts” are the living units within the cell. In 1898, Carl Benda stained these organelles by crystal violet and saw that they are of thread-shape but other time they appear like granules[4]. He coined the term “mitochondrion” from the Greek words “mitos” (=thread) and “chondrion” (=granule).

Structure of mitochondria. Mitochondria look like membrane-coated organelles, but their construction is more complex. In addition to the external mitochondrial membrane forming the shape of mitochondria, inside is also an inner mitochondrial membrane, which is shrouded in numerous “cristae”[3] (see **Figure 1**). Between both membranes, intermembrane space is located. Internal compartment matrix is area surrounded by inner membrane. Enzymes of respiratory chain are incorporated into the inner mitochondrial membrane, whilst tricarboxylic acid ([TCA]; citric acid; Krebs) cycle, fatty acid oxidation etc. are performed inside matrix. Mitochondrial shape and size may differ according to cell line (e.g., in hepatocytes and fibroblasts mitochondria have 3-4 µm in length and approximately 1 µm in diameter and have a typical oblong "sausage-like” shape)[3]. Cristae founded in inner mitochondrial membrane can also have a different shape (lamellar or tubular). However, the number of mitochondria and cristae are the most important parameters for function. The number of mitochondria in one cell vary in different cell types and ranges from a few hundred to thousands (e.g. the liver cell contains approximately 800 mitochondria, while the human oocyte counts to > 100,000 mitochondria)[3]. Similarly, number of cristae vary in different cell lines. For example, mitochondria in muscle cells, have high-folded, lamellar cristae with a large surface area leading to high respiratory rate[3].

Chemiosmotic theory. In 30’s, there were first attempts to isolate mitochondria, and, in early 50’s, it was well-described that mitochondria contain the enzymes of the TCA cycle, fatty acid oxidation and oxidative phosphorylation. In 1961, Peter Mitchell proposed his chemiosmotic

hypothesis suggesting that synthesis of ATP in respiring cells is generated via the electron transport chain located in inner mitochondrial membrane[3].

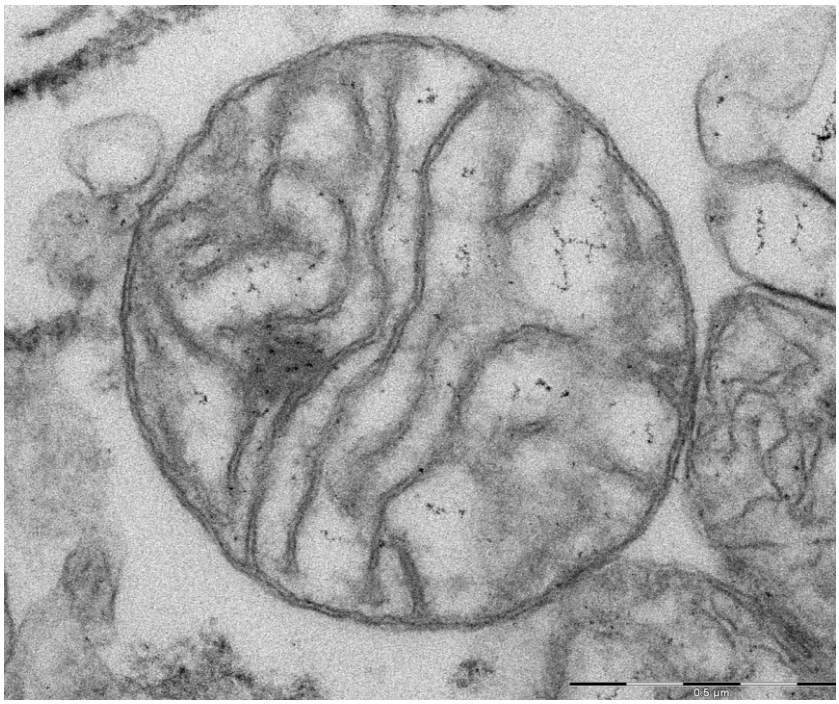

Figure 1. Electron microscopy picture of human heart muscle mitochondria. Scale bar: 0.5 µm. Krajčová et al., 2018[5].

Energy production. Mitochondria can utilize both pyruvate from glucose and fatty acids as fuel. Pyruvate and fatty acids are transported across the inner mitochondrial membrane and then converted to the metabolic intermediate Acetyl Coenzyme A (Acetyl-CoA), either by enzyme pyruvate dehydrogenase or enzymes of fatty acid oxidation, both located in the mitochondrial matrix. Acetyl-CoA is then oxidized as a substrate for TCA cycle in series of chemical reactions resulting in a production of reduced coenzymes nicotinamide adenine dinucleotide (NADH) and flavin adenine dinucleotide ($FADH_2$) and CO_2 as a waste molecule. According to *chemiosmotic* theory, electrons from reduced coenzymes (NADH and $FADH_2$) generated during catabolic pathways (glucose metabolism, TCA cycle, fatty acid oxidation), are transferred along electron transfer chain (ETC) consisting of 4 complexes of respiratory chain (I, II, III, IV) in the inner mitochondrial membrane to final acceptor oxygen[3]. The reducing equivalents (electrons) enter the ETC at two sites: complex I (NADH: ubiquinone oxidoreductase) or complex II (succinate: ubiquinone oxidoreductase) and undergo sequential oxidation reduction reactions. Complex I and II reduce ubiquinone (coenzyme Q) to ubiquinol. Complex III (ubiquinone: cytochrome c

oxidoreductase) couples the oxidation of ubiquinol to cytochrome c reduction. Complex IV (cytochrome c: oxygen oxidoreductase) catalyses the oxidation of cytochrome c, reducing molecular oxygen and producing water. Energy released during redox states is used for pumping the protons across the inner mitochondrial membrane from matrix into the intermembrane space at three sites: complex I, III, and IV. Inner mitochondrial membrane is impermeable for protons and they accumulate in intermembrane space creating electrochemical gradient. The enzyme F_1F_0-ATPase, which is translocated in the inner mitochondrial membrane, allows protons to diffuse back into the matrix through its molecule. During the process, ATPase undergoes conformational changes leading to formation of adenosine triphosphate molecule from adenosine diphosphate and inorganic phosphate. In summary, proton-motive force is used for ATP synthesis. The process is called *oxidative phosphorylation,* and, during physiological conditions, couples respiration with ATP production. *Fatty acids transport and oxidation.* Fatty acids, as fuel for energy production, firstly need to be transported through outer and inner mitochondrial membrane into the matrix, where enzymes of fatty acid oxidation (β-oxidation; FAO) are located. Long chain-fatty acids (e.g. palmitate) need for the transport carnitine shuttle. Fatty acids are esterified with Coenzyme A to form acyl-CoA, when they enter the cell. Coenzyme A cannot cross the mitochondrial membranes to enter the matrix. Acyl-CoA therefore undergoes reaction with carnitine, by enzyme CPT-1 (carnitine palmitoyl transferase 1) resulting in formation of acylcarnitine and CoA. Acylcarnitine then gets into the intermembrane space by Carnitine-acylcarnitine translocase and crosses the inner membrane, where it transfers acyl group onto CoA, which is freely available in mitochondrial matrix. The reaction is catalysed by CPT-2 (carnitine palmitoyl transferase 2) and its product – acyl-CoA enters fatty acid oxidation in matrix. Fatty acid oxidation includes a series of reactions catalysed by 4 enzymes leading to production of Acetyl-CoA. Of note, through the process, $FADH_2$ is also generated which enters respiratory chain by electron transfer flavoprotein (ETF) dehydrogenase. Short-chain and medium-chain fatty acids can enter mitochondria as independently on carnitine. They are activated in the mitochondrial matrix where short-chain and medium-chain acyl-CoA synthetases are located.

In conclusion, defects of energy production can be caused by inhibition of substrate pathways, inhibition of FAO and inhibition in electron transfer chain, either by defects of complexes I, II, III, IV and ETF dehydrogenase/or electron carriers: coenzyme Q or cytochrome c.

2. Drug-induced mitochondrial dysfunction

Increasing number of reports reflect that mitochondria, either as a primary or secondary target to drugs[6], and their dysfunction, can play a key role in drug-induced adverse effects[7]. Drugs can affect mitochondria either directly (by uncoupling or inhibition of electron transport chain, inhibition of mitochondrial transport pathways, inhibition of fatty acid oxidation or fatty acid uptake, the citric acid (tricarboxylic acid; Krebs) cycle, mitochondrial DNA transcription, protein production)[2] or indirectly (by increasing reactive oxygen species production leading to mitochondrial DNA mutation, membrane depolarization and decreased antioxidant production)[6]. For example, adriamycin-induced mitochondrial cardiomyopathy is a well-known complication of this commonly used chemotherapeutics caused by interference with mitochondrial metabolism via inhibition of ATP production (by uncoupling of oxidative phosphorylation) and production of reactive oxygen species[8]. Liver toxicity is a side effect of valproic acid, widely used antiepileptic drug[9]. It was observed in an *in vitro* study, that sodium valproate decreases oxygen consumption rate and mitochondrial membrane potential[10]. Statins, a class of drugs used for hypercholesterolaemia treatment, are well-known for their two important side effects, elevation of liver enzymes and myotoxicity, which could vary from mild myopathy to serious rhabdomyolysis[11]. Recent studies are suggestive of their impact on mitochondrial function, causing directly complex III inhibition[12] or coenzyme Q_{10} deficiency[13]. Statins inhibit HMG-CoA reductase producing mevalonate, a precursor of both cholesterol and coenzyme Q_{10}[14]. Amiodarone, a class III antiarrhythmic agent causing micro-vesicular steatosis of the liver is associated with inhibition of fatty acid oxidation in mitochondria[15,16]. Antibiotics, such as tetracyclines or chloramphenicol, impair mitochondrial respiration[17] by inhibition of fatty acid oxidation[18] or mitochondrial protein synthesis and decreasing ATP production[19]. Acetylsalicylic acid, one of the non-opioid analgesics, caused inhibition of fatty acid oxidation[20] in patients who developed Reye's syndrome. Metformin is a widely used oral antidiabetics from class of biguanides, which inhibits activity of complex I of respiratory chain leading to decreased ATP synthesis in mitochondria[21].

One of the agents which are suggestive to have an impact on mitochondrial metabolism is phenol derivative propofol, which is one of the most commonly used drugs in anaesthesia. Its rare but fatal complication "propofol infusion syndrome" is known from 1990 and includes metabolic acidosis, cardiac failure, arrhythmias, rhabdomyolysis, renal failure, hypertriglyceridemia and fever[22]. Previous animal studies and its clinical symptoms are suggestive of its mitochondrial

origin, but exact mechanism remains unknown. Specific treatment doesn't exist, and mortality is high.

3. Propofol in clinical practice

Propofol is an intravenous sedative agent used for an induction and maintenance of anaesthesia and sedation in the intensive care units (ICUs) from 1980's[23,24]. It is a short acting lipophilic hypnotic agent with a chemical structure of an alkylphenol derivative (2,6-diisopropylphenol; see **Figure 2**), which is administered as 1 or 2% solution in 10% Intralipid infusion. Propofol acts by potentiating γ-aminobutyric acid type A ($GABA_A$) receptors to achieve the sedative hypnotic effect[25]. It has become widely used both in children and adult patient population[26], due to its multiple favourable effects including rapid onset of action, short half-life and less incidence of postoperative adverse effects (e.g. nausea and vomiting) in comparison with previously commonly used anaesthetics as thiopental and methohexital[27,28]. Moreover, it has been shown that propofol is a suitable replacement for etomidate for sedation in cardiac surgery patients[29] and it has also gained popularity in the population of neurosurgical patients with trauma head injury due to its ability to maintain or reduce intracranial pressure, while maintaining an adequate cerebral perfusion pressure[30]. Propofol had been generally considered safe and efficacious[31], but in the early 1990's fatal complications after its administration were firstly reported[32,33].

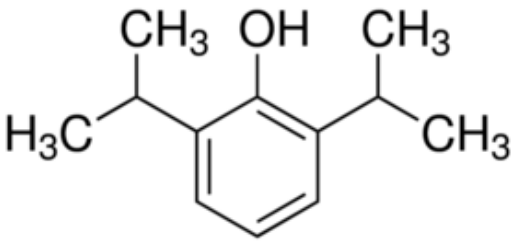

Figure 2. Chemical structure of propofol (2, 6 – diisopropylphenol).

4. Chemical structure and properties of propofol

Propofol is chemically described as 2,6-diisopropylphenol, a simple phenol substituted with two isopropyl groups positioned on each side of a hydroxyl group (see **Figure 2**)[34]. Its pure substance has a slightly yellowish colour and it has an oil consistence at room temperature. The

molecule of propofol is insoluble in aqueous solution because of its highly lipophilic benzene ring and isopropyl side groups[35]. Due to its high lipophilicity propofol was firstly administered as 1% active agent dissolved in solution containing 16% polyethoxylated castor oil (Cremophor EL), but this formulation was soon withdrawn as the stabilizing agent was found to cause anaphylactic reactions[36]. Nowadays, propofol is commercially available as 1 or 2% (10 or 20 mg/mL, resp.) active agent 2,6-diisopropylphenol dissolved in 10% Intralipid emulsion[37], which consists of soybean oil (100 mg/mL), egg yolk lecithin (12 mg/mL) and glycerol (22.5 mg/mL)[35]. Due to this Intralipid vehicle, which also serves as a parenteral nutritional agent, propofol is famed for its "milky" appearance. The pH of the emulsion is adjusted with sodium hydroxide to around 7.0 – 8.5 for optimal emulsion stability[35]. Lipid vehicle can be conducive to bacterial growth[38]. Thus, propofol infusion also contains 0.005% of the chelating agent disodium edetate (EDTA), which acts as an antimicrobial agent[39].

5. Pharmacokinetics and pharmacodynamics of propofol

Propofol is a phenol derivative which is structurally and chemically unrelated to barbiturates and other previously used anaesthetic agents[40]. Anaesthetic properties of propofol were discovered in 1973[41,42] by Imperial Chemical Industries in the United Kingdom (UK) investigating the sedative effects of phenol derivatives in animal models[34]. The early study in humans demonstrated that propofol it the effective and safe induction agent with pain after injection as the only known side-effect[43]. During 1980's, it became very popular in anaesthesia and intensive care because of its favourable pharmacokinetic profile including particularly rapid onset, short duration of action and fast recovery. Its pharmacokinetics involves a three-compartment model consisting of plasma, rapidly and slowly equilibrating tissues[44]. Propofol has a fast onset and short duration of action due to its rapid penetration of the blood-brain barrier[40]. Its initial distribution half-life is very short (around 2–8 min)[45]. Propofol rapid distribution to the central nervous system is followed by its fast redistribution to inactive tissue depots (muscle and fat tissue) and then it is slowly returned from these peripheral compartments into the blood[40]. Loss of consciousness is achieved within 20 to 40 seconds after intravenous administration[46]. After initial bolus, propofol concentration in human plasma rapidly decreases because of the fast redistribution from brain to peripheral tissues[46] and because of its rapid elimination[45]. Propofol administration is characterized by lack of accumulation on repeated boluses and lack of excitatory effects on induction and during maintenance and recovery[47]. Propofol is rapidly metabolized in the liver to inactive glucuronide, sulphate conjugates and corresponding quinol metabolites,

producing water-soluble compounds which are excreted mainly by the kidneys[45,48,49]. It also undergoes 4-hydroxylation by cytochrome P450 to 2,6-diisopropyl-1,4-quinol, which can also undergo glucuronide conjugation and excretion in the urine[49]. Clearance of propofol is extremely high and recovery occurs rapidly after drug discontinuation[50]. Rate of recovery is even ten times higher than e.g. that of thiopental[51]. These pharmacokinetic properties make propofol suitable and popular for short procedures when sedation is needed for only a few minutes[50]. Renal and hepatic diseases have no clinically significant effect on the metabolism of propofol[48]. Propofol has significant pharmacodynamic effects in cardiovascular system as it causes 15-25% decrease in blood pressure and systemic vascular resistance without a compensatory increase in heart rate, and cardiac output is decreased by 20%[48]. Propofol can cause profound bradycardia, possibly through resetting of the baroreceptor reflex and rarely even make asystole[48]. Propofol administration influences also respiratory system – the only bolus can produce apnoea of variable duration (30 to ≥60 seconds) and suppression of laryngeal reflexes[48]. In the central nervous system, propofol causes a dose-dependent decreased level of consciousness and reduces cerebral blood flow, intracranial pressure, and cerebral oxygen consumption. Propofol is therefore often used in cases requiring decrease in intracranial pressure, e.g. patients with trauma head injury.

Propofol action is related to the major inhibitory neurotransmitter GABA (γ-aminobutyric acid) in the central nervous system. $GABA_A$ receptors are located in the postsynaptic membrane and mediate neuronal inhibition in brain[52]. Propofol binds to $GABA_A$ receptors potentiating the inhibition and resulting in its sedative and hypnotic effect[53]. The binding to the receptors induces opening of chloride channels and increases chloride conductance across the neuron resulting in the hyperpolarization of the cell membrane[52]. In addition, propofol inhibits glutamate receptors[54] and reduces extracellular glutamate levels[55].

6. History of propofol infusion syndrome (PRIS)

6.1 PRIS in the paediatric population

The first case report of fatal complication after propofol administration was documented in Denmark in 1990[32]. 2-year old girl with upper respiratory infection received propofol infusion at dose of 10 mg/kg per hour for duration of 4 days. The child developed severe metabolic acidosis, hypotension and multiple organ failure of unknown etiology leading to death. Authors related these fatal complications to propofol infusion. Two years later, Parke et al. published similar cases

in the United Kingdom[33]. Five children, aged between 4 weeks and 6 years, developed serious complications leading to death after propofol administration. All children were admitted to intensive care unit for upper or lower respiratory infection and intubated within 24 hours from admission. In all cases, propofol was used for sedation at the average dose of 7.4-10 mg/kg per hour for duration of 66-115 hours. Every patient subsequently developed increasing metabolic acidosis followed by hyperlipidaemia and bradyarrhythmia proceeding to progressive myocardial failure that was resistant to resuscitation. Some of them suffered also by fever, hepatomegaly, pulmonary oedema, acute renal failure, hypocalcaemia or hyperkalaemia. Echocardiography and necropsy showed no evidence of structural heart disease or cardiomyopathy. Furthermore, there was no evidence of viral myocarditis, Reye's syndrome or sepsis. Propofol infusion was considered the presumable cause of the death[33]. In June 1992, Committee on Safety of Medicine in the United Kingdom issued a warning against propofol use for sedation in the population of paediatric patients, although there was no evidence of a direct effect of propofol or its vehicle in children receiving propofol infusion[56,57]. Investigation of Food and Drug Administration (FDA) in United States did not find a direct link between propofol administration and death of these paediatric patients, but further study was conducted[58,59]. A few weeks later, the first case of successful treatment of these serious adverse effects was described[60]. 20-month old child with acute epiglottitis was administered with propofol infusion at the dose of 5-10 mg/kg per hour for duration of 56 hours. The third day of propofol administration the child developed metabolic acidosis, hyperlipidaemia, bradycardia, hypotension and oliguria. Laboratory blood test revealed high concentration of creatine kinase and muscle biopsy showed necrosis. Bradycardia rapidly proceeded to asystole, which successfully responded to pharmacological treatment. Veno-venous hemodiafiltration was initiated and after that replaced by peritoneal dialysis. The patient gradually recovered and was discharged from the hospital[60]. In following years, number of case reports describing these propofol complications increased[61,62] and manufacturer warned against propofol use as a sedative agent in intensive care units in paediatric patients in 1994[58]. Several authors had still doubts about whether propofol could be the cause of the death in these cases and considered propofol to be safe drug[63], but other similar reports of propofol-induced death continued to be documented in literature[64–68].

In 2001, the unpublished randomized controlled trial (reviewed by FDA) observed 28-day mortality in 327 patients sedated by propofol in paediatric ICUs in United States. Results showed increased mortality in patients with propofol sedation in comparison with control group: mortality was about 11% for group of patients receiving 2% propofol, and 8% for group of patients receiving

1% propofol. Patients with non-propofol sedation had about 4% mortality. FDA and Canadian Health Board issued a warning against propofol use for long-term sedation in children[69]. Short-term administration was generally still considered safe but few children developed these adverse effects even after several hours, 2.5 hours[70] and 5 hours[67].

6.2 PRIS in the adult population

Although the syndrome was initially documented solely in children, few reports were published in the population of adult patients[71–73]. In 1996, Marinella et al. described a case of 30-year-old woman with acute respiratory failure, who needed a mechanical ventilation and propofol sedation[74]. After only 2 hours she developed metabolic acidosis and blood test showed increased lactate level. After discontinuation of propofol infusion, laboratory values normalized and patient recovered and remained without any consequences[74]. In 2000, Perrier et al. reported the first case of death caused by propofol infusion in adults[73]. 18-year-old patient with trauma head injury developed metabolic acidosis, hyperkalaemia, elevated levels of creatine kinase and arrhythmias progressing to asystole that was resistant to treatment[73]. Similar cases in adults were subsequently described[71,72,75]. Cremer et al. published in *The Lancet* a landmark paper of seven cases of PRIS in the neurosurgical ICU and was the first to highlight that the cumulative dose of propofol was the main risk factor for its development[72]. In 2002, guidelines for population of adult patients were issued[76]. Jacobi et al. recommended to avoid propofol administration in concentrations higher than 83 μg/kg/min because of increased risk of cardiac arrest in adults[76]. Authors also recommended to monitor patients receiving propofol for unexplained metabolic acidosis or arrhythmias[76]. In 2006, the FDA updated the labelling information and limited the maximum dose of propofol recommended for sedation to 4 mg/kg per hour[77]. At the same time European regulatory authorities suggested that patients should be monitored for metabolic acidosis, hyperkalemia, rhabdomyolysis or elevated creatine kinase level and signs of heart failure. In case of development of these signs they recommended reduction or discontinuation of propofol[58,78].

7. Definition of PRIS

In 1998, propofol infusion syndrome was defined by Bray et al.[65]. Authors summarized all cases concerning adverse effects of propofol used for sedation documented in literature within this year and described clinical and laboratory signs of the syndrome. In most cases propofol was

used to provide sedation during mechanical ventilation. The syndrome was defined as: (1) a sudden, or relatively sudden, onset of a marked bradycardia, resistant to treatment and progressing to asystole, and also the appearance of one of the following symptoms: (2) the presence of lipaemic plasma; (3) a clinically enlarged liver or histological evidence of fatty infiltration of the liver found at autopsy; (4) the presence of metabolic acidosis (with a base deficit > 10 at least once in a patient's arterial blood sample); (5) the presence of muscle involvement with evidence of rhabdomyolysis or myoglobinuria[65]. In following years, many patients with PRIS developed tachycardia instead of bradycardia. Therefore, some authors suggested modification of Bray's definition and used "the presence of heart failure and arrhythmias" as one of the signs of PRIS[58,79,80].

A current view on the syndrome is quite different from previous Bray's definition in 90's. In our first publication in *Critical Care*, we analyzed data from 153 patients with PRIS from case reports and case series published between 1990 and 2014 and we looked at the presence of individual signs of the syndrome[81]. In many cases, patients developed only mild unexplained acidosis and elevation of creatine kinase, sometimes with worsening of acute kidney injury and arrhythmia, but other features of PRIS were often missing[82–86]. In some of reported cases, mild unexplained acidosis was even the only sign of possible PRIS development, which completely disappeared after propofol withdrawal[74]. Because symptoms can occur in any combination and order and can range from the very mild to severe in each individual patient, it is very difficult to determine a precise definition of PRIS.

8. Epidemiology of PRIS

PRIS is a rare complication of propofol administration and its incidence is still unknown. It is well known that development of PRIS depends on the presence of risk factors e.g. propofol infusion rate or duration[72,79,81]. In 1998, Bray et al. observed 33% incidence of PRIS in a group of paediatric patients receiving propofol at the mean dose higher than 4 mg/kg per hour for a minimum of 48 hours[65]. In 2001, Cremer et al. reported the incidence of PRIS in adult head-injured patients[72]. PRIS occurred in 17% of patients receiving propofol at the dose of 5 to 6 mg/kg per hour and in 31% of patients receiving propofol at the dose greater than 6 mg/kg per hour[72]. Cravens et al. recorded the occurrence of metabolic acidosis in the group of adult patients undergoing radiofrequency ablation[87]. 24% patients who were administered with propofol at the high-dose of 20 mg/kg per hour for a duration of 7 hours developed metabolic acidosis. Authors

selected solely the cases, where propofol agent was considered the only possible cause of acidosis[87]. In 2008, Fong et al. proposed results of their retrospective analysis of all case reports with PRIS published in MEDLINE system between 1989 and 2005[22]. Authors searched for the reports where patients developed at least one of the clinical symptoms of PRIS. Of 1139 patients with suspected PRIS, 30% were fatal[22]. Higher mortality was associated with young age, male sex and concomitant administration of vasopressors or presence of cardiac abnormalities, metabolic acidosis, renal failure, hypotension, rhabdomyolysis or hypotension[22]. In 2009, Smith et al. showed 6% incidence of the syndrome in population of patients with severe head trauma injury[88]. According to the results, concomitant use of vasopressors was associated with development of PRIS in this cohort[88]. Roberts et al. analysed the group of 1017 critically ill adult patients receiving propofol at least for 24 hours[83]. The incidence of PRIS slightly exceeded 1% and in most cases (91%) PRIS development was associated with the concomitant vasopressor administration[83]. Iyer et al. analysed the group of patients admitted to ICU with refractory status epilepticus who received propofol[89]. 45% patients developed features of PRIS and mortality of the cohort was about 6%[89]. In 2014, Schroeppel et al. examined the cohort of 207 patients with trauma brain injury and found 2.9% incidence of PRIS[85].

Although the number of published case reports of PRIS worldwide was less than 200 until 2018, we believe that in fact the syndrome occurred in many cases that were unrecognized or never documented by clinicians.

9. Clinical manifestation and laboratory findings of PRIS

In 2008, Fong et al. reviewed all reported cases of PRIS and analysed its most common clinical and laboratory signs[22]. Most frequent features included the following: cardiac failure or arrhythmias (43,7%), hypotension (34%), rhabdomyolysis (27%), hepatic insufficiency (24,1%), renal insufficiency (23,5%), metabolic acidosis (20,1%), hypoxia (17,5%), hyperthermia (11,6%) and dyslipidaemia (5,3%)[22].

Cardiovascular system. The most frequent changes seen in PRIS were related to the cardiovascular system. Arrhythmias: in 2008, Bray et al. defined the presence of bradycardia that is resistant to treatment and proceeding to asystole as a criterion essential for diagnosis of PRIS[65]. In following years, some patients with PRIS developed ventricular or supraventricular tachycardia, right bundle branch block or atrial fibrillation instead of bradycardia[79,80]. Electrocardiographic changes: in 2006, Vernooy et al. analysed data from previously published study in the group of

neurological patients with PRIS[90] and described their electrocardiographic changes[91]. Six of the seven patients with PRIS developed electrocardiogram (ECG) changes preceding malignant arrhythmias and sudden cardiac death after several hours[91]. The first described abnormality on ECG was elevation of ST-segments (in precordial leads V1-V3) that was similar to ECG pattern of Brugada syndrome. Subsequently, all six patients developed prolonged QT interval, idioventricular rhythm, ventricular tachycardia or ventricular fibrillation. All six patients died within 10 ± 12 hours after initiation of ECG changes. Propofol rate was 7.9 ± 1.2 mg/kg/hour at the time of ECG changes. Study also documented case report of 15-year-old child, who developed rhabdomyolysis, renal insufficiency, ST elevations in right precordial leads and inversion of T waves on ECG after several days of propofol administration[91]. In that case, propofol infusion was immediately withdrawn with normalization of ECG (except persisting T waves inversions) and patient survived[91]. Vernooy et al. concluded that development of coved-type ST-segment elevation (similar to that present an ECG pattern of Brugada syndrome) in the right precordial leads is the first warning sign of electrical instability and imminent sudden cardiac death related to PRIS[91]. Authors recommended ECG monitoring during high-dose propofol administration. In case of Brugada-like pattern on ECG, physicians should be alert to danger of serious cardiac rhythm disturbances[91]. Weiner et al. reported the case of critically ill patient who developed Brugada ECG pattern after high-dose propofol infusion[92] (see **Figure 3**). When ECG pattern was recognized, the propofol was withdrawn and the ECG pattern resolved. The patient was discharged home with no signs of arrhythmia. In summary, various ECG changes were documented in many cases of patients with PRIS. According to Robinson et al., arrhythmias might develop even in the absence of profound acidosis or myocardial failure[93].

Metabolic changes. Metabolic acidosis was present in most of PRIS cases. According to Koch et al., lactic acidosis might be an early stage of PRIS[94]. Although significant lactic acidosis frequently occurred within a few hours after propofol initiation[67,70,74,82,92,94–98], some patients developed either only mild metabolic acidosis[93,99] or PRIS occurred even without acidosis[100,101]. Most patients with PRIS had hyperlipidemia[33,68] which was considered an early sign of PRIS[102]. Hypertriglyceridemia is thought to be secondary to altered lipid kinetics in liver due to Intralipid infusion[103]. Gottschling et al. described that short-term propofol administration at the standard dose and rate might significantly increase serum triglycerides and pancreatic enzyme levels in healthy individuals not developing PRIS[104].

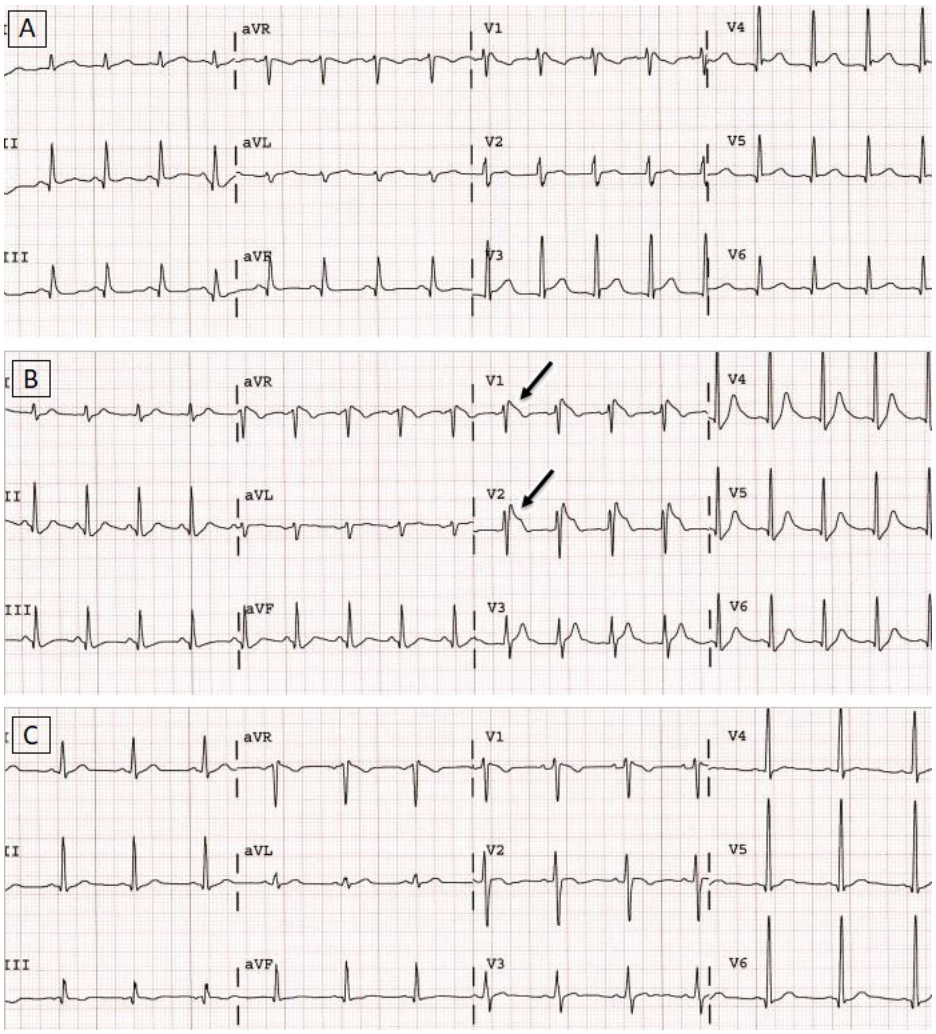

Figure 3. Electrocardiogram (ECG) of the patient who developed Brugada-like pattern after high-dose propofol infusion[92]. A) ECG 2 hours after initiation of propofol administration showing sinus tachycardia with diffuse ST segment elevation with a rSr' pattern in V1-V2. B) ECG 13.5 hours after the initial electrocardiogram with development of Brugada pattern with coved ST segment elevation in V1 and V2 (indicated by black arrows). C) ECG 2 days after propofol discontinuation: ST segment elevation resolved leaving only a rSr' pattern similar to the initial electrocardiogram. Adapted from Weiner et al., 2010[92].

Liver. Hepatomegaly is quite often and well described clinical feature of PRIS[33,65,95,100,105,106]. Histological examination showed micro-vesicular fatty liver infiltration[33] and 10% zone III necrosis with fat changes similar to those seen in acetaminophen poisoning[107]. In several patients with PRIS, propofol increased aspartate and alanine aminotransferase serum levels[89,106–110].

Muscle injury and rhabdomyolysis. Rhabdomyolysis, skeletal and cardiac muscle injury might be presented in PRIS and are associated with specific laboratory findings, e.g. elevated serum creatine kinase levels, troponin I or potassium concentration[111]. Histological tissue examination in patients with PRIS revealed a focal necrosis in skeletal[60,112] or cardiac muscle[113].

Renal system. Acute renal injury might occur in PRIS as the consequence of rhabdomyolysis and myoglobinuria[33,67,89,100,109,114–123]. Histological findings in the patients with PRIS showed acute tubular necrosis and presence of myoglobin casts in kidney tubules[90,124]. Depending on the degree of injury, serum creatinine levels might be elevated in blood samples[56,68,86,91,92,100,109,112,114,115,117–119,125]. Green discoloration of the urine is other known adverse effect of propofol treatment and is caused by propofol metabolites (4-sulfate and 1- or 4-glucuronide conjugates of 2,6-diisopropyl-1,4-quinol)[126]. Although urine discoloration has been described in many cases of PRIS[106,107,115,116,127], it can occur also in patients not developing the syndrome[126].

Another laboratory findings observed in patients with PRIS were hyperbilirubinemia[60], coagulopathy or hyperphosphatemia[116]. In 2001, Wolf et al. performed detailed biochemical analyses of patient with PRIS that revealed increased levels of malonyl-carnitine and C5-acylcarnitine suggesting propofol impact on fatty acid oxidation[68]. In the study from 2004, Withington et al. described an increased levels of acylcarnitine intermediates (especially medium-chain fatty acids) in patient with PRIS[116].

10. Pathophysiology of PRIS

In accordance with previous studies, propofol is suggestive to cause an impairment of electron transfer chain and fatty acid oxidation in mitochondria, but exact mechanism remains unknown.

10.1 Inhibition and uncoupling of electron transfer chain

According to the pilot animal *in vitro* studies, propofol is thought to act as an inhibitor of electron transport chain[128–131] and probably a mild uncoupler of inner mitochondrial membrane[130,132]. In early studies, Branca et al. briefly exposed isolated rat and heart liver mitochondria to various concentrations of propofol[128,129,132]. Isolated rat liver mitochondria were exposed to a range of propofol concentrations up to 100 µmol/L, which led to a linear dose-dependent reduction of respiratory chain capacity and transmembrane potential, but no impairment of ATP synthesis up to 75 µmol/L propofol[128,132]. Complex I was more sensitive to

propofol than complex II and, in addition, propofol (at range of 25–400 μmol/L) caused proton leak through the inner mitochondrial membrane[130]. In mitochondria isolated from rat hearts, inhibition of ATP synthesis was observed only at high dose concentrations (>300 μmol/L) of propofol[129].

In an *in vitro* study performed on isolated perfused guinea pig hearts, supratherapeutic propofol concentrations (50–200 μmol/L) caused a delay in myoglobin desaturation and cytochrome c reduction after exposure to ischaemia, consistent with inhibition of the respiratory chain, but not with uncoupling of inner mitochondrial membrane[131]. Decreased activity of cytochrome c oxidase (complex IV) was independently revealed in the skeletal muscle biopsies obtained from two patients who developed PRIS[67,107]. Another study found significantly reduced activities (of complex II+III and complex IV) of the respiratory chain in the skeletal muscle in the patient who died of PRIS[133].

Vanlander et al. was the first who emphasized on the structural similarity of propofol with strongly lipophilic Coenzyme Q (CoQ), which works as an electron-carrier in the inner mitochondrial membrane transferring electrons from complexes I and II to complex III[133]. In a series of experiments performed on rats (combining *in vivo* and *in vitro* exposure to propofol), authors demonstrated that propofol in therapeutic levels probably incorporates into the inner mitochondrial membrane, where interacts with CoQ molecule: possibly by electron acceptance from complexes I and II instead of CoQ and blocking electron transfer further to complex III, whilst much higher concentrations of propofol are needed to block the activities of individual complexes[133]. To confirm this hypothesis, they tested 3 minutes pre-incubation of propofol and then supplementation with CoQ. The results showed that inhibition of complex II+III by propofol was preventable with CoQ supplementation[133]. In the very high concentration, propofol caused inhibition of complex IV activity of the respiratory chain[133].

10.2 Inhibition of fatty acid oxidation

Another proposed mechanism of PRIS is an impairment of fatty acid metabolism, formulated by Wolf et al.[68,134] and Withington et al.[116] The authors found accumulated intermediates of fatty acid oxidation and increased plasma concentrations of acyl-carnitines in children with PRIS[68,116,134]. The levels normalized after cessation of propofol infusion suggesting a propofol-induced defect of fatty acid metabolism[135].

Animal study performed on rabbits showed an inhibition of the transport of fatty acids into mitochondria probably by propofol-induced inhibition of carnitine-acyl transferase I[136]. This enzyme is activated by adenosine monophosphate-activated kinase (AMPK). If propofol interferes with signalling function of Coenzyme Q[133], it may attenuate the activation of fatty acid oxidation by AMPK, but the activity of this enzyme has been increased in the myocardium of propofol-sedated rabbits[137]. PRIS was also associated with a ketogenic diet[138]. Prolonged propofol infusion seemed to be a crucial factor in the impairment of fatty acid oxidation: in the patient receiving propofol infusion (at the dose of 4.1–6.6 mg/kg per hour) plasma C4-carnitine species elevated steadily over the period of 5 days[134].

In summary, previous *in vitro* studies observed an acute effect of propofol exposure and mitochondrial metabolism was assessed after only several minutes of incubation. On contrary, propofol infusion syndrome mostly occurs after a prolonged administration (>48 hours)[72,76,134]. To induce a demonstrable effect after such a short exposure, propofol concentrations used in acute experiments need to be much higher than those found in human plasma (up to 10 μg/mL) during propofol anaesthesia[139] or sedation[140,141]. In extremely high concentrations, propofol mostly caused direct inhibition of respiratory chain complexes or uncoupling of inner membrane. The recent landmark paper of Vanlander et al. focused on the structural similarity of propofol molecule with Coenzyme Q[133], which needs to be further examined together with propofol-induced impairment of fatty acid metabolism.

11. Risk factors and prevention of PRIS

Risk factors for PRIS include prolonged propofol infusion, critical illness, low carbohydrate intake, hepatic dysfunction, catecholamine administration[72], glucocorticoids, systemic inflammation, cytokine production, young age, subclinical mitochondrial disease, lean body mass index[142] and head-injury[124]. According to Cremer et al., head-injured patients in neurosurgical ICUs are at particular risk for PRIS development, because high anaesthetic doses of propofol are often required in these patients to control intracranial hypertension rather than to simply maintain sedation[124]. In addition, the frequent use of vasopressors, which are supposed to act as triggering factor, are used to maintain an acceptable cerebral perfusion pressure[72]. Cremer et al. suggested to avoid propofol infusion at the rate higher than 5 mg/kg/hour for long-term sedation in ICU patients[72]. In 2002, the Society of Critical Care Medicine in alliance with the American College of Chest Physicians published guidelines warning that prolonged use (>48 hours) of high doses of

propofol (>66μg/kg/min) may be associated with development of lactic acidosis, bradycardia and lipaemia in children, and infusions of >83μg/kg/min could be associated with increased risk of cardiac arrest in adults. [115]. Although, the prolonged high-dose propofol infusions are typical for development of PRIS, the syndrome was described also in patients administered short-term propofol infusions[74,94,96,118]. Liolios et al. advised to be aware of the potential occurrence of the syndrome even when high-dose of propofol infusions are used for short time[118]. In 2006, Merz described the first case of PRIS-induced death, when patient was administered by propofol at the low infusion rate[143]. According to Kumar et al., body mass index and body habitus may also play a role in the volume of distribution of propofol and may reach toxic levels in lean patients[142].

12. Treatment of PRIS

Up to now, specific treatment of PRIS doesn't exist. The therapy is based on the supportive care including fluid resuscitation, sodium bicarbonate infusion and transvenous pacing. Nonetheless, many patients with PRIS diagnosis die and mortality of the syndrome remains high[22,69]. On the contrary, several procedures of successful treatment were described in the last two decades[60,107,114,116,117,127]. In 1992, Barclay et al. successfully used hemodiafiltration subsequently replaced by peritoneal dialysis in the case of 20-month-old child with PRIS[60]. It was the first reported case when child with PRIS survived[60]. In 1996, Cray et al. successfully treated PRIS patient by plasmapheresis followed by continuous veno-venous hemofiltration[107]. Following cases reported other successful methods: extracorporeal membrane oxygenation[144], hemoperfusion[116] or hemodialysis[116,117]. In 2004, Culp et al. reported a case report of 13-year-old child with PRIS in cardiogenic shock who successfully recovered after treatment by extracorporeal membrane oxygenation (ECMO)[144]. Further case reports of successful ECMO support were documented in literature[110]. In 2010, Guitton et al. described the case of adolescent PRIS patient who developed cardiocirculatory arrest[110]. ECMO was used for the treatment, cardiocirculatory function improved rapidly and patient fully recovered[110]. According to the authors, ECMO should be considered in cases of cardiocirculatory failure[110]. In 2010, Da Silva et al. described a case report of 4-year-old boy in whom previously described methods (haemodialysis, hemoperfusion or ECMO) was limited because of severe hemodynamic instability[127]. The patient was treated the partial-exchange blood transfusion continued by veno-venous haemodialysis when he became haemodynamically stable[127]. The treatment was successful, and authors recommend to use this procedure as a bridge during a period of severe hemodynamic instability[127]. In many other cases

with PRIS survivors, authors believe that the development of the syndrome was averted simply by the early recognition of PRIS, immediate cessation of propofol infusion and, if necessary, its replacement by another anaesthetic, e.g. midazolam[74,96].

13. Meta-analysis of 153 published PRIS case reports and case series

In our publication "Propofol infusion syndrome: a structured review of experimental studies and 153 published case reports" (reported in *Critical Care*, 2015) we analyzed data from 153 patients case reports and case series published between 1990 and 2014[81].

13.1 Aims of the study

We primary aimed to determine the relationship of propofol administration with PRIS clinical and laboratory outcomes and to analyze the factors increasing mortality[81]. The secondary aim was to find a link between the clinical presentations with proposed cellular mechanisms and to describe trends over time[81].

13.2 Methods and statistical analysis

We searched for all cases about PRIS published between 1990 and 2014. Consent for the study was not required, as the reports had been previously published[81]. A three-stage search method was performed when looking for all articles[81]. Firstly, we started with a general keyword search on the PubMed database using terms "Propofol-infusion syndrome" which yielded 275 articles[81]. We sorted all the articles related to PRIS and obtained the full-texts. We worked without any language limitation and included articles in English, German, Spanish, Chinese, Danish and Norwegian[81]. Google Translate was used to extract the data from articles in Scandinavian languages and the English abstract only for one article in Chinese[81]. Secondly, we searched references of these papers for further articles fulfilling the eligibility criteria described above but not identified during our original search[81]. Finally, we also included reports of unexpected metabolic acidosis and arrhythmia in patients on propofol published prior to the 1998 definition of PRIS[81]. This resulted in the total number of 94 manuscripts reporting on 153 patients with suspected PRIS[81].

In these papers we specifically searched and extracted data describing patients' demographic characteristics (sex and age), underlying diseases (traumatic brain injury, respiratory infection, status epilepticus, other neurological cause or others), average propofol

rate (mg/kg per hour) and duration (hours), unexplained metabolic acidosis, arrhythmias, other ECG changes, cardiac failure, acute respiratory distress syndrome, hypotension, acute kidney injury (AKI; any report of oliguria, anuria or increased creatinine), rhabdomyolysis (or elevated creatine kinase or myoglobin), lipaemia (or increased plasma triglycerides), liver damage and unexplained fever[81]. We considered a sign as being present if the original case report authors described it as a sign of PRIS: in most case reports this causation is suspected if a sign occurred or worsened after propofol administration and disappeared or improved after discontinuation of propofol administration[81]. We did not analyze concomitant medication (vasopressors and steroids) as these data were missing in >50 % of published cases[81]. In each case, the outcome was defined as "survived" (if the patient was reported to recover from PRIS) or "died", regardless of the report authors' opinion on the cause of death[81].

In order to describe trends over time, simple linear regression was used for statistical analysis[81] and cases were divided into three groups (n = 27, 53 and 72, resp.) demarcated by the years of publication: 2001 (the year of banning prolonged propofol infusion in children and the acceptance of the existence of PRIS in adults) and 2006 (the year when the safety limit of 4 mg/kg per hour was recommended)[81]. Multiple logistic regression was used to analyze risk factors for mortality and calculate the influence of every single independent variable on mortality[81]. All calculations were performed using Stata Software (version 13.1; Stata Corp. Ltd., USA), and *p* values <0.05 were considered significant.

13.3 Results

13.3.1 Changes of features of PRIS over time

90 % patients developed PRIS as a complication of non-procedural sedation in ICUs and remaining 10 % as a complication of propofol use during anesthesia[81]. The duration of infusion in reported cases of PRIS raised over time and the mean propofol infusion rate decreased, resulting in an overall decrease in the cumulative propofol dose leading to PRIS[81]. Mean age of patients in reported cases increased over time, and this trend was apparent even if pediatric cases were excluded from the analysis[81]. There was no change in the underlying disease of patients with PRIS over time, but the incidence of some reported signs of PRIS changed[81] (see **Figure 4**). Arrhythmia, other ECG changes, hypertriglyceridemia and fever occurred with less frequency over time[81]. Metabolic acidosis remained the most common symptom of PRIS with a constant incidence at around 77 % in reported cases[81].

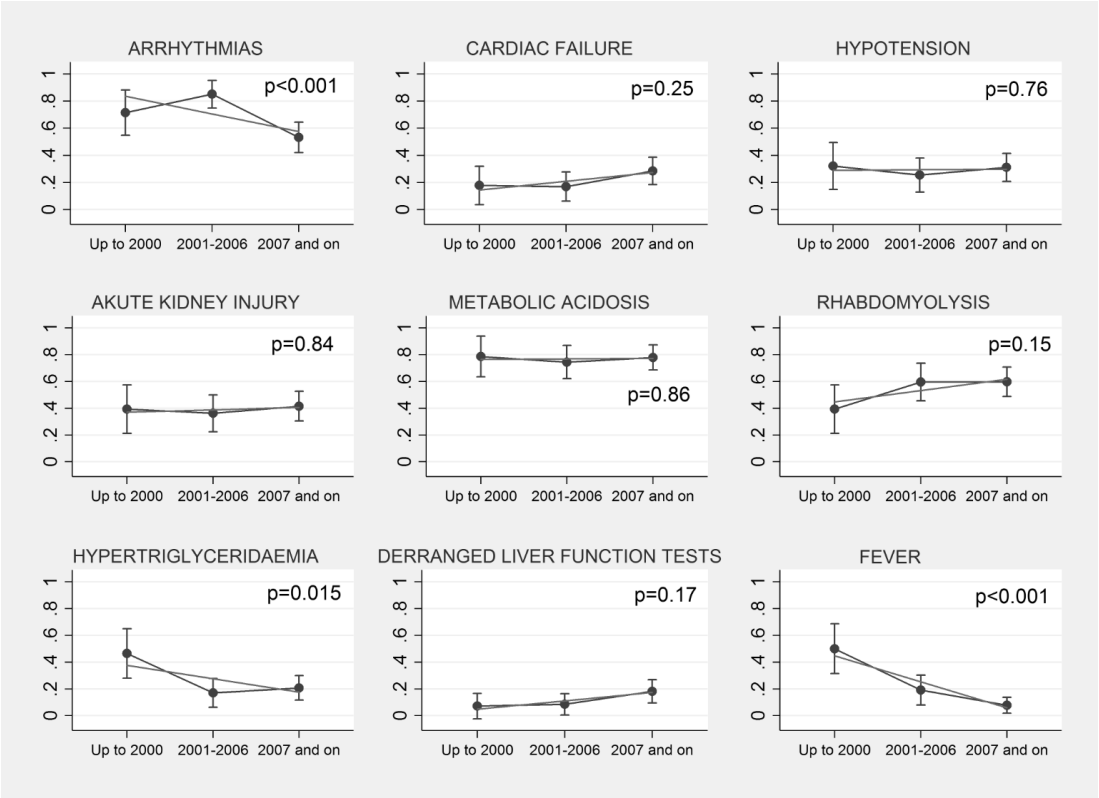

Figure 4. **Frequency of symptoms in reported cases of PRIS over time.** Data presented as means, vertical bars are 95 % confidence intervals. Krajčová et al., 2015[81].

13.3.2 Influence of propofol infusion rate and duration on signs of PRIS

Propofol infusion rate significantly influenced the frequency of fever (which occurs in <5 % of patients with an infusion rate <4 mg/kg per hour, but in >40 % with an infusion rate above 8 mg/kg per hour) (see **Figure 5**)[81]. There is a trend to similar dose dependency for cardiac failure and metabolic acidosis, which both occur more frequently with the dose above 4 mg/kg per hour[81]. Other signs occur in similar frequencies across the range of propofol infusion rates. When looking at the influence of the duration, arrhythmia and other ECG changes occur more frequently after 48 hours of infusion (see **Figure 6**)[81]. The incidence of rhabdomyolysis and hypertriglyceridemia increase after 96 hours of administration. On the contrary, metabolic acidosis occurs more frequently in cases reporting a shorter duration of propofol administration leading to PRIS development[81].

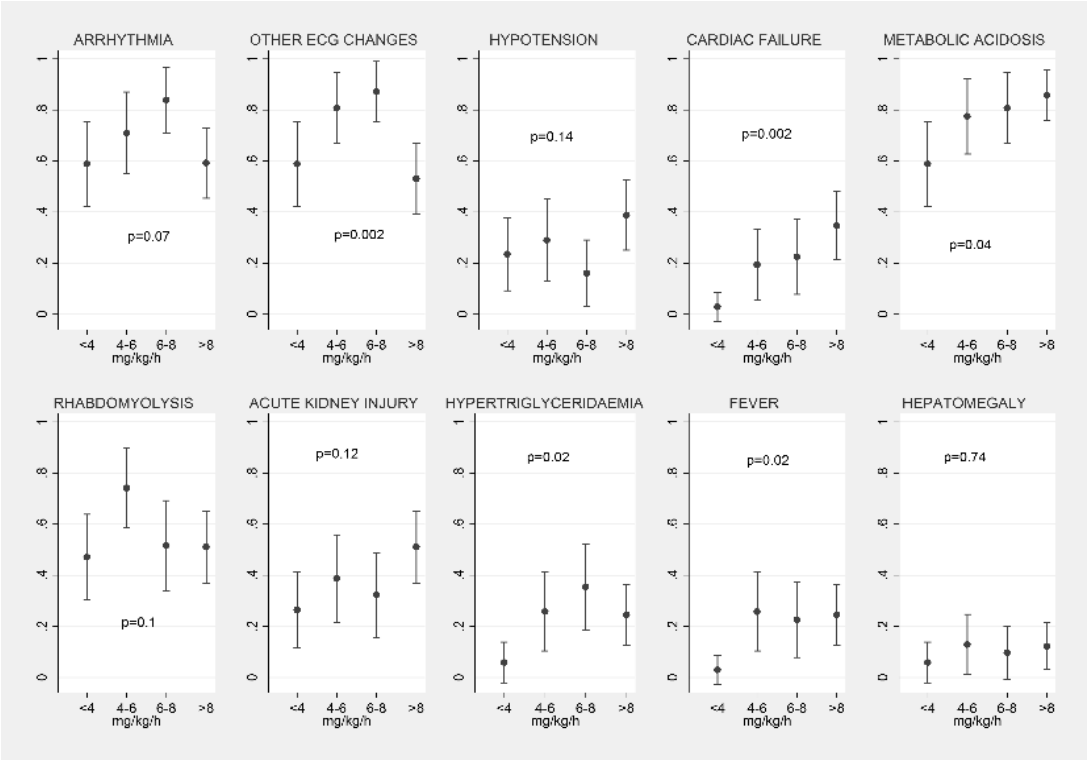

Figure 5. Relative frequency (y axis) of symptoms in patients divided into four quartiles of reported propofol infusion rate. Data presented as means, vertical bars are 95 % confidence interval. Krajčová et al., 2015[81].

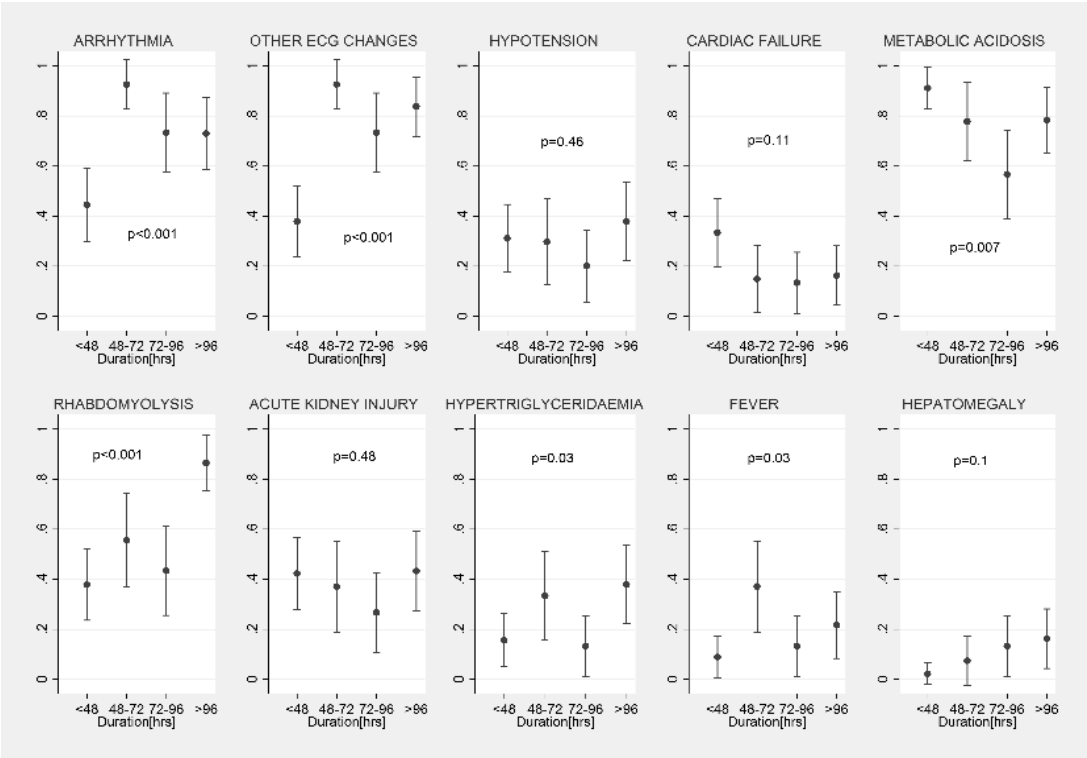

Figure 6. Relative frequency (y axis) of symptoms of PRIS in patients divided into four quartiles of reported propofol infusion duration. Data presented as means, vertical bars are 95 % confidence intervals. Krajčová et al., 2015[81].

13.3.3. Factors influencing mortality in published cases of PRIS

PRIS continues to be reported in the literature in both adult and paediatric population without a clear trend to a reduction[81]. Mortality was higher than 51%[81] and decreased over time from 74% before 2001, to 64 % between 2001 and 2006, and to 32% in cases reported after 2006[81]. Multivariate logistical regression performed on 128 cases with complete datasets identified higher dose, longer duration of infusion, development of fever and the presence of TBI as factors associated with increased mortality of PRIS[81].

14. Aims and hypotheses

Experimental data from our meta-analysis from 153 published case reports suggested that early, dose-dependent signs of PRIS (metabolic acidosis and cardiac failure) may be caused by inhibition or uncoupling of electron transfer chain, whilst late, time-dependent signs (arrhythmias, ECG changes and rhabdomyolysis) can be caused by inhibition of fatty acid oxidation and fatty acids accumulation after prolonged administration[81].

In the *in vitro* experiments, we aimed to test long-term propofol effect (at concentrations resembling its levels in human plasma during sedation or anaesthesia) on mitochondrial functions in human skeletal muscle-derived cells. Firstly, we hypothesized that mitochondrial functions are affected by one of the following substances:

1) propofol agent alone (2,6-diisopropylphenol), or
2) lipid vehicle Intralipid/or non-esterified fatty acids (NEFA) mixture resembling Intralipid composition contained in the propofol infusion, or
3) the combination of both substances

Further aims were focused on detailed mechanism of propofol-induced mitochondrial impairment. We hypothesized that propofol:

1) leads to a dose-dependent uncoupling of the inner mitochondrial membrane resulting in the reduced production of ATP, dysfunction and muscle damage and possible overproduction of heat
2) causes the reduction of spare respiratory capacity
3) causes the direct inhibition of one of the complexes of the electron transfer chain leading to the reduction of ATP production
4) inhibits fatty acid oxidation

15. Methods

15.1 Study subjects

Skeletal muscle cells were isolated from biopsies obtained from patients (n = 30; age, 71.8 ± 7.1; body mass index, 28.5 ± 4.8) undergoing hip replacement surgery at the Department of Orthopedic Surgery of Královské Vinohrady University Hospital in Prague (for more information see **Table 1**). Muscle cells were obtained by open technique during surgery. Patients more than 18 years of age, who were given non-propofol anesthesia (e.g. midazolam, etomidate), were eligible for the study. Patients receiving propofol during surgery as well as patients with history of known mitochondrial disorders were excluded. In addition, for [1-^{14}C] palmitate experiments, we obtained vastus lateralis samples under local anesthesia from five healthy volunteers by needle biopsy technique (Bergström technique)[145] in the Department of Pharmaceutical Biosciences at the University of Oslo. This part of study was performed in cooperation with laboratory group of professor Arild Rustan from University of Oslo. The study protocols were approved by respective research ethics boards in both institutions. All patients provided a prospective written informed consent.

15.2 Biopsy of m. vastus lateralis: open technique vs. Bergström technique

In our previous work, we compared two techniques of biopsy of musculus vastus lateralis obtained from orthopaedic patients[146]. During the study, the surgeon was asked to gain two muscle samples from the same subject (n=6)[146]. When vastus lateralis muscle was exposed during the surgery, one sample was taken by open technique using a scalpel or scissors and the second sample from the same muscle using 5 mm Bergström needle attached to a suction catheter[146]. The surgeon involved in the study was trained in the use of Bergström needle. Further processing of both samples was identical. In that study, we prepared muscle tissue homogenates and, after that, we analyzed global mitochondrial parameters in both groups[146]. We did not find any significant differences in mitochondrial functional indices between needle and open biopsy techniques in human skeletal muscle homogenates[146]. Therefore, we believe that different technique of biopsy had no impact on mitochondrial function in our experiments with propofol performed on cell culture.

Patient	Sex	Age	Height [cm]	Weight [kg]	BMI	Medical history
1	F	72	165	83	30.5	OA, hypercholesterolemia
2	F	72	172	83	28.1	OA, hypertension, hypercholesterolemia, hypothyreosis
3	F	70	164	64	23.8	OA, hypercholesterolemia, spondylosis, spondyloarthrosis, nephrolithiasis
4	F	77	150	86	38.2	OA, hypertension, hypothyreosis
5	F	67	162	78	29.7	OA, hypertension, ischemic heart disease, Parkinson's disease
6	M	60	180	79	24.4	OA, hypothyreosis, diabetes mellitus, trombofilia
7	F	73	168	83	29.4	OA, hypertension, diabetes mellitus
8	F	71	171	103	35.2	OA, hypertension, hypothyreosis, ischemic heart disease
9	F	80	175	78	25.5	NOF#, hypertension, chronic ischemic heart disease
10	M	73	172	86	29.1	NOF#, hypertension, diabetes mellitus, Parkinson disease
11	F	67	169	88	30.8	OA, hypothyreosis, obesity, hypersomnia
12	M	80	174	60	19.8	hypertension, OA - reoperation after hip replacement surgery
13	F	59	160	85	33.2	NOF#, hypertension
14	F	66	158	50	20.0	NOF#, hypertension, dyslipidemia, bronchial asthma
15	F	80	158	60	24.0	OA, hypertension, paroxysmal atrial fibrillation, chronic ischemic heart disease, chronic renal insufficiency, dyslipidemia
16	M	60	178	80	25.3	NOF#, hypertension, anxiety-depressive disorder, diabetes mellitus, ischemic heart disease, chronic renal insufficiency
17	F	82	160	60	23.4	OA, hypertension
18	F	77	166	87	31.6	OA, arterial hypertension, rheumatoid arthritis, hypothyreosis, dyslipidemia
19	F	71	176	80	25.8	NOF#, hypertension, hyperlipidemia

20	F	68	180	118	36.4	OA, hypertension, obesity, hyperlipidemia, hypothyreosis
21	F	83	153	80	34.2	OA, hypertension, chronic kidney disease, dyslipidemia, rheumatoid arthritis
22	M	61	178	110	34.7	OA - reoperation after hip replacement surgery, hypertension, dyslipidemia
23	F	84	154	80	33.7	NOF#, OA, hypertension, ischemic heart disease, glaucoma
24	M	80	171	66	22.6	OA, ischemic heart disease, atrial fibrillation, chronic kidney disease, hypertension, hyperlipidemia
25	F	72	158	64	25.6	OA, thyroiditis
26	M	72	181	80	24.4	OA, hypertension
27	F	76	158	73	29.2	OA, genu valgum, diabetes mellitus, hypertension, hyperlipidemia
28	F	68	166	82	29.8	OA, osteoporosis, dyslipidemia, chronic back pain, insomnia
29	F	67	162	74	28.2	OA
30	M	65	178	94	29.7	OA, hyperlipidemia

Table 1. Detailed characteristics of study subjects on biopsy day. OA = osteoarthritis of the hip, NOF# = neck of femur fracture. Krajčová et al., 2017[147].

15.3 Transport of muscle samples

At least~ 150 mg of skeletal muscle tissue was used for isolation of satellite cells according to protocol of Thompson et al.[148]. Immediately after biopsy, muscle sample was inserted into 50 mL falcon tube with pre-cold "Transport Medium" which consisted of Dulbecco's Modified Eagle's Medium with 5.56 mM glucose, 1 mM pyruvate, 3.7 mM glutamine and phenol red (Thermo Fisher Scientific, Inc., MA, USA). The medium was supplemented with antibiotics (1% solution of 100 U/mL penicillin and 100 µg/mL streptomycin) and antimycotics (0.1% fungizone) to prevent contamination of cells. Biopsy sample was then transferred from operating room to the laboratory in falcon tube with Transport Medium placed on ice.

15.4 Cell culture isolation and cultivation of myoblasts

Satellite cells were subsequently isolated and cultured as previously described[149]. Firstly, skeletal muscle tissue was transferred to Petri dish and weighted on analytical scale. After that, connective tissue, fat and vessels were removed under microscope with forceps and scissors as much as possible. Muscle tissue (150-250 mg) was then transferred into new Petri dish with fresh and sterile "Transport Medium" placed in laminar box. Sterile forceps and scissors were used for other steps of isolation procedure. Muscle tissue was firstly carefully minced with scissors into fine fragments at room temperature. Medium with floating tissue fragments was then pipetted from Petri dish into 50 mL falcon tube and diluted with Hank's balanced salt solution to obtain large volume. Skeletal muscle fragments were then centrifuged (350 xg, 25°C) for 5 minutes. After that, supernatant was cautiously discarded with vacuum aspirator, pellet with tissue fragments was rinsed with colourless Hank's balanced salt solution and centrifuged again. The step was repeated 2-3 times until the colour of solution was clear. After last centrifugation, supernatant was aspirated, and 0.25% Trypsin/0.68% Collagenase solution was added to the pellet with fragments. Cells were subsequently dissociated by incubation in the solution in a shaking water bath at 37°C for 30 minutes. Fetal bovine serum containing protease inhibitors (α_1-antitrypsin, α_2-macroglobulin) was then added to stop dissociation by inhibition of trypsin activity. Next step for isolation of skeletal muscle cells was pre-coating of all dissociated cells on uncoated Petri dish as non-coated surface is preferentially used for adhesion by fibroblasts cells, in comparison with skeletal muscle-derived cells which prefer to growth on collagen or gelatine-coated surface. Therefore, dissociated cells were pre-plated in pre-warmed "Growth Medium" consisting of Dulbecco's Modified Eagle's Medium supplemented with 15% fetal bovine serum, 5.56 mM glucose, 1 mM pyruvate, 1% solution of 100 U/mL penicillin and 100 µg/mL streptomycin, 0.05 µg/mL fungizone, 0.4 µg/mL dexamethasone, 0.5 mM L-glutamine on uncoated Petri dish at 37°C in the atmosphere of 5% CO_2 for 60 minutes to remove fibroblasts. Gelatine-coated flasks were simultaneously prepared for attachment and growth of myoblasts. Bottom of flasks was coated by a small amount of liquid gelatine solution (1-2 ml per 25 cm^2 flask), which was then closed and incubated in 37°C in 5% CO_2. After 30 minutes of incubation, gelatine was removed by aspirator and opened flasks with unscrewed lid were left to dry in sterile laminar box at room temperature. After pre-plating on uncoated Petri dishes, muscle fragments were subsequently carefully transferred into gelatine-coated flasks and cultured in "Growth Medium" at 37 °C in a humidified atmosphere of 5 % CO2. After 24 hours, 10 ng/mL of epidermal growth factor, 1 ng/mL of

fibroblast growth factor and 10 µg/mL of insulin were added. The "Growth Medium" was changed every 2 or 3 days.

Rate of proliferation. Human myoblasts are rapidly growing and dividing cells with the average doubling time of 24-36 hours[150]. In our previous study, we exposed human skeletal muscle cells to different glutamine levels in culture media (0; 100; 200; 300; 500; 5000 µM) and observed its effect on cell bioenergetics and proliferation[149] (see **Figure 7**). Surprisingly, supra-physiological concentrations of glutamine (5000 µM) as recommended by many protocols for *in vitro* cell cultures[151–154], including human myoblasts[155], did not bring any additional benefit in terms of myoblast proliferation[149]. Since cells had a high rate of proliferation at 500 µM glutamine, which is normal level in human plasma[149], we preferred to cultivate myoblasts in medium with this lower concentration in our further studies.

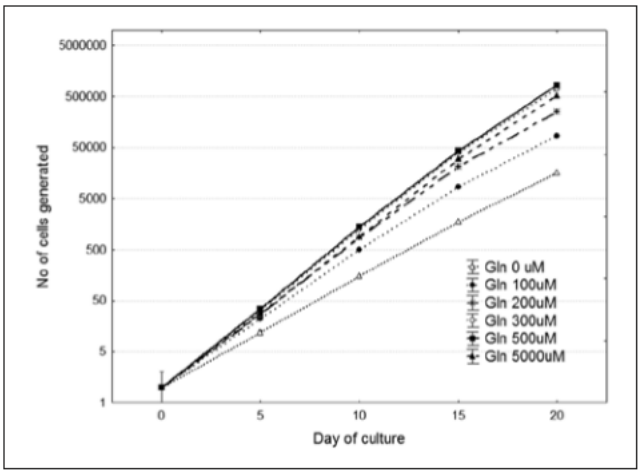

Figure 7. Proliferation rate of human myoblasts in relation to glutamine concentration in the media. Mean number of cells formed from a single cell at day 0. Krajčová et al., 2015[149].

The cell line is growing on the bottom of flasks or dishes in a monolayer. Growth of cell culture is typically divided into 3 phases (see **Figure 8**): initiation with short *lag phase*, when cells adapt to new conditions and don't grow; *log phase*, when growth of cells begins, and number of cells is increasing exponentially; *phase of plateau*, when cells slow down and stop to grow. In this stationary period, cells reach a high density and have no space to divide and grow because cell monolayer covers the most of the surface of flask bottom. At this time, cells switch into the phase of "contact inhibition"[156], when stop proliferating upon contact formation. Cell crowding, depletion of nutrients and accumulation of waste finally result in cell death[157].

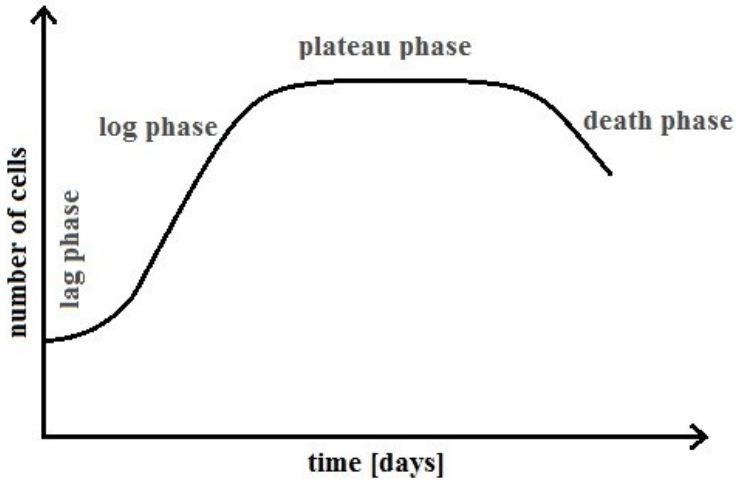

Figure 8. Simplified scheme of growth rate of cell culture.

Therefore, upon 80-90% confluency, cells were passaged and seeded into new gelatine-coated flasks, plates or Petri dishes. During subculturing, trypsin-EDTA solution was used as dissociation agent for release of myoblasts attached to the bottom of flask. Old culture medium was discarded without disturbing of cell monolayer prior to addition of trypsin-EDTA. Cells were subsequently rinsed with Dulbecco's Phosphate-Buffered Saline (DPBS) without calcium and magnesium (Thermo Fisher Scientific, Inc., MA, USA) to remove the rest of FBS which could inactivate trypsin. Small amount of trypsin was then added into flask with cells and incubated for 3-5 minutes in 37°C until it was possible to visualize under microscope that almost all cells were floating in trypsin solution. Growth medium supplemented with FBS was then added to stop trypsin activation. Cells were manually counted with haemocytometer and small aliquot of cell suspension was added to new gelatine-coated flask. Seeding density was at least 3500 cells/per cm^2 according to recommendation for human skeletal muscle cells[158]. During trypsinization, floating cells are of round shape. Few hours after cells settle down to the bottom of flask and attach gelatine-coated surface, they typically change the shape from round to fibrous and cylindrical (see **Figure 9, parts A** and **C**).

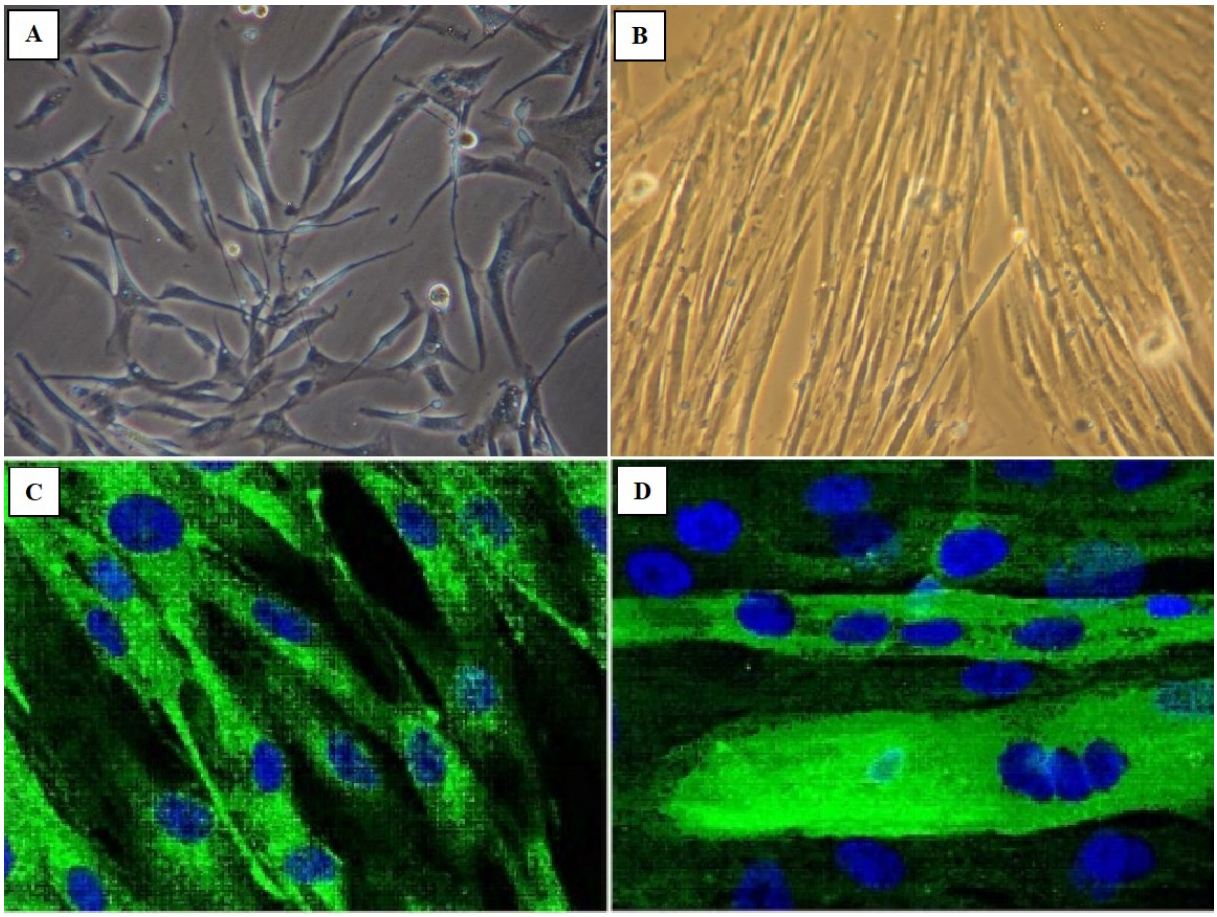

Figure 9. Cell culture of myoblasts and myotubes. Myoblasts in growth medium (A) and myotubes in differentiation medium (B) under binocular inverse microscope and appearance of myoblasts (C) and myotubes (D) stained for desmin (AB 907 rabbit anti–desmin polyclonal antibody [Millipore, Billerica, MA, USA]) under confocal microscopy. Krajčová et al., 2015[149].

15.5 Differentiation into myotubes

Myotubes differentiated from myoblasts were used for all experiments according to Aguer et al.[155] as they are generally considered an *in vitro* model of human skeletal muscle. When myoblasts reached ~ 90% confluency, "Growth Medium" was replaced by "Differentiation Medium" consisted of Dulbecco's Modified Eagle's Medium containing reduced concentration of serum to stop growth of cells and initiate the process of differentiation and fusion into myotubes. We used 2% horse serum in medium supplemented with 1% solution of penicillin and streptomycin, 25 mM Glucose and 10 µg/mL of insulin. After 7 days, cells were differentiated into multi-nuclear cylindrical myotubes (see **Figure 9, parts B** and **D**).

15.6 Indirect immunofluorescence and confocal microscopy

We used indirect immunofluorescence and confocal microscopy to confirm the purity of cell line[155]. We stained both myoblasts and myotubes. Cells (myoblasts) were grown on gelatine-coated coverslips until they reached 80% confluency. Firstly, they were fixed with 4% paraformaldehyde. The coverslips were then washed four times in DPBS for 5 min (placed on the orbital shaker; speed 80 rpmi) and subsequently permeabilized with 0.5 mL of 0.1 % saponin for 10 min. Cells were then washed three times again in PBS, labelled with primary antibody rabbit anti-desmin AB907 (dilution 1:50, 1:100, 1:200; Millipore, Billerica, MA, USA) and incubated in the covered humid chamber for 60 minutes. After that, cells coverslips were washed with solution of 0.05% Tween and DPBS and incubated with Goat Anti-Rabbit IgG H&L secondary antibody (Alexa Fluor® 488; ab150077; dilution 1:200; Abcam plc, Cambridge, UK) for 60 min at room temperature. Finally, the rinsed coverslips were fixed on glass slides using Prolong GOLD with DAPI (4´,6´-diamidino-2-phenylindole) and sealed with nail polish. Indirect immunofluorescence was performed using confocal microscopy LEICA TCS SP5 (see **Figure 9, part C**). In case of myotubes, the same procedure with all described steps was performed but cells were differentiated into myotubes (by incubation in Differentiation Medium for 7 days) on coverslips prior to staining (see **Figure 9, part D**).

15.7 Cell culture exposure to various conditions

After 7 days of differentiation, cells were cultivated in different conditions. Individual components of propofol infusion were tested on cells both separately and in combination. Each condition was performed in triplicates or tetraplicates.

15.7.1 Duration of exposure

Previous experiments performed on animal models tested propofol effect on mitochondria in high doses and after acute exposure[128–130,132]. Since the risk of PRIS increases with prolonged duration of propofol administration, we decided to test propofol on human skeletal muscle cells after long-term exposure. In addition, in our meta-analysis of 153 published PRIS case reports we found that some signs (e.g. rhabdomyolysis) occurred more frequently after propofol infusion longer than 96 hours. Therefore, we chose the duration of 4 days (= approximately 96 hours) for incubation of cells in propofol.

15.7.2 Myotubes exposed to different concentrations of propofol and Intralipid

Chemical structure of propofol is a strongly hydrophobic alkylphenol derivative 2,6-diisopropylphenol. Due to its high lipophilicity, 1% propofol is administered soluted in 10% intralipid emulsion. Therefore, we decided to test propofol agent as well as its lipid vehicle. The cells were cultured in four different concentrations (1, 2.5, 5 and 10 μg/mL) of propofol (2,6-diisopropylphenol; Sigma-Aldrich, USA) corresponding to its clinical concentrations in human plasma during propofol infusion (anaesthesia and sedation) or in medium containing 10% Intralipid (Intralipid® 10%; Fresenius Kabi, Germany). Control groups of cells were, in parallel, incubated either in fresh medium alone or ethanol which was used for propofol stock preparation (see below).

15.7.3 Myotubes exposed to different concentrations of propofol and non-esterified fatty acids (NEFA)

In human plasma, triglyceride levels are elevated after Intralipid infusion[159]. Triglycerides are subsequently hydrolyzed releasing free fatty acids[160,161]. Considering this Intralipid *in vivo* effect, we incubated cells also in NEFA mixture resembling fatty acids composition of Intralipid (with the ratio of fatty acids: 55% of linoleic acid, 27% of oleic acid and 10.5% of palmitic acid)[162] at the total concentration of 500 μM. In the experiments, cells were cultivated in two different concentrations of propofol alone (2.5 and 10 μg/mL). Another groups of cells were exposed to medium containing same concentrations of propofol (2.5 and 10 μg/mL) combined with NEFA mixture as well. Control groups of cells were cultured either in fresh medium or medium supplemented with NEFA.

15.8 Preparation of reagents for experiments

15.8.1 Preparation of propofol stock

Prior to all experiments, propofol stock was prepared. Commercially produced propofol is available as 1 or 2% (10 or 20 mg/mL) active agent 2,6-diisopropylphenol[37] dissolved in 10% Intralipid emulsion. For our experiments, 2,6-diisopropylphenol (Sigma-Aldrich, Corp., St. Louis, MO, USA) was used as an active agent. The stock was prepared fresh before every experiment or addition of propofol into medium to cell culture. Propofol was firstly diluted in purified ethanol and then in "Differentiation Medium" to obtain final concentration of 1 mg/per mL. After that, propofol stock was added into myotubes whilst diluted in their "Differentiation Medium" to obtain

lesser concentrations. Different aliquots of the stock were pipetted to cell culture medium to gain various levels of propofol, but we wanted to maintain the same concentration of ethanol vehicle in each sample at the same time. Therefore, we prepared a range of propofol stocks (1 mg 2,6-diisopropylphenol/mL), where ethanol amount was always adjusted to obtain the same final ethanol concentration when pipetted into the medium of every group of cells. By this way, we obtained cell groups incubated at the range of propofol concentrations, where each of them was diluted in the same amount of ethanol. Resulting ethanol concentration in cell culture was very low (< 0.01 %), which should not be toxic for cells. We confirmed this also by cell viability tests (see below).

15.8.2 Preparation of Intralipid vehicle and NEFA

10% Intralipid® emulsion (Fresenius Kabi, AG, Germany) was used for all experiments. NEFA (linoleic acid, oleic acid, palmitic acid) were prepared as previously described[163,164] at the total concentration of 500 µM. Concentration of fatty acids was calculated using commercial kit (NEFA Randox). Fatty acids were stored in -20°C for maximum of 2 months.

15.8.3 Preparation of substrates, uncouplers and inhibitors

All reagents were obtained from Sigma-Aldrich, Corp., St. Louis, MO, USA. Substrates (malate, glutamate, succinate, ascorbate and N,N,N',N'-tetramethyl-p-phenylenediamine [TMPD]) and adenosine diphosphate (ADP) were diluted in distilled water and stored in -20°C for maximum of 2 months. Duroquinol was prepared always fresh prior to experiment from its oxidized form duroquinone as previously described[165]. ATPase inhibitor oligomycin, uncoupler carbonyl cyanide-4-(trifluoromethoxy) phenylhydrazone (FCCP) and inhibitors antimycin A and rotenone were diluted in dimethyl sulfoxide (DMSO) and stored in -20°C. Inhibitor malonate was prepared by dilution in distilled water and stored in -20°C. Saponin for permeabilization of cells was prepared always fresh. pH of all reagents was adjusted to 7.4. All media were purchased from Thermo Fisher Scientific, Inc., MA, USA and stored in temperature up to + 4°C.

15.9 Experiments

Protocol design of the main experiments are illustrated at **Figure 10**.

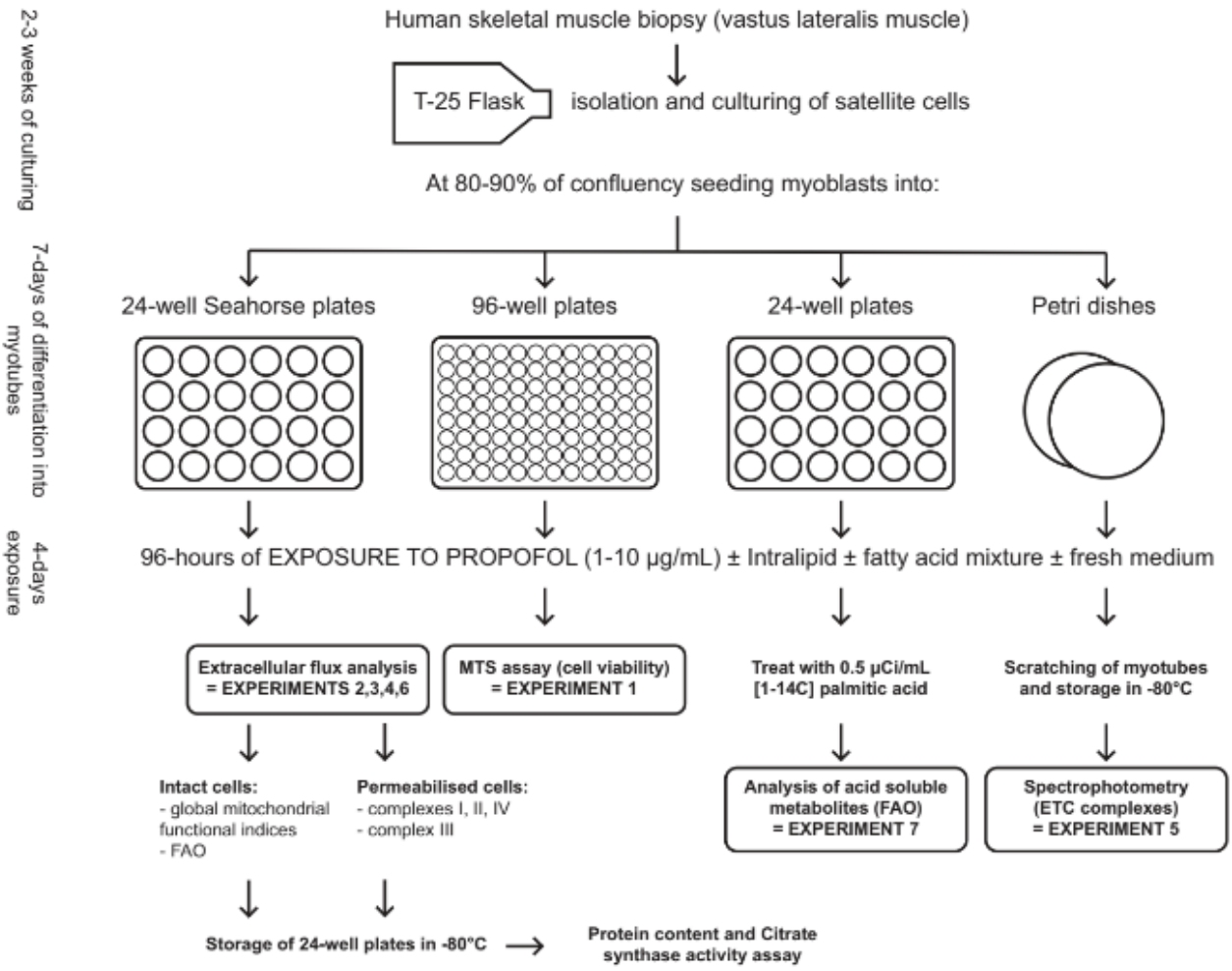

Figure 10. Overview of study design of all experiments. Note: ETC = Electron transfer chain, FAO = Fatty acid oxidation, MTS = 3-(4,5-dimethylthiazol-2-yl)-2,5-diphenyltetrazolium bromide. Krajčová et al., 2017[147].

15.9.1 Cell viability measurement

Firstly, we determined cell viability after exposure of cells to different propofol concentrations. Cell viability was analyzed by CellTiter 96® AQueous Non-Radioactive Cell Proliferation Assay (Promega, Corp., Madison, WI, USA) as previously described[166]. In literature, the assay is known as "MTS viability assay". It is a colorimetric method, which is routinely used for determining the number of viable cells. Assays are performed by adding a small amount of the Solution Reagent (containing a tetrazolium compound (MTS; [3-(4,5-dimethylthiazol-2-yl)-5-(3carboxymethoxyphenyl)-2-(4-sulfophenyl)-2H-tetrazolium, inner salt]) and an electron-coupling reagent (PES; phenazine ethosulfate) directly to wells with cells. Cells are then incubated for 1–4 hours in a humified atmosphere in 5% CO_2 incubator at 37°C and, after incubation, absorbance at 490 nm is measured using spectrophotometer. The quantity of formazan product as measured by the amount of 490 nm absorbance is directly proportional to the number of living cells in culture. In our experiments, prior to exposure, myoblasts were seeded at density of 1 x 10^4 cells per well on 96-well gelatine-coated microplate. After 24 hours of incubation in "Growth Medium", the cells reached confluence and medium was changed to "Differentiation Medium". Differentiated myotubes were treated for 96 hours with a range of propofol concentrations (1, 2.5, 5, 10, 25 and 50 μg/mL) diluted in ethanol, Intralipid vehicle (see **Figure 11, part A**) and mixture of non-esterified fatty acids at the total concentration of 500 μM (see **Figure 11, part B**) or the combination of propofol either with Intralipid or NEFA. Control cells were incubated either in the differentiation medium alone or medium containing 0.01 % ethanol. After exposure, MTS reagent with electron coupling agent phenazine methosulfate was added into each well of cells. After 2 hours of incubation, absorbance was recorded at 490 nm using spectrophotometer (TECAN Infinite PRO). Each experiment was performed in triplicates. This assay helped us to determine concentrations suitable for other experiments. Since the highest concentrations (25 and 50 μg/mL) of propofol range significantly decreased viability of cells (see Results), we excluded them from other experiments.

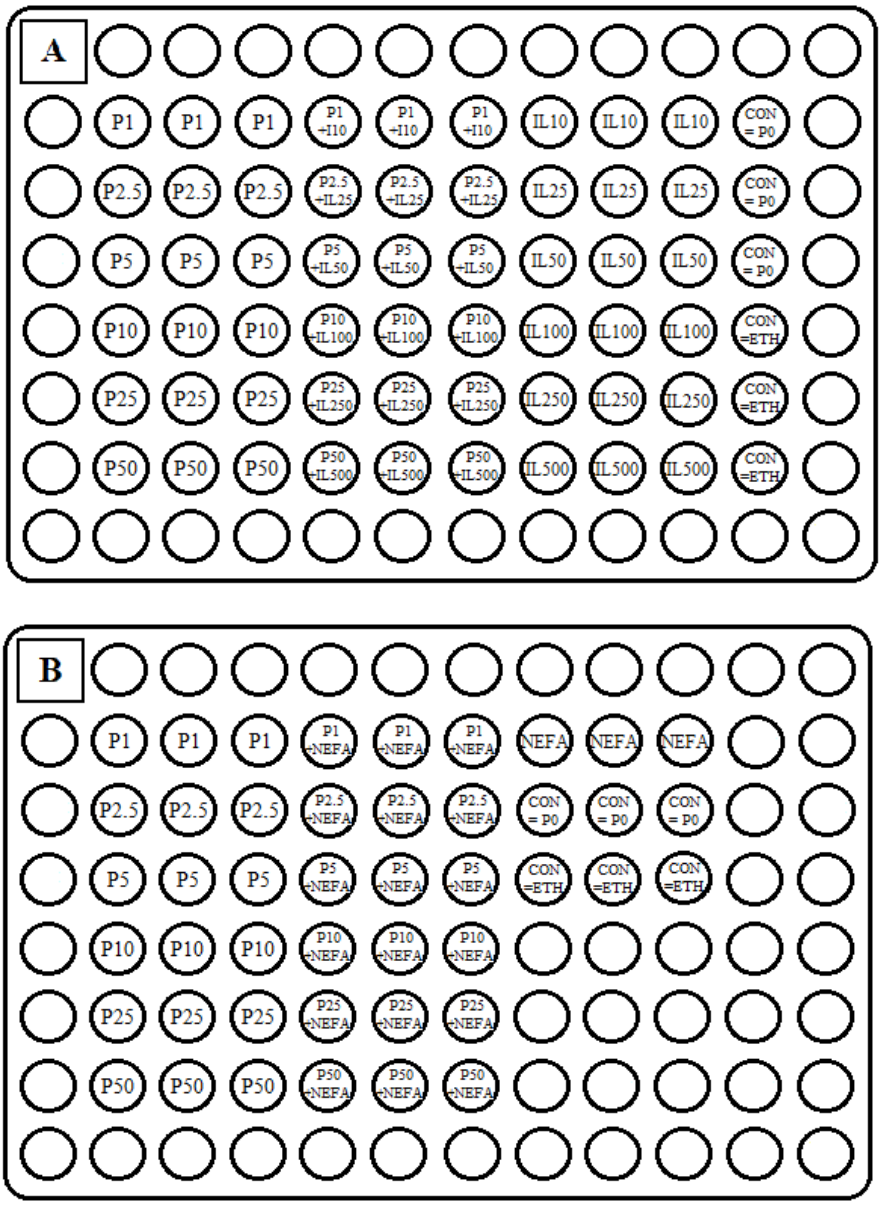

Figure 11. MTS viability assay on 96-well microplate. Myotubes (10 000 cells/per well) were exposed for 96 hours to various conditions. **Part A.** CON=P0: control = propofol at concentration 0 µg/mL (= differentiation medium alone); CON=ETH: control = 0.01% ethanol; P1-50: propofol at concentrations 1-50 µg/mL; IL10-500: Intralipid at concentrations 10-500 µg/mL; P1-50+IL10-500: mixture of propofol and Intralipid at concentrations 1-50 µg/mL and 10-500 µg/mL, resp.; **Part B.** NEFA: non-esterified fatty acids = fatty acid mixture resembling fatty acid composition of Intralipid = linoleate: oleate: palmitate in ratio 6:3:1 at the total concentration of 500 µM; P1-50+NEFA: mixture of propofol and non-esterified fatty acids at concentrations 1-50 µg/mL and 500 µM, respectively. Edge wells of microplate were left empty because of risk of evaporation.

15.9.2 Extracellular Flux Analysis

Bioenergetic profile of cells was studied using XF-24 Extracellular Flux Analyzer (Seahorse Bioscience [Agilent Technologies Inc., Santa Clara, CA, USA]).

Principle of XF-24 Extracellular Flux Analyzer. The method measures simultaneously the oxygen consumption rate (OCR) and extracellular acidification rate (ECAR) with oxygen-sensing fluorophores and pH sensors. The technology uses a piston to reversibly enclose a small volume (7 µl) above the microlayer of cells seeded in a 24-microwell plate (see **Figure 12**), monitoring oxygen uptake in that volume for 2–5 min and then raising the piston[167], allowing the bulk incubation medium (~1 ml) to re-equilibrate[168,169]. The amount of dissolved oxygen and free protons in microchamber is measured at baseline of experiment and after addition of up to 4 test agents. Any drug or tested compound can be added to cell culture to screen its effect on bioenergetics either prior to experiment (e.g. for a model of chronic exposure) or it can be injected as one of the 4 agents during the measurement process (rather a model for acute exposure). The dynamics of OCR enables to assess energy metabolism. Four wells are usually used as background control, with the remaining 20 wells for testing samples (cells or some cellular organelles) at different conditions in tri- to tetraplicates. XF-24 Extracellular Flux Analyzer can be used to monitor the respiration of cells and organelles that can be attached to the multi-well plate[167], either spontaneously in the case of cultured cells[168] (= attachment on the plastic bottom of wells or surface coated by e.g. fibronectin, collagen or gelatine according to specific cell line) or by centrifugation of isolated mitochondria[169] or synaptosomes[170]. A novel approach was developed for assessment of mitochondrial function in pancreatic islets[171].

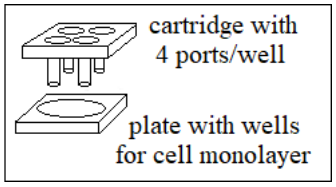

Figure 12. Simplified schema of XF-24 Extracellular Flux Analysis: cartridge with 4 ports for 4 compounds, firstly manually pipetted into ports, and then injected automatically during measurement into well with cell monolayer on 24-well microplate, which is settled under cartridge.

Seeding of cells in a 24-well plate. In our experiments, we used either intact or permeabilized cells. For seeding cells and measurement on XF-24 Extracellular Flux Analyzer, we used protocol previously described by our group[149]. In this study in preliminary experiments, we determined a suitable number of cells seeded in each well of microplate. We tried to achieve a sufficient levels of oxygen consumption rate (reflecting adequate and clear response to injected agents) and to avoid a rapid depletion of oxygen concentration at the same time. We tried

concentrations between 20 000 and 75 000 cells/per well, as this is usual for most of cell lines. According to the results, we chose the number of density for 30 000 cells/per well[149].

Prior to exposure, myoblasts were seeded at the density of 30 x 10^4 cells per well overnight on gelatine-coated 24-well XF-24 V7 cell culture microplates (Seahorse Bioscience [Agilent Technologies Inc., Santa Clara, CA, USA]). During the seeding, 30 000 cells were seeded per well in volume of 100 µL of "Growth Medium". After 60 minutes incubation in 5% CO_2 atmosphere, cells were sufficiently attached to gelatine-coated surface and 150 µl of "Growth Medium" was added to each well to get the final volume of 0.25 mL. These steps enabled cells to evenly cover and spread on the bottom surface of the well preventing their accumulation in the edge of the well. Cells were seeded overnight and reached the confluency of~ 80-90 %. Next day, "Growth Medium" was switched into "Differentiation Medium". On plate, cells were divided into 6 groups and various experimental conditions were formed. 20 wells were used for testing cells at different propofol concentrations (0, 1, 2.5, 5 and 10 µg/mL) and controls: fresh medium and either ethanol or Intralipid in tri- or tetraplicates (see **Figure 13, part A**). Each tested group with propofol contained the different concentration of 2,6-diisopropylphenol, but the same amount of ethanol (0.01%).

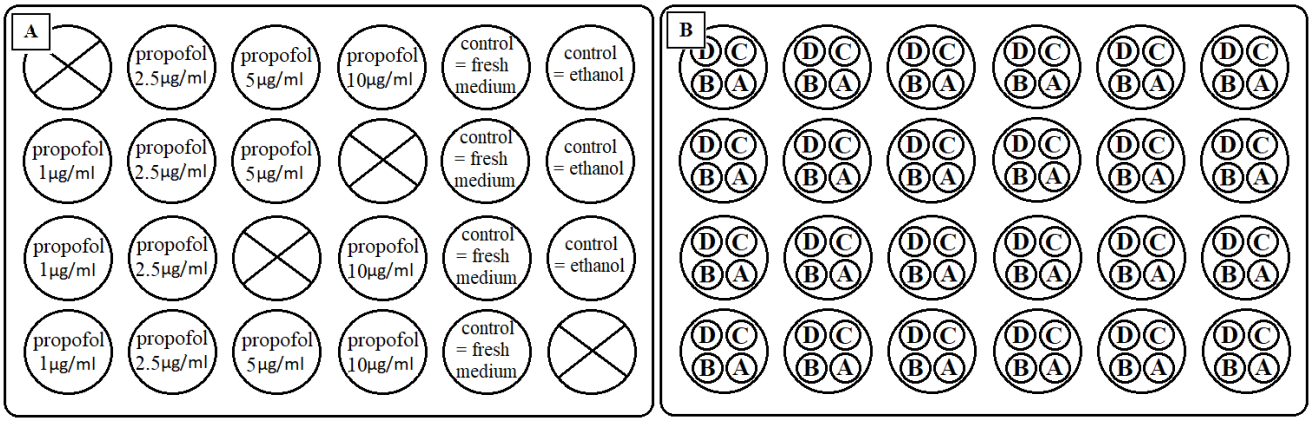

Figure 13. Part A. 24-well microplate with cells. Myotubes (30 000 cells/per well) were exposed to various conditions. 4 groups represent myotubes incubated in 4 different propofol concentrations (1, 2.5, 5 and 10 µg/mL). Control groups were defined as cells cultivated in fresh medium alone without propofol (0 µg/mL). The last tested group was either intralipid vehicle (100 µg/mL) or 0.01% ethanol. Group of 4 wells on plate ⊗ represent background control (=wells where cells were not seeded). **Part B. "Seahorse" cartridge plate.** Each well has 4 ports: A, B, C, D. Into each port, a compound (substrate/uncoupler/inhibitor) is pipetted prior to measurement. During measurement, compounds are gradually automatically injected in time slots.

Preparation a day before the Experiment. Seahorse cartridge was hydrated with XF Calibrant and incubated in humified non-CO_2 37°C incubator overnight according to manufacturer instructions[172]. The temperature in XF-24 Extracellular Analyzer was settled down to 37°C and kept during the whole experiment.

Preparation during a day of the Experiment. Cells seeded on 24-well microplate were checked under a microscope before measurement. The cells were then carefully rinsed with pre-warmed DPBS and XF Assay Medium (Seahorse Bioscience [Agilent Technologies Inc., Santa Clara, CA, USA]) with 4 mM Glucose, 1 mM pyruvate and 2 mM Glutamine (pH of medium was adjusted to 7.4 at temperature of 37°C). After that, 500 µL of XF Assay Medium was pipetted to each well and cells were pre-incubated in the incubator without 5% CO_2 at temperature 37°C, whilst all the substrates, uncouplers and inhibitors were pipetted to "Seahorse" cartridge plate (see **Figure 13, part B**), which was immediately inserted into Extracelular Flux Analyzer. After calibration, 24-well microplate with cells was inserted into the machine (below the level of cartridge, see **Figure 12**) and experiment was initiated.

In our study, we assessed global mitochondrial parameters, respiration linked to individual complexes and fatty acid oxidation:

A. Global mitochondrial functional parameters

In the first phase of experiment, we evaluated main components of mitochondrial function in intact cells (see **Figure 14**): basal respiration, ATP turnover, proton leak, maximum respiratory capacity and non-mitochondrial respiration.

Basal respiration is the state in initial phase of experiment, when cells have only endogenous substrates, which are oxidized and slowly exhausted, but no exogenous substrates or ADP is added to stimulate oxygen consumption[173]. After oxidation of endogenous substrates, only non-mitochondrial respiration remains[173]. *Non-mitochondrial respiration* is based on activity of non-mitochondrial oxygen consuming enzymes. Some cell lines, e.g. macrophages, have highly activated non-mitochondrial NADPH oxidases[167]. Most other cells have low but significant non-mitochondrial oxygen consumption, around 10% of total, caused by different desaturase and detoxification enzymes[167]. Mitochondrial respiration is assumed to be constant[167]. Other states are usually corrected for non-mitochondrial respiration[174]. *ATP turnover.* Since oxidative phosphorylation is linked with respiration, the rate of mitochondrial ATP synthesis is determined from the decrease in respiration by inhibiting the ATP synthase with ATPase inhibitor

oligomycin[167]. *Proton leak* across the mitochondrial membrane can be directly measured after enzymatic inhibition of the phosphorylation system[167]. Leak respiration is generated by flux of protons along the electrochemical proton gradient across the inner mitochondrial membrane[175] and represents a dissipative component of respiration which is not available for performing biochemical work and thus related to heat production[176]. A large increase may mean that the mitochondria are severely damaged (uncoupled)[167]. *Maximum respiratory capacity* is measured as oxygen consumption in the noncoupled state at optimum uncoupler concentration[177]. This optimum concentration is obtained by stepwise titration of an established protonophore to induce maximum oxygen flux[177]. Uncoupler effect leads to proton leakage through the inner mitochondrial membrane and allows electron transport chain to work in its maximum rate.

In our experiment, basal respiration was measured at the start of measurement (*phase 1,* see **Figure 14**)[149]. Subsequently, we used the sequence of 3 added agents to test global mitochondrial indices: an ATPase inhibitor oligomycin (*phase 2*), followed by an inner membrane uncoupler, FCCP (carbonyl cyanide-4-[trifluoromethoxy]phenylhydrazone, *phase 3*). Finally, we blocked the respiratory chain complex III with Antimycin A (*phase 4*). Oxygen consumption after exposure to Antimycin A is considered non-mitochondrial (see **Figure 14**). Basal OCR was calculated as OCR *Phase 1* – OCR *Phase 4*. When comparing OCR before and after exposure, the absolute cell number is irrelevant since the same population of cells is compared. Therefore, most parameters of energy metabolism were expressed as a percentage of baseline value. ATP turnover was calculated as 100*(OCR *Phase 1* – OCR *Phase 2*)/Basal OCR [%]. Leak through the inner mitochondrial membrane was calculated as 100*(OCR *Phase 2* – OCR *Phase 4*)/Basal OCR [%]. By analogy, respiratory chain capacity (or maximum respiration) was calculated as 100*(OCR *Phase 3* – OCR *Phase 4*)/Basal OCR. From obtained data from the experiment, we determined extracellular acidification rate, which relates to lactate production and is used as a measure of the rate of anaerobic glycolysis[167].

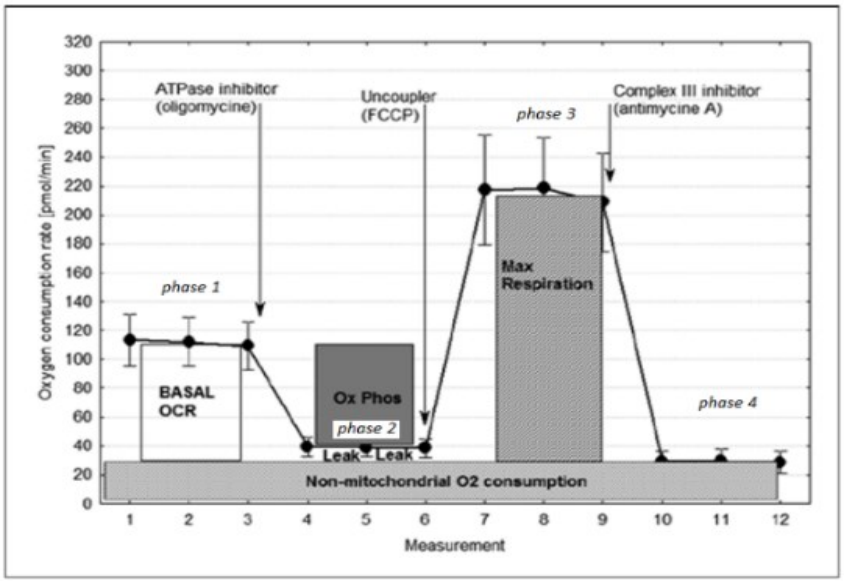

Figure 14. The principle of Extracellular Flux Analysis: basic experimental design ("stress test") for assessment of global mitochondrial parameters. FCCP, carbonyl cyanide-4-(trifluoromethoxy)phenylhydrazone; OCR, oxygen consumption rate; Ox Phos, oxidative phosphorylation. Krajčová et al., 2015[149].

Optimizing the XF-24 Extracellular Flux Analysis protocol for human myoblasts. Titration of uncouplers and inhibitors. Since it is critical to titrate the ATPase inhibitor and the uncoupler in each new cell line and condition[167], we firstly had to determine optimum concentrations of these agents. We performed our experiment with propofol-exposed cells according to our previous study, where we had compared the effects of 0.75, 1, and 1.5 µM oligomycin achieving maximum inhibition of ATPase with 1 µM[149]. This concentration was therefore used for the rest of the experiments. Similarly, we had compared uncoupling effects of 0.5, 1, and 2 µM FCCP and achieved maximum OCR with 1 µM[149]. Finally, to verify the ability of 4 µm Antimycin A to inhibit the respiratory chain, we had performed an experiment in which we added 0.6 M KCN (complex IV inhibitor) after Antimycin A. No additional decrease in OCR was seen with the addition of cyanide[149]. *Duration of measurement.* We have an experience that prolonged duration on Extracellular Flux Analyzer can have a negative impact on some cell lines, as we were able to observe their minimal response to oligomycin after long period. We hypothesize that this could probably mean that mitochondria in cells are uncoupled after too long period staying inside the machine. In this case, it is needed to shorten the time of measurement. In our cell line, we determined the safe duration of experiment for 240 minutes. In the pilot study, we checked that in control wells (which were left without addition of inhibitors during measurement), OCR

remained stable during the whole period. Moreover, oligomycin-induced decrease of OCR (in wells with injection of agents) was sufficient.

Design of protocol on XF-24 Extracellular Flux Analyzer. In this experiment, we did not use port D, as we added only 3 agents in ports A, B and C. Baseline OCR was measured in 3 cycles (3 minutes mixing, 2 minutes waiting and 2 minutes measuring). Then the 3 cycles (3 minutes mixing, 2 minutes waiting and 3 minutes measuring) were repeated after adding oligomycin (1 μM), FCCP (1 μM) and Antimycin A (4 μM).

B. Respiration linked to individual complexes of electron transfer chain

Changes in respiration may correlate to altered mitochondrial substrate oxidation. Therefore, examining the effect of specific substrates for individual complexes of respiratory chain is one approach to determine the mechanism underlying the observed differences[178]. Since the basic measurement in our study showed us changes between mitochondrial function of propofol-treated cells and control cells (see Results), we continued to test electron transfer system in more detail and measured the respiration linked to individual complexes (C I, II, III and IV) of electron transport chain. Energy metabolism was studied under both ATP-coupled and uncoupled respiration.

Seeding of cells in 24-well plate. In this experiment studying the function of respiratory complexes, we used the same design of cell exposure as in previous one (described above for assessment of global mitochondrial parameters; see **Figure 13, part A**). Similarly, differentiated cells were exposed to four different concentrations of propofol (1, 2.5, 5 and 10 μg/mL), control groups were defined as cells cultivated in fresh "Differentiation medium" without propofol (0 μg/mL) and the last tested group was exposed to either Intralipid (100 μg/mL) or 0.01% ethanol.

Preparation of cells for experiment including permeabilization step. We used the same protocol as mentioned above. The differences in protocol design were performed at the day of experiment on Extracellular Flux Analyzer. It is needed to add ADP and substrates with high molecular weight for testing individual complexes of respiratory chain. These macromolecules cannot freely cross cell membranes. Therefore, it is necessary to permeabilize cell membrane. This can be achieved by mechanical cell disruption or chemical permeabilization using detergents[179]. Usually, cell lines are in an *in vitro* studies permeabilized with classical chemical detergents: saponin, digitonin or novel agent recombinant perfringolysin O (rPFO; XF PMP reagent; Seahorse Bioscience [Agilent Technologies Inc., Santa Clara, CA, USA])[178]. For our experiments, we used

saponin detergent, which interacts with membrane cholesterol, selectively removing it and leaving holes in the membrane[180]. Cholesterol-containing membranes (including cell membrane and membranes of endoplasmic reticulum, the Golgi apparatus or lysosomes) are readily permeabilised by saponin whilst membranes with lack of cholesterol (inner nuclear membrane and mitochondrial membrane) remain intact[181]. Saponin is a cholesterol-like sugar-containing compound produced by several plants, which has a large lipophilic region that inserts into membranes and interacts with steroids, phospholipids and proteins, disrupting cholesterol-phospholipid interactions to create ring-shaped complexes with pores of 12-15 nm diameter, which allows the entry of macromolecules[181]. According to electron microscopy, the rest of plasma membrane is relatively intact[181]. In preliminary experiments, we optimized permeabilization protocol for human skeletal muscle cells, because this process is highly dependent on reagent concentration, exposure time and temperature and can differ in each cell line. Saponin concentration must be sufficient to enable macromolecules entry across the membrane inside the cell, but it should not be too high because of risk of mitochondrial and cell damage. Damage of mitochondria by saponin is usually evident only at concentrations of >25 μg/mL saponin[182]. For our experiments on human myotubes, we observed that concentration of 5 μg/mL saponin with 4-5 minutes of incubation was effective and safe.

Preparation during a day of Experiment. All media and solutions were prepared fresh shortly before experiment. For measurement with permeabilized muscle cells, we used Mitochondrial Assay Solution (MAS) instead of XF Assay Medium according to the manufacturer recommendations[183]. MAS is a non-ionic mannitol and sucrose-based buffer used in permeabilization assays[183]. Our solution consisted of 220 mM mannitol, 70 mM sucrose, 10 mM KH_2PO_4, 5 mM $MgCl_2$, 2 mM HEPES, 1 mM bovine serum albumin (BSA), EGTA, 0.2% BSA and distilled water. BSA was included into the MAS buffer, because it is essential for maintaining well-coupled mitochondria following permeabilization[182]. We made sure that all BSA was properly dissolved, then warmed MAS to 37°C and adjusted pH to 7.4. To avoid a prolonged exposure and contact of cells to MAS which could be harmful for cells[184], we needed to shorten the length of both preparation and measurement as much as possible. In addition, shortened measurement helped us to prevent rapid burst of ADP. Therefore, we pipetted all substrates and inhibitors into 4 ports of seahorse cartridge, inserted the cartridge into the machine and initiated calibration. Whilst the process of calibration (~ 25 minutes) was running, we were preparing plate with cells. Firstly, we gently aspirated the old "Differentiation Medium", washed cells with pre-warmed MAS alone and incubated them in MAS with 5 μg/mL saponin for 4-5 minutes in air at room

temperature. During the process we were careful not to touch the plate. After that, we carefully discarded the medium with saponin and added pre-warmed MAS supplemented with 4 mM ADP and substrates for complex I: 2.5 mM malate and 15 mM glutamate (pH of MAS supplemented with substrates was again checked and adjusted to 7.4). Immediately after the change of medium and pipetting MAS, plate was inserted to calibrated XF-24 Extracellular Flux Analyzer. The whole process of cell preparation for measurement did not take more than 20-25 minutes.

Mitochondrial indices obtained during measurement on permeabilized cells. In our first experiments, we analysed main mitochondrial functions on experimentally uncoupled respiration in intact cells. FCCP and inhibitors can freely cross the cell membrane and get into mitochondria in comparison with macromolecules as ADP or substrates. In permeabilised cells, we used both uncoupled and coupled respiration.

During oxidative phosphorylation (OXPHOS), metabolites are oxidized donating reducing equivalents to coenzymes nicotinamide adenine dinucleotide (NAD^+) and flavin adenine dinucleotide (FAD) to generate NADH+H_2 and $FADH_2$[185]. After that, electrons enter the electron transport chain complexes in the mitochondrial inner membrane and pass down a decreasing energy potential gradient. The resulting energy release drives proton pumping across the inner mitochondrial membrane from the matrix to the intermembrane space by complexes I, III, and IV[185]. The electrochemical gradient, or proton motive force (Δp), that is established by proton pumping, then drives protons back into the mitochondrial matrix through the ATP synthase to generate ATP. Finally, electrons are transferred to complex IV, cytochrome c oxidase, and then donated to molecular oxygen leading to H_2O production[185]. In summary, oxidative phosphorylation is the oxidation of reduced fuel substrates by electron transfer to oxygen which is chemiosmotically *coupled* to the phosphorylation of ADP to ATP[186].

Uncoupling of oxidative phosphorylation means a loss of coupling between the rate of electron transport in the respiratory chain (respiration) and ATP production (phosphorylation) without affecting respiratory chain[187]. *Uncoupled* respiration, experimentally induced by addition of protonophore (e.g. FCCP), is a maximum electron flow in mitochondria without ATP formation and reflects the capacity of mitochondria to response to increased demand.

Respiratory states. In the first part, we simply described testing of the global mitochondrial parameters: basal respiration, proton leak, ATP production and maximum respiratory capacity. According to the classical work of Chance and Williams from 1955[188], we can describe the different conditions during experiment as several „respiratory states" for assessment of mitochondrial

functions. This can be useful particularly when assessing ADP-stimulated respiration. Oxygen consumption is measured at baseline in the presence of only inorganic phosphate (P_i) (= *State 1*)[173,182]. Substrates such as glutamate plus malate or succinate are then added to measure ADP-independent respiratory activity (= *State 2*)[182]. Addition of ADP is signed as *State 3* respiration, which is defined as the ADP -stimulated respiration in the presence of high ADP and P_i concentrations supported by a defined substrate or substrate combination at saturating oxygen levels. In this phase, addition of ADP leads to fast oxygen consumption rate and the formation of ATP. When ADP is depleted, respiration returns to rates similar to that of *State 2* (= *State 4*)[182]. *State 4* respiration is also induced by addition of ATPase inhibitor oligomycin[182] and represents LEAK respiration. An uncoupler may be added to mitochondria in *State 4* or in the absence of ADP (but in the presence of oxygen and fuel substrates), which leads to an increase of respiration to a rate equal to that in State 3 or higher. This state is used as *State 3u (uncoupled)* and represents noncoupled state of electron transfer capacity[189].

*Design of the first experiment: CI, II and IV-linked respiration (see **Figure 15**).* Cells were incubated in medium with 4 mM ADP and substrates for complex I (2.5 mM malate and 15 mM glutamate). OCR was immediately measured at baseline. During the experiment, we continued with injection of complex I-linked inhibitor (3 µM rotenone) followed by the substrate for complex II (10 mM succinate). After that, respiration was blocked with complex II-linked inhibitor (5 mM malonate). Finally, we added 10 mM ascorbate with 0.2 mM TMPD (N,N,N',N'-tetramethyl-p-phenylenediamine) to assess complex IV-linked respiration.

*Design of the second experiment: CIII-linked respiration (see **Figure 16**).* 15 mM glutamate, 2.5 mM malate and 10 mM succinate were added to the permeabilized cells prior to the start of assay. During the measurement, cells were initially uncoupled by FCCP and respiration was subsequently inhibited by complex I and II-linked inhibitors (3 µM rotenone plus 5 mM malonate). Complex III-linked respiration was measured as oxygen consumption rate after addition of 0.6 mM duroquinol, which was prepared from its oxidized form duroquinone (Sigma-Aldrich, Corp., St. Louis, MO, USA) as previously described[165]. In the last step, respiration was blocked by 4 µM Antimycin A.

Design of the third experiment: Correlation between the capacity of any of the respiratory complexes and ETC spare capacity. We measured respiration linked to individual complexes and global mitochondrial parameters (see **Figure 14**) in parallel from the same subject to determine a possible correlation between capacity of any of the respiratory complexes and ETC spare capacity.

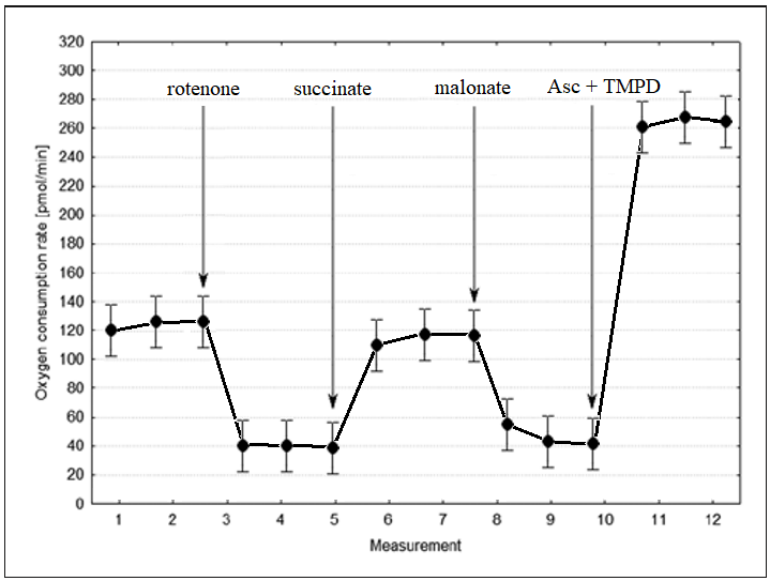

Figure 15. Extracellular Flux Analysis: measurement of complex I-, complex II- and complex IV-linked respiration (coupled respiration). Cells were incubated in medium supplemented with glutamate + malate as substrates for complex I and ADP. Reagents injected during the experiment: rotenone was used as complex I inhibitor, succinate as substrate for complex II, malonate as complex II inhibitor and, finally, ascorbate (Asc) with TMPD (N,N,N',N'-tetramethyl-p-phenylenediamine) as substrates for complex IV.

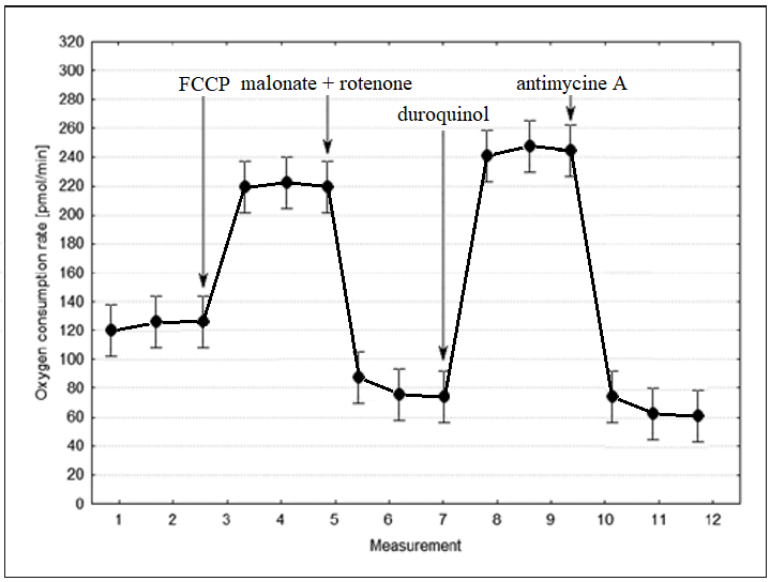

Figure 16. Extracellular Flux Analysis: measurement of complex III-linked respiration (uncoupled respiration). Cells were incubated in medium supplemented with glutamate + malate + succinate (substrates for complexes I and II). Reagents injected during the experiment: cells were uncoupled by addition of FCCP ([carbonyl cyanide-4-(trifluoromethoxy)phenylhydrazone]; uncoupled complex I and II respiration) and subsequently malonate + rotenone were added as inhibitors.

Then, duroquinol was injected as substrate for complex III. Finally, Antimycin A as complex III inhibitor was added.

Duration of measurement on Extracellular Flux Analyzer. As we previously mentioned, we tried to maximally shorten period of measurement to avoid prolong incubation of cells in MAS medium and, in case of coupled respiration, to prevent rapid exhausting of ADP. Baseline OCR was measured in 3 cycles (0.5 minute mixing, 0.5 minute waiting and 2 minutes measuring). Then the 3 cycles (0.5 minute mixing, 0.5 minute waiting and 2 minutes measuring) were repeated after injection of agents in ports A, B, C and D. The length of experiment was not longer than 70 minutes (including calibration and equilibration of cartridge plate and plate with cells resp.).

C. Fatty acid oxidation

It was hypothesized that propofol could have an impact on fatty acid oxidation[68,116]. In our experiment, we wanted to test possible impact of long-term incubation of both 2,6-diisopropylphenol and its vehicle in propofol infusion on skeletal muscle cell mitochondria. We tried to reflect the fact that after administration of intralipid infusion, it is *in vivo* hydrolysed releasing free fatty acids in human plasma[160,161]. Therefore, to investigate fatty acid metabolism we slightly modified a design of cells exposure to propofol before measurement on XF-24 Extracellular Flux Analyzer.

Seeding of cells and exposure to experimental conditions in 24-well plate before measurement. Prior to exposure, cells were cultivated as usual and differentiated to form myotubes for 7 days. After that, cells started to be exposed to various conditions for 96 hours. Two groups were exposed to propofol alone (2.5 and 10 μg/mL; see **Figure 17**). Another groups of cells were exposed to medium containing same concentrations of propofol (2.5 and 10 μg/mL) combined with NEFA, which were prepared to resemble fatty acid composition of Intralipid (with the ratio of fatty acids: 55% of linoleic acid, 27% of oleic acid and 10.5% of palmitic acid)[162] at the total concentration of 500 μM. Control groups of cells were cultured either in fresh "Differentiation medium" alone or NEFA mixture.

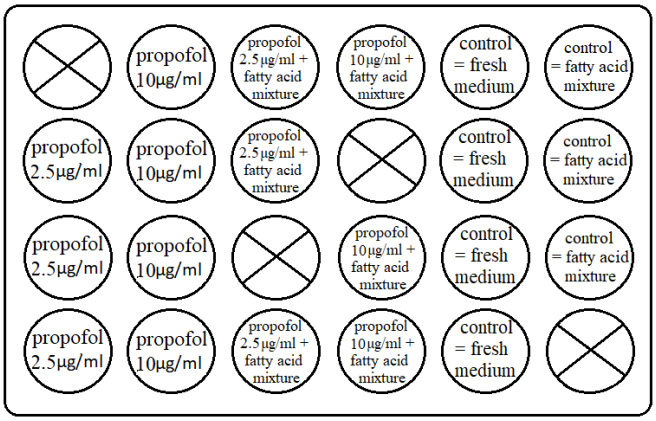

Figure 17. 24-well microplate with cells for FAO experiment. Myotubes (30 000 cells/per well) were exposed to various conditions. 2 groups represent myotubes incubated in 2 different propofol concentrations (2.5 and 10 µg/mL). Control groups were defined as cells cultivated in fresh "Differentiation medium" without propofol (0 µg/mL) or cells incubated in non-esterified fatty acids (NEFA) mixture (with the ratio of fatty acids: 55% of linoleic acid, 27% of oleic acid and 10.5% of palmitic acid). Last 2 groups were exposed to both propofol (2.5 and 10 µg/mL) and NEFA mixture.

Aim of this experiment was to test mitochondrial response to addition of fatty acids as substrates (by injection of sodium palmitate on Extracellular Flux Analyzer). We used palmitate as a standard long-chain fatty acid which enabled us to test whole pathway including both enzymes that are involved in fatty acid transport into mitochondria and enzymes that ensure fatty acid metabolism itself (see **Figure 27** in Discussion). We wanted to look at the differences in individual groups of cells and to compare myotubes exposed to 2,6-diisopropylphenol alone and myotubes incubated in propofol with propofol with NEFA mixture.

Fatty acid oxidation and carnitine transport. Long-chain fatty acids are transported through plasma membrane by fatty acid transporter CD36 and then activated by esterification to CoA-SH, which is catalysed by acyl-CoA synthetases[190]. For transport into mitochondria fatty acyl-CoA molecules need to be transported by carnitine through action of carnitine palmitoyltransferase-I (CPT-I). A carnitine/acyl-carnitine translocase (CACT) then shuttles acyl-carnitines into mitochondria, where carnitine palmitoyltransferase-II (CPT II) regenerates the acyl-CoA molecule which is then oxidized in process of fatty acid oxidation (β-oxidation)[190]. This multiple reaction process results in production of Acetyl-CoA, which serves as fuel for TCA cycle. In addition, the process generates also reducing equivalents $FADH_2$ and $NADH+H^+$, which are then

passed to Coenzyme Q, through electron transfer flavoprotein (ETF) dehydrogenase and to complex I, respectively[190].

For experiment, we therefore used non-permeabilised intact cells incubated in respiration medium supplemented with 0.5 mM carnitine.

Preparation during a day of Experiment. Prior to the experiment, we prepared KHB medium containing 111 mM NaCl, 4.7 mM KCl, 2 mM $MgSO_4$, 1.2 mM Na_2HPO_4 and distilled water according to manufacturer recommendations[191]. 2.5 mM Glucose and 0.5 mM carnitine were prepared fresh and added to KHB medium. The solution was pre-warmed to 37°C and pH was adjusted to pH 7.4. Cells were firstly checked under microscope and old medium was carefully discarded. After that, they were washed with pre-warmed KHB medium and then KHB was added to the cells. Plate with cells was inserted to humified non-CO_2 incubator for 50-60 minutes. Whilst cells were incubated, the seahorse cartridge was prepared as usual and 4 agents were pipetted to ports A, B, C and D. *Preparation of sodium palmitate.* Sodium palmitate was used as a substrate for fatty acid utilization and prepared as previously described[192]. Bovine Serum Albumin (BSA) was used as a carrier for insoluble palmitate, because palmitate conjugation to BSA creates an aqueous-soluble reagent that can be easily absorbed and utilized by cells. 1 mM sodium palmitate was prepared in 150 mM NaCl and 0.17 mM BSA in 150 mM NaCl. Sodium palmitate solution was heated to 70°C on a heated stir plate until its colour became clear, and then an equal volume of hot sodium palmitate was added to the BSA solution (the molar ratio between palmitate and BSA was 6:1). After that, the solution was stirred at 37°C for 1 hour and the pH was adjusted to 7.4. The stock of sodium palmitate was stored in -20°C for up to maximum of 2 months.

*Design of protocol on Extracellular Flux Analyzer (see **Figure 18**).* Firstly, intact myotubes were uncoupled by injection of 1 µM FCCP (port A) to achieve maximum respiration rate. Fatty acid oxidation was then measured as etomoxir-induced inhibition of oxygen consumption rate after repeatable addition of sodium palmitate (at the total concentration of 200 µM; ports B and C). 40 µM etomoxir was injected after that (port D). Baseline OCR was measured in 3 cycles (0.5 minute mixing, 0.5 minute waiting and 2 minutes measuring). Then the 3 cycles (2 minutes mixing, 2 minutes waiting and 3 minutes measuring) were repeated after injection of each agent.

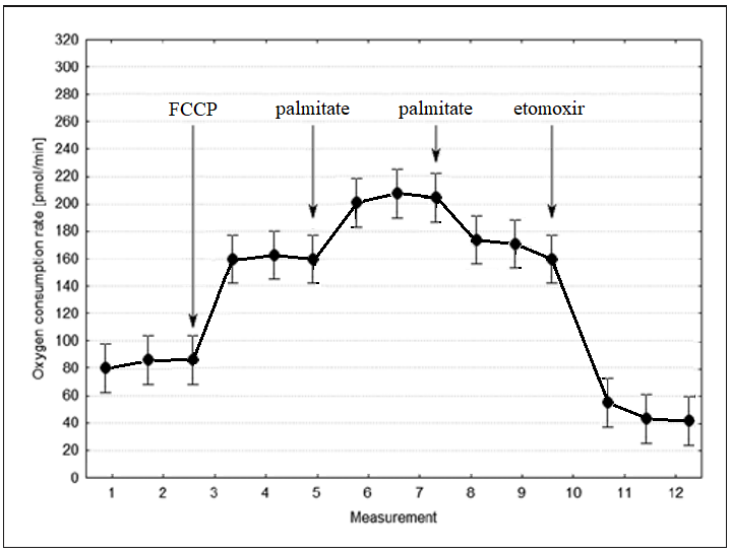

Figure 18. Extracellular Flux Analysis: measurement of fatty acid oxidation. Intact cells were incubated in KHB medium supplemented with 0.5 mM carnitine. Firstly, cells were uncoupled with FCCP (carbonyl cyanide-4-(trifluoromethoxy)phenylhydrazone). After that, sodium palmitate was repeatedly added as a substrate for FAO (at the total concentration of 200 µM). Fatty acid oxidation was then measured as etomoxir-induced inhibition of oxygen consumption rate.

15.9.3 Protein content and Citrate synthase activity

After each experiment performed on XF-24 Extracellular Flux Analyzer, cells were checked under microscope. The respiration medium was carefully discarded, and cells were washed with pre-cold PBS. Cell buffer lysis (150 µL/well) and protease inhibitor cocktail (2 µL/well) were added into each well with cells and plates were stored immediately at – 80°C for further analysis of Citrate synthase (CS) activity and protein content.

Citrate synthase is the initial enzyme of TCA cycle, which catalyses the reaction between acetyl-CoA and oxaloacetic acid to form citric acid. Citrate synthase is widely used as a marker of the mitochondrial density[165,193]. CS activity was analysed using CS Assay kit (Sigma-Aldrich, Corp., St. Louis, MO, USA) and measured according to manufacturer's instructions[194]. Briefly, we prepared all the solutions as recommended before this assay (Assay buffer with 200 mM Tris with 0.2% Triton, adjusted to pH 8; 10 mM 5,5'-Dithiobis-(2-nitrobenzoic acid) [DTNB]; 30 mM Acetyl-CoA and 10mM Oxaloacetate [OAA], prepared fresh at the day of assay). The 24-well plate was gradually thawed slowly shaking on ice, samples from the bottom were thoroughly harvested and transferred to small Eppendorf tubes and centrifuged for 10 000 xg, for 10 minutes at 4°C. After that, 100 µL of supernatant from each sample in Eppendorf tube was mixed with 86 µL of Assay buffer with addition of 2 µL of 10 mM DTNB and 2 µL of 30 mM Acetyl-CoA. Spectrophotometric Assay was then initiated by measuring absorbance at 412 nm to obtain baseline[194]. For spectrophotometry TECAN Infinite M200 Pro microplate reader was used. Subsequently, we added 10 µL of 10 mM OAA solution to each well at the same moment using multichannel pipette to initiate the reaction and measurement of absorbance at 412 nm was then repeated. The principle of reaction could be described as followed: hydrolysis of the thioester of acetyl-CoA resulted in the formation of CoA with a thiol group (CoA-SH)[194]. The thiol reacted with the DTNB in the reaction mixture to form 5-thio-2-nitrobenzoic acid (TNB)[194]. This yellow product (TNB) was then observed spectrophotometrically by measuring absorbance at 412 nm[194].

Reaction catalysed by Citrate synthase: Acetyl CoA + OAA → Citrate + CoA-SH + H^+ + H_2O

Colorimetric reaction: CoA-SH + DTNB → TNB + CoA-S-S-TNB

Protein content was determined using Bradford assay as described elsewhere[195].

15.9.4 Analysis of acid soluble metabolites

In 2016, we started to cooperate on this project with research team of professor Arild Rustan (School of Pharmacy, University of Oslo, Norway) as he offered us to perform analysis of acid soluble metabolites which is not possible to do at our faculty. We sent our Norwegian colleagues the frozen cell cultures, which had been previously used for our experiments and then stored in liquid nitrogen. Unfortunately, these cells could not be used for other techniques because of transport difficulties. After arrival to Norway, cells were not viable. Therefore, our Norwegian colleagues had to use skeletal muscle cells obtained from vastus lateralis biopsies from healthy volunteers in Norway (n = 5). The biopsy technique, which they used, was performed by Bergström needle[145]. All conditions including isolation, cultivation, differentiation and exposure of cells to propofol, were the same as ours. After 4 days of propofol treatment, the medium was completely removed before addition of 0.5 µCi/mL [1-^{14}C] palmitic acid (PerkinElmer NEN®, Boston, MA, USA), given in DMEM-Glutamax™ (low glucose, 5 mmol/L) with L-carnitine (1 mmol/L) and BSA (40 µmol/L). The cells were incubated at 37°C for 4 hours before the incubation media were collected. Oxidation of [1-^{14}C] palmitic acid to acid-soluble metabolites (ASMs) was measured by acid precipitation of the incubation media. ASMs reflect incomplete fatty acid oxidation in the mitochondria and consist mainly of tricarboxylic acid cycle metabolites. In brief, 100 µL of the incubation media were added 30 µL BSA (6%) and 300 µL $HClO_4$ (1 mol/L) and centrifuged at 10.000 rpm / 4°C / 10 min. Then 200 µL of the supernatant was counted by liquid scintillation (Packard Tri-Carb 1900 TR).

15.9.5 Spectrophotometric analysis of individual activities of respiratory complexes and octanoyl-dehydrogenase activity

After 96-hours incubation in various conditions (medium with propofol concentration of 2.5 and 10 µg/mL vs. “Differentiation medium” [=0 µg/mL propofol] for control group), myotubes were washed by phosphate buffer saline, harvested from Petri dishes using cell scraper (Biologix) and then centrifuged at 350 xg for 10 minutes at room temperature. The supernatant was discarded, and the pellet was frozen and stored in -80 °C for further spectrophotometric analysis. When all samples were collected, the frozen pellets were thawed in the “Homogenisation Medium” (10 mM Tris-Cl, 10 mM KCl, 150 µM $MgCl_2$, 250 mM sucrose, pH 6.5) and mechanically disrupted with a 2 mL glass tight-fitting Dounce homogenizer (Wheaton type B). The homogenate was then exposed to 3 further cycles of rapid freezing thawing. The homogenate was then

centrifuged at 500 xg at 4 °C and the supernatant was taken for assays. The activities of enzymes were assayed spectrophotometrically using TECAN Infinite M200 Pro microplate reader. Complex I, II, III and IV activities were performed as described in detail elsewhere[196]. In brief, frozen samples were thawed and homogenized and then exposed to 3 further cycles of rapid freezing thawing. *Complex I* assay was performed in the assay mixture consisting of 25 mM potassium phosphate, 3.5 g/L BSA, 2 mM ethylenediaminetetraacetic acid (EDTA), 60 µM DCIP, 70 µM decylubiquinone, 1 µM Antimycin A and 0.2 mM reduced nicotinamide adenine dinucleotide (NADH), pH 7.8[196]. Changes in absorbance were followed at 600 nm. Rotenone sensitive activity was calculated by subtracting the activity of wells with 10 µM rotenone. *Complex II* activity was measured in the assay mixture composed of 80 mM potassium phosphate, 1 g/l BSA, 100 mM EDTA, 10 mM succinate, 80 µM dichlorophenollindophenol (DCIP), 50 µM decylubiquinone, 1 µM Antimycin A and 3µM rotenone, pH 7.8[196]. Changes in absorbance were followed at 600 nm. Malonate sensitive activity was calculated by subtracting the activity of wells with 20 mM malonate. *Complex III* activity was measured in the assay mixture containing 50 µM ferricytochrome c, 25 mM potassium phosphate, 4 mM sodium azide, 0.1 mM EDTA, 0.025% Tween 20 and 50 µM decylubiquinol, pH 7.4[196]. Changes in absorbance were followed at 550 nm. Antimycin A sensitive activity was calculated by subtracting the activity of wells with 10 µM antimycin A. *Complex IV* activity was measured in the assay buffer containing 30 mM potassium phosphate and 25µM of freshly prepared ferrocytochrome c, pH 7.4[196]. Changes in absorbance were followed at 550 nm. The absorbance of samples oxidized with 10 µl of 0.5 M potassium hexacyanoferrate (III) was subtracted from all measurements, and then the natural logarithm absorbance was plotted against time and compared to untreated control. Acyl-CoA dehydrogenase activity was measured by modifying the protocol Ijlst and Wanders[197]. We followed the reduction of 2,6-dichloroindophenol (DCIP) at 600 nm instead of ferricenium hexafluorophosphate. The assay mixture contained 20 mM Tris-Cl (pH adjusted to 8.0), 0.1 % Triton X-100 and 10 mM DCIP and 10 µL of homogenate. A600 was followed at 37°C with 30 seconds interval until the signal was stable, then 20 µM octanoyl-CoA was added to initiate the reaction.

15.10 Statistics

For statistical analysis, we used software Stata 14.2 (Stata Corp., LLC, College Station, TX). In order to deal with hierarchical structure of the data, we used a four-level mixed effect model of linear regression[147]. In the fixed part, the model consists of a dependent continuous variable (e.g., a bioenergetic variable) and an independent variable, which is a categorical variable describing the experimental condition (e.g., the concentration of propofol)[147]. In the random part, the model reflects the following four levels: subjects, experimental condition, well, and repeated measures in each well[147]. The data are presented as the difference (with a 95% CI and p value) between the mean value of the dependent variable of reference cells and the mean value of the dependent variable under the given experimental condition[147].

16. Results

16.1 Cell viability and effect of propofol on mitochondrial and protein content

Cell viability test (MTS test) was the first method that we used to observe propofol effect on human skeletal muscle cells. 96 hours exposure of myotubes to propofol up to 10 μg/mL did not cause detectable changes in cell survival measured by cell viability test, but higher concentrations (25 and 50 μg/mL) were highly toxic (see **Figure 19**)[147]. Therefore, we excluded them from other experiments. Neither NEFA nor Intralipid alone affected cell survival[147]. On the contrary, when cells were exposed to combination of propofol with either Intralipid or NEFA, it seemed that these compounds had protective effect, as viability of cells was higher in comparison with groups exposed to propofol alone. In all experiments, exposure to propofol caused a degree of dose-dependent reduction of both protein and mitochondrial contents (measured as Bradford assay or Citrate synthase activity, respectively; see **Figure 20**)[147]. These changes were mirrored in changes of basal OCR. Thus, we normalized all functional mitochondrial parameters derived from extracellular flux analysis to basal OCR[147].

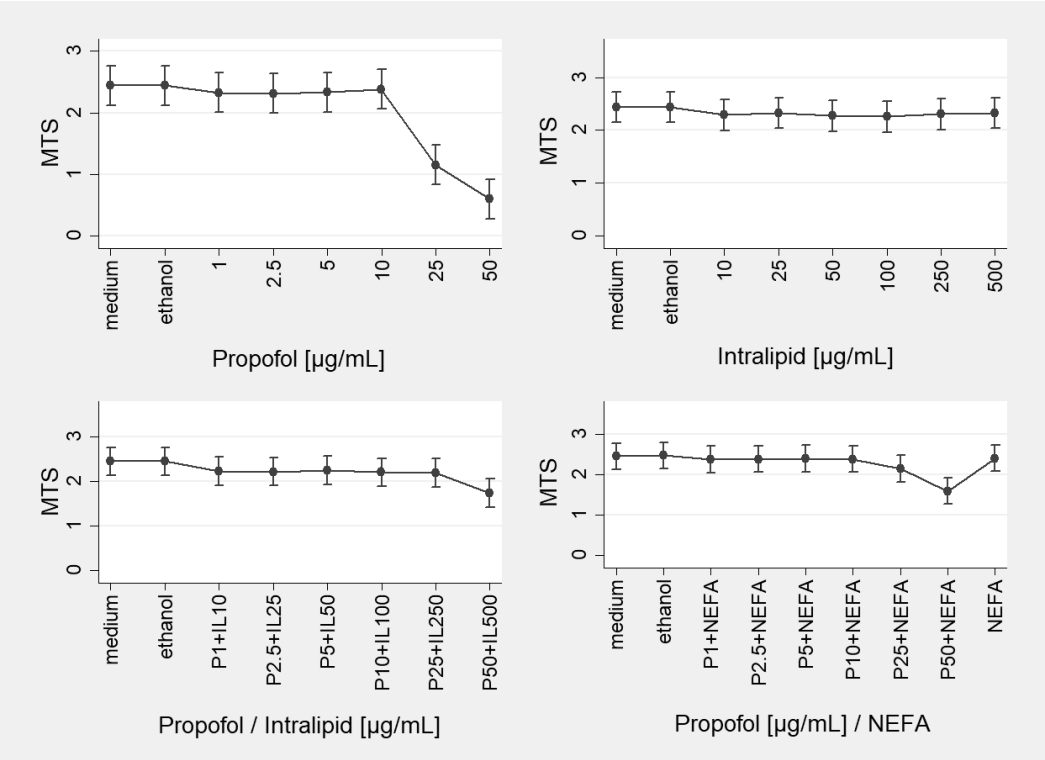

Figure 19. Results of MTS test. The absorbance on y-axis (arbitrary units) is directly proportional to number of viable cells. Protective effects of Intralipid and NEFA (500 µM) are apparent. Krajčová et al., 2017[147].

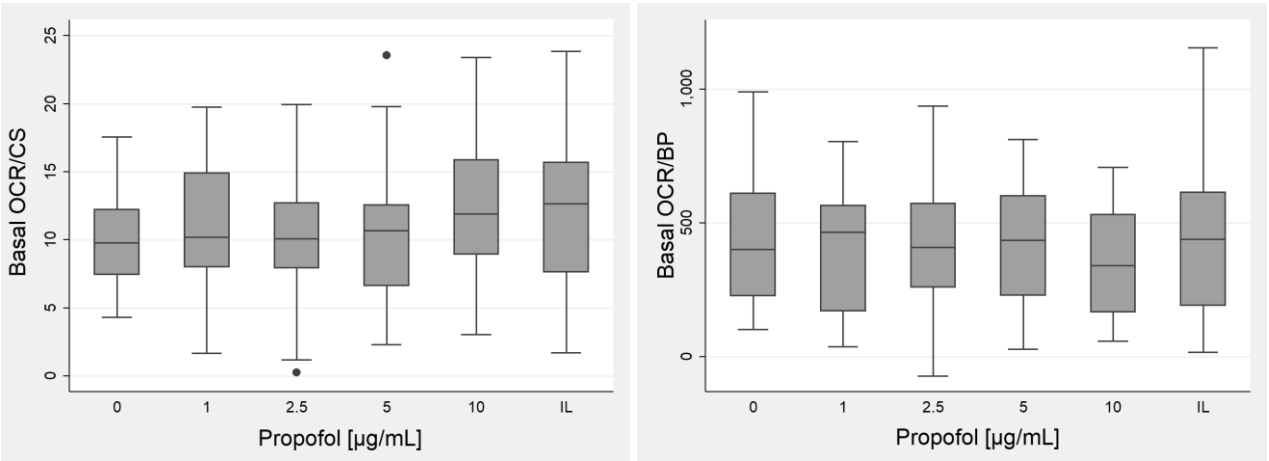

Figure 20. Relation between basal oxygen consumption rate (OCR) and Citrate Synthase (CS) activity (on the left) and between basal OCR and Bradford protein (BP) content (on the right). Krajčová et al., 2017[147].

16.2 Global mitochondrial functional parameters

Basal oxygen consumption rate was only affected by the highest tested concentration: 10 µg/mL propofol (see **Figure 21, part A**)[147]. Proton leak through the inner mitochondrial membrane tended to be increased in a non-concentration dependent manner (from 21% of basal OCR in controls to 24–40% in cells exposed to propofol), but this effect only reached statistical significance with 2.5 µg/mL of propofol (see **Figure 21, part B**)[147]. Spare ETC capacity in control cells was 378% ± 135% of basal OCR. It was significantly reduced across all propofol concentrations (to 113% ± 96%, 111% ± 77%, 245% ± 155%, 245% ± 188% for 1.0, 2.5, 5.0, and 10 µg/mL of propofol, respectively, $p < 0.01$ for all differences) (see **Figure 21, part C**)[147]. No effect was observed after incubation of cells in the Intralipid vehicle. Anaerobic glycolysis (as measured as the ECAR) was highly variable and only reduced by 10 µg/mL of propofol (see **Figure 21, part D**)[147].

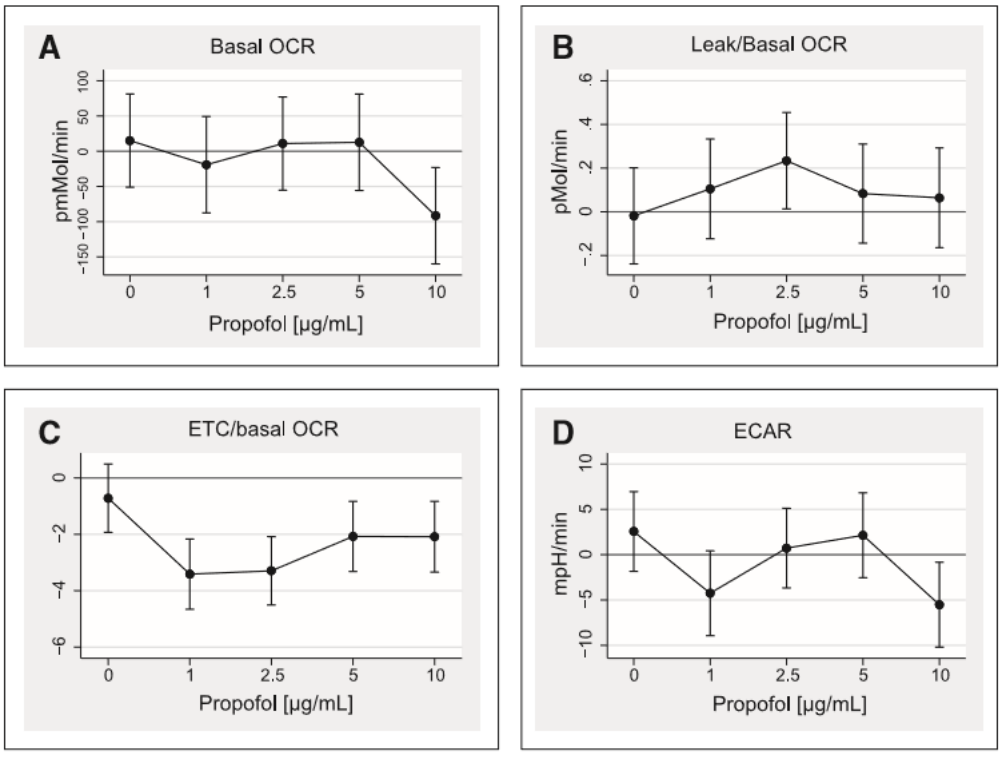

Figure 21. Global mitochondrial parameters. Differences in bioenergetic variables (y-axis) caused by a range of propofol concentrations (x-axis) diluted in 0.01% ethanol (propofol = 0 refers to ethanol alone) compared with reference cells cultured in "Differentiation medium" alone (mean from n = 6; vertical bars represent 95% CIs). A, Basal oxygen consumption rate (OCR). B, Leak/ basal OCR ratio. C, Electron transfer chain capacity (ETC)/basal OCR ratio. D, The Extracellular Acidification Rate (ECAR) reflects the rate of anaerobic glycolysis. Krajčová et al., 2017[147].

16.3 Fatty Acid Oxidation: Extracellular Flux Analysis and Analysis of Oxidation of [1-^{14}C] palmitic acid to acid-soluble metabolites

By Extracellular Flux Analysis, we found a profound inhibition of FAO which decreased to 36% and 33% of values in control cells with 2.5 or 10 µg/mL of propofol, respectively ($p < 0.01$ for both; see **Figure 22, part A**)[147]. In Experiment with assessment of oxidation of [1-^{14}C] palmitate acid to acid-soluble metabolites, we observed a significant decrease of FAO with 2.5, 5, and 10 µg/mL of propofol (see **Figure 22, part B**)[147].

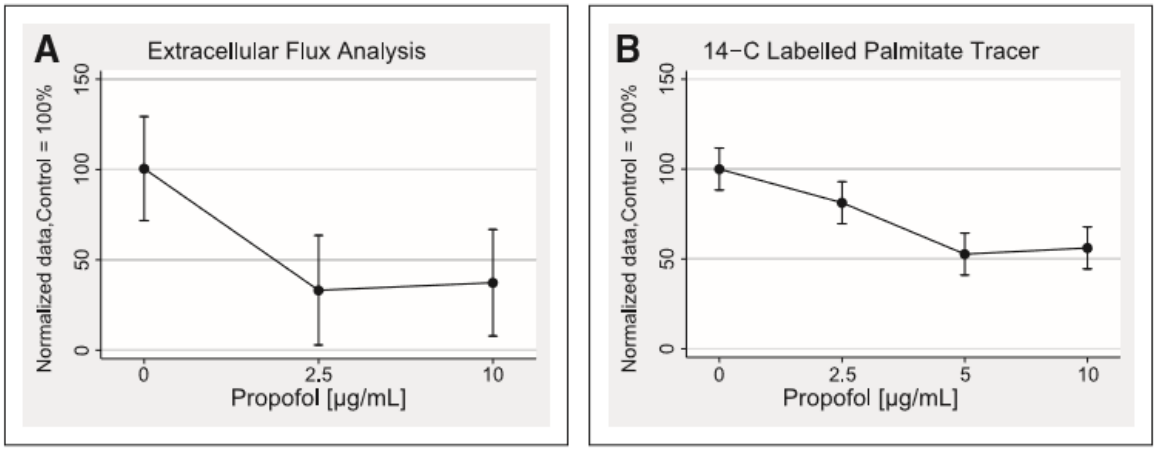

Figure 22. Effect of propofol on fatty acid oxidation. Changes in fatty acid oxidation rate caused by propofol measured by Extracellular Flux Analysis (A) and by [1-^{14}C] palmitate technique (B). Data expressed as mean % of value in reference cells (i.e., cultured without propofol), which are arbitrarily set as 100%. Vertical bars are 95% CI. Krajčová et al., 2017[147].

16.4 Respiration linked to individual complexes of electron transfer chain: Extracellular Flux Analysis and Spectrophotometric Assay

When measured isolated activities of individual complexes (Spectrophotometric Assay), we have not found any inhibition by propofol of the capacity of respiratory complexes II–IV nor ACAD (see **Table 2**)[147]. In intact mitochondria of saponin-permeabilized myotubes (Extracellular Flux Analysis), there was no effect of propofol 2.5 µg/ mL on ETC complexes either, but with 10 µg/mL, there was a reduction of the activity of the complexes III and IV (see **Table 2** and **Figure 23**)[147]. We observed no correlation between the activity of any of these complexes and ETC spare capacity (data not shown).

Mitochondrial Enzymes	Spectrophotometry ($n = 6$)		Extracellular Flux Analysis ($n = 6$)	
	Mean Enzyme Activity (Normalized to Citrate Synthase) Expressed as % of Controls (95% CI)		Mean Complex Capacity (Normalized to Basal Oxygen Consumption Rate) Expressed as % of Controls Without Propofol (95% CI)	
	Propofol Concentration: 2.5 μg/mL	Propofol Concentration: 10 μg/mL	Propofol Concentration: 2.5 μg/mL	Propofol Concentration: 10 μg/mL
Complex I	N/A	N/A	102 (93–112)	108 (98–117)
Complex II	102 (92–112)	124[a] (114–134)	104 (97–110)	101 (94–109)
Complex III	123 (100–146)	109 (86–131)	82 (44–120)	41[a] (10–92)
Complex IV	131[a] (111–151)	104 (83–124)	85 (62–108)	73[a] (46–99)
Acyl-CoA dehydrogenase	108 (85–130)	97 (74–119)	N/A	N/A

Table 2. Activity of individual complexes of electron transfer chain analysed using Spectrophotometric assay. Mean activities (95% CIs) of individual mitochondrial enzymes expressed as % of values in control cells cultured in the absence of propofol. N/A = not applicable. [a]$p < 0.05$. Krajčová et al., 2017[147].

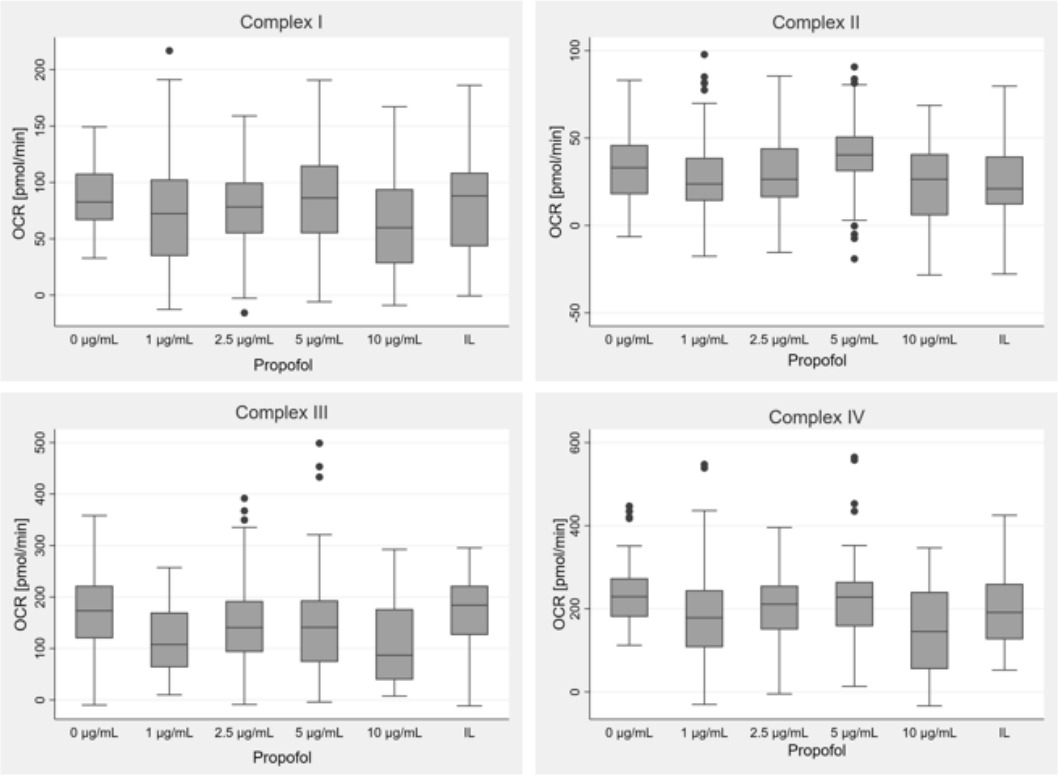

Figure 23. Effect of the range of propofol concentrations on respiration linked to individual complexes of electron transport chain analysed by XF-24 Extracellular Flux Analyzer.

In addition, we looked specifically at complex III-linked respiration and transfer of electrons from complexes I and II to complex III by Coenzyme Q (see **Figure 27** in Discussion). To assess its function, we looked at the results of experiment where cells were in respiration medium supplemented with substrates for complexes I and II (malate+glutamate and succinate, resp.) prior to measurement on XF-24 Extracellular Flux Analyzer (see **Figure 16** in Methods). After that, agents were sequentially added as follows: uncoupler FCCP to maximally stimulate respiration, followed by inhibitors of complexes I and II (rotenone and malonate, resp.). Subsequently, complex III substrate (duroquinol) was added and respiration was inhibited by inhibitor for complex III (Antimycin A). From the measured values, we obtained data reflecting the differences between pathway from complex I and II to complex III (= electrons are transferred using Coenzyme Q) and pathway where electrons were sent directly to complex III (by addition of duroquinol) bypassing Coenzyme Q. We calculated the difference as: OCR after FCCP – OCR after duroquinol. OCR after Antimycin A reflecting non-mitochondrial respiration was subtracted from the values. According to the results, it seemed that low concentrations of propofol (1 and 2.5 µg/mL) inhibited respiration linked to complex I+II (see **Figure 24**). At higher concentrations there was a trend of propofol-induced direct inhibition of complex III, but the results were not statistically significant.

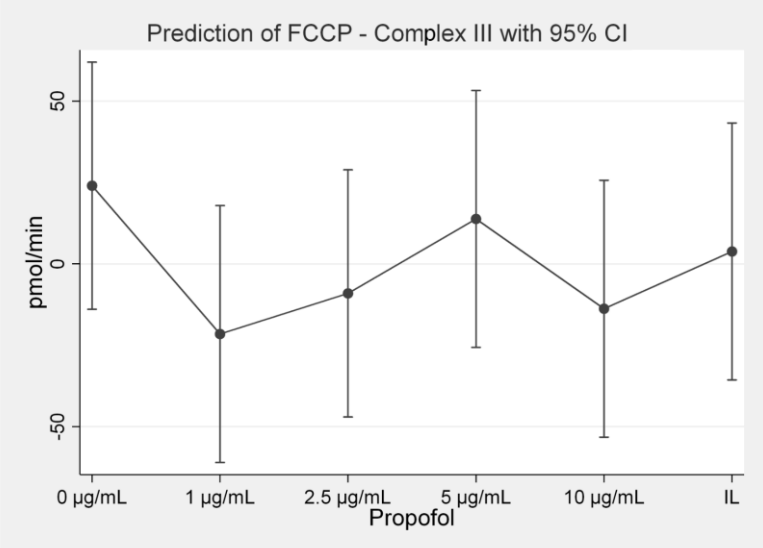

Figure 24. Effect of the range of propofol concentrations on respiration linked to complex I+II and respiration linked to complex III of electron transfer chain analysed by XF-24 Extracellular Flux Analyzer.

16.5 Influence of NEFA on propofol-induced changes in mitochondrial metabolism

Cells were exposed to propofol (2.5 and 10 µg/mL) with and without NEFA for 96 hours to test their possible effect on propofol induced-changes of mitochondrial metabolism. Addition of NEFA alone to the media did not affect cell survival (see **Figure 19**) or global mitochondrial functional indices, but it mitigated the inhibitory effects of propofol on basal OCR (see **Figure 25, part A**) and normalized spare ETC capacity (see **Figure 25, part B**) in cells co-exposed to propofol[147].

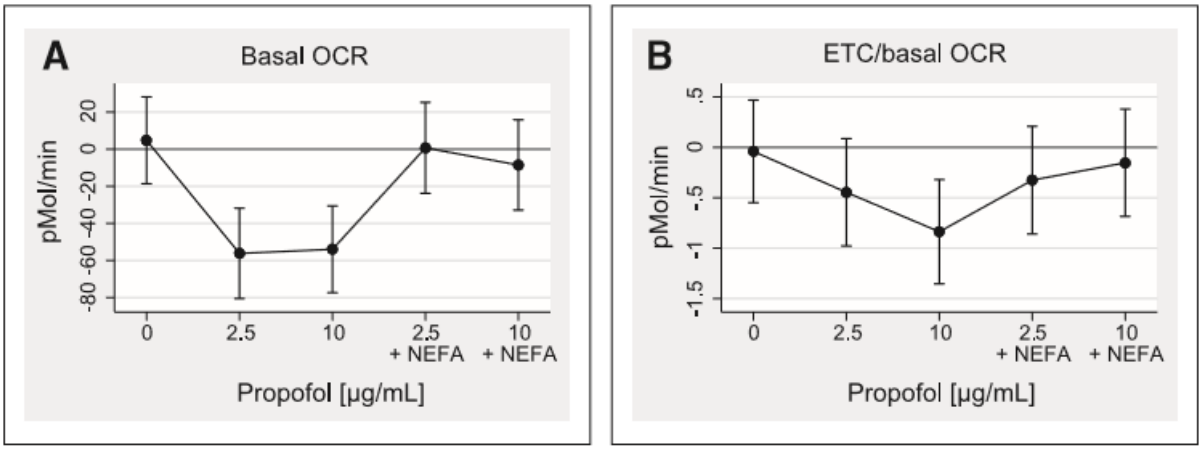

Figure 25. Impact of NEFA on propofol-induced changes in mitochondria. Interaction of propofol diluted in 0.01% ethanol with increased non-esterified fatty acids (NEFA) in culture media. Reference cells were cultured in the fresh "Differentiation medium" alone (propofol = 0 are cells cultured in 0.01% ethanol). (A) Changes in basal oxygen consumption rate (OCR). (B) Changes in spare capacity of electron transfer chain ratio to basal OCR. ETC = electron transfer chain capacity. Krajčová et al., 2017[147].

17 Discussion

Firstly, we looked at all 153 PRIS case reports and case series published between 1990 and 2014[81]. Our analysis of reported cases shows that PRIS has changed over the last 24 years[81]: a typical patient who died with PRIS in the early 1990s was a child with respiratory infection who developed PRIS after having received an excessive dose of propofol[32,33]. Nowadays, PRIS is more likely to be seen in an adult or elderly patient sedated by a usual dose of propofol in an ICU in whom mild unexplained acidosis and elevation of creatine kinase is noted[81], sometimes with worsening of acute kidney injury and arrhythmia, but other features of PRIS are often missing[82,83,85]. This can be a consequence of changes of prescription habits, with more ICU patients exposed to propofol, but a smaller proportion of them exposed to dangerously high doses[81].

We looked also at the factors associated with higher mortality. Our multivariate analysis showed that there are only a few independent predictors of death[81]. The most important of these seemed to be the cumulative dose of propofol, being represented by both mean infusion rate and the duration of infusion[81]. Out of all the other features of PRIS, which seem to increase the probability of death in univariate analysis, only the presence of trauma brain injury and fever were significantly related to PRIS mortality[81].

We also looked at the dependency of the frequency of PRIS signs on the rate and duration of propofol infusion and we observed that dose-related signs of PRIS occurred more frequently with higher infusion rates, irrespective of the duration of infusion, and included: cardiac failure, metabolic acidosis, fever, and perhaps hypotension[81]. Signs of PRIS dependent on duration of infusion occurred more frequently with longer propofol infusions (mostly >48 hours) irrespective of dose and included arrhythmia and other ECG changes[81]. Rhabdomyolysis and hypertriglyceridemia occurred most frequently with high doses of propofol after 96 hours of administration and seemed to be dependent on cumulative dose rise in frequency with both the dose and time of administration[81].

However, in some of reported cases, mild unexplained acidosis was even the only sign of possible PRIS development, which completely disappeared after propofol withdrawal[74]. A current view on PRIS is therefore quite different from previous Bray's definition in 90's. Because symptoms can occur in any combination and order and can range from the very mild to severe in each individual patient, it is very difficult to determine a precise definition of PRIS[81].

Our finding that cardiac failure and metabolic acidosis occurred early and in a dose-dependent manner is consistent with a direct inhibition of aerobic phosphorylation observed in experimental studies[81]. The heart muscle is highly reliant on aerobic ATP production[198] and acidosis may represent a combination of hypoperfusion and cytopathic hypoxia in tissues[81]. Fever was reported more frequently with higher propofol infusion doses that might reflect mitochondrial uncoupling from ATP production and energy dissipation as heat[81]. On the contrary, arrhythmia and ECG changes occurred more frequently in PRIS cases caused by prolonged propofol infusions which could be explained by the fact that arrhythmia and ECG changes are caused by elevated free fatty acids, which steadily increase over days during propofol administration[68] and are known to be proarrhythmogenic[199] (even more so in combination with metabolic acidosis)[81]. Similarly, rhabdomyolysis (a common feature of inborn defects of fatty acid oxidation[200,201]) was associated with the duration of propofol administration and might also be related to the propofol-induced defect of fatty acid oxidation[81]. The frequency of hypertriglyceridemia seemed to also increase with cumulative dose of propofol[81]. If the dose of lipid emulsions exceeds the capacity of hydrolysis in plasma, triacylglyceroles accumulate in the blood and are taken up by the reticulo-endothelial system, causing hepatosplenomegaly, jaundice, and clotting disturbances ("fat overload syndrome"[202]). Recommended lipid dose for parenteral nutrition is 29–54 mg/kg per hour[203]. To match this dose, propofol as a 1 % solution in 10 % intralipid has to run at 2.9–5.4 mg/kg per hour. Most of the patients with PRIS exceeded this rate[81]. Nonetheless, it seems that excessive doses of lipid emulsions are generally well tolerated; rapid infusions of lipid emulsions even in a range of 170–5000 mg/kg per hour have been accidentally administered without side effects[204]. In animal models of PRIS[137,205], elevated triglycerides was the only sign observed in control animals receiving intralipid alone.

In conclusion, the main limitation of our meta-analysis is the risk of publication bias, i.e. that the published cases are not representative of the population of patients with PRIS. In summary, we found out that cardiac failure and metabolic acidosis occur early in a dose-dependent manner and could be caused by inhibiting aerobic phosphorylation and fever by mitochondrial uncoupling while arrhythmia, other ECG changes and rhabdomyolysis appear more frequently after prolonged propofol infusions, irrespective of dose[81]. In addition, in our meta-analysis of 153 published PRIS case reports we found that some signs (e.g. rhabdomyolysis) occurrs more frequently after propofol infusion longer than 96 hours. This finding helped us to design our further experimental *in vitro* study when selecting the length of propofol exposure: we chose the duration of 4 days (= approximately 96 hours) for incubation of cells in propofol.

In 90's, soon after the first case of PRIS, the pathogenesis of syndrome started to be extensively studied. First *in vitro* studies were performed on animals, mostly by exposing isolated mitochondria from rat liver[128,130,132] or heart[129] to very high doses of propofol for a very short time (at the range of minutes). According to them, propofol was thought to act as an inhibitor of electron transport chain[128–131] and a mild uncoupler of the inner mitochondrial membrane[130,132]. The main limitation of these studies was the short action of propofol on mitochondria at concentrations which mostly several times exceeded propofol levels found *in vivo* in human plasma (up to 10 μg/mL) during anaesthesia[139] or sedation[140,141].

The only study of long-term *in vivo* exposure to propofol was published in 2015 by Vanlander et al.[133] In the study, authors discussed a structural similarity of propofol and Coenzyme Q (CoQ) molecule[133]. They observed eight rats, who were sedated for up to 20 hours with gradually increasing doses of propofol (from 20 to 80 mg/per kg/hour) in comparison with group of control rats. Liver, skeletal and heart muscle biopsies were performed in different time intervals after initiation of propofol administration (after 6; 12; 3.5-8 hours). Tissue samples were homogenized to prepare homogenates suitable for spectrophotometric analyses[133]. The activities of respiratory chain complexes (nicotinamide: adenine dinucleotide: coenzyme Q reductase [complex I], succinate coenzyme Q reductase [complex II], succinate cytochrome c reductase [complex II+III activity], cytochrome c ubiquinol reductase [complex III], cytochrome c oxidase [complex IV]) were then measured. The analysis demonstrated that the enzyme succinate cytochrome c reductase (specific for complexes II and III) was the enzyme that was the most sensitive to propofol exposure in skeletal and heart muscle homogenates even at the lowest used concentrations (20 and 25 μM, resp.) and in liver at the higher concentration of propofol (40 μM)[133]. In contrast, the activities of the individual complexes (I, II, III) were not affected[133]. Complex IV was the only enzyme of respiratory chain that was decreased by propofol exposure (from concentration $>$ 40 μM)[133]. Vanlander et al. also performed *in vitro* experiments using control samples taken from rats before the drug was administered[133]. Samples (skeletal muscle homogenates) were exposed for a short time (3 min) to different concentrations of propofol (100; 200 and 400 μM) and all above-mentioned spectrophotometric analyses were repeated. The results showed no significant impact of lower doses of propofol (100 μM) on activities of respiratory chain complexes[133]. These results were contrary to previously described *in vivo* experiments demonstrating inhibition (especially of complex II+III activity) caused even by 20 μM propofol in skeletal muscle. Only at a 10-fold higher concentration of propofol (200 μM), an inhibitory effect on the respiratory chain activities (complex I, complex II+III, complex III and complex IV) was seen *in vitro*[133]. An inhibition of complex

II activity was seen only after exposure of 400 μM propofol[133]. However, *in vivo* experiments observing long-term effect of propofol sedation reflected more physiological conditions than influence of multiple-fold higher (>100 μM) concentration of propofol on mitochondria after only 3 minutes of duration. The authors explain the difference between *in vivo* and *in vitro* effects by different distribution of propofol within mitochondria and different incubation time (in the *in vivo* experiments at the range of hours in comparison with only 3 minutes preincubation in the *in vitro* experiments)[133]. A significant decline in activity of complex II+III after propofol exposure seen in *in vivo* experiments contrasted with analyses of individual activities of complex II and III demonstrating no decrease. Vanlander et al. explained that this could be a consequence of possible interference of propofol with Coenzyme Q because of structural similarities of both molecules (see **Figure 26**)[133].

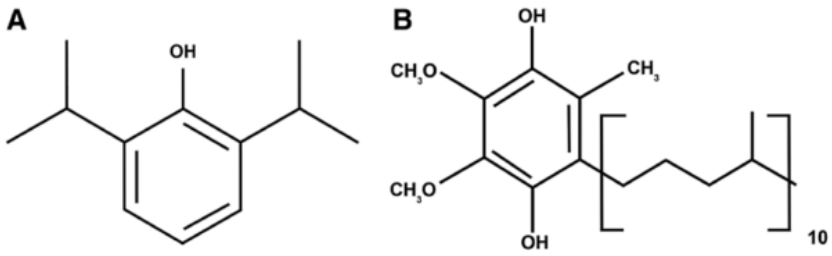

Figure 26. Structural similarity of propofol and Coenzyme Q[133]. (A) Molecular structure of propofol (2,6-diisopropylphenol); (B) Molecular structure of ubiquinol (reduced form of Coenzyme Q). Vanlander et al., 2015[133].

Coenzyme Q is a lipophilic molecule located in the inner mitochondrial membrane. It consists of a redox active benzoquinone ring conjugated to an isoprenoid chain[206]. The length of chain in humans contains 10 isoprenyl units and is designed CoQ_{10}[206]. Coenzyme Q shuttles electrons from complex I and II and transfers them to complex III of the respiratory chain (see **Figure 27**). Coenzyme Q acts also as an antioxidant and scavenger of reactive oxygen species[206]. In addition, it is involved in other cellular functions: DNA replication and repair through its role in pyrimidine synthesis and the regulation of the physicochemical properties of cellular membranes[207,208]. *In vivo* experiments of the study of Vanlander et al. showed no impact of propofol on complex II nor complex III when tested individually[133]. In comparison with this, complex II and III activity was affected suggesting that propofol interferes with Coenzyme Q and disrupts electron flow from complex II to complex III. Based on this fact, authors performed a set

of experiments with coenzyme Q supplementation in the *in vitro* experiments[133]. To confirm the hypothesis of possible propofol interference with Coenzyme Q, authors exposed homogenates to propofol for 3 minutes and then tested effect of exogenously added Coenzyme Q: one group was supplemented with 0.13 mM Coenzyme Q and the second one by 0.26 mM Coenzyme Q. The results showed that inhibition of complex II+III by propofol was preventable with Coenzyme Q supplementation, reinforcing the hypothesis of a disturbing effect of propofol on the biologic function of coenzyme Q[133]. Authors summarized, that according *in vivo* tests propofol probably incorporated into the inner mitochondrial membrane where starting to accept the electrons from the complexes I and II in the respiratory chain without transferring them to complex III[133]. In the *in vitro* test, sample was exposed to propofol only for 3 minutes. The contact of drug with the sample was therefore shorter and time of exposure might be insufficient for incorporation of the molecule into the inner mitochondrial membrane. An additional effect on complex IV can be due to the interference of propofol with the cytochrome in complex IV (aa3) and with cytochrome c[133].

Apart from propofol-evoked changes of electron transfer chain, propofol-induced inhibition of FAO was discussed as the possible underlying mechanism of PRIS[68,116]. Patients with PRIS developed some clinical signs similar to inborn defects of FAO, including cardiac arrhythmias, rhabdomyolysis and skeletal myopathy. In FAO disorders, these abnormalities can be triggered by prolonged fasting or low-carbohydrate, ketogenic diet[209]. One case report described a child developing PRIS after simultaneous administration of propofol sedation and ketogenic diet[138]. In addition, children with PRIS were often screened falsely positive for inborn defect of FAO as acyl-CoA derivatives are elevated in their blood[68,111,116] and sometimes these changes normalized in PRIS survivors after propofol withdrawal[68]. One animal study also demonstrated an inhibition of the transport of fatty acids into mitochondria at the level of carnitine-acyl transferase I, which is an enzyme activated by adenosine monophosphate-activated kinase (AMPK)[136]. If propofol interferes with signalling function of coenzyme Q[133], it may attenuate the activation of fatty acid oxidation by AMPK[210], but other study showed that the activity of this enzyme has been increased in the myocardium of propofol-sedated rabbits[211].

In our experimental study "Effects of Propofol on Cellular Bioenergetics in Human Skeletal Muscle Cells", we used an *in vitro* model of human skeletal muscle and studied the effects of propofol on major bioenergetics pathways[147]. Human myotubes were exposed to propofol concentrations in a range 1–10 μg/mL for 96 hours in order to resemble levels achieved in patients during sedation in the ICU (1.2–4.5 μg/mL[139,140]) or during induction of general anaesthesia (10.5

μg/mL[139]). We not only measured activities of individual ETC complexes but also studied effects of propofol on bioenergetics in a culture of intact or permeabilized cells by Extracellular Flux Analysis[147], which we had previously adapted for the use in human myotubes[149].

Duration of propofol infusion seems to be a crucial factor for development of PRIS[81]. According to our meta-analysis of 153 published PRIS case reports, we found that some signs (e.g. rhabdomyolysis) occurred more frequently after propofol infusion longer than 96 hours[81]. Therefore, we chose the duration of approximately 96 hours for incubation of cells in propofol. Ours is the first study looking at the long-term effects of propofol in an *in vitro* model of human tissue.

Although the highest propofol concentrations (10 μg/mL) affected mitochondrial and protein content, and to some extent also activities of isolated respiratory complexes and cell survival, none of these effects were observed for lower concentrations of propofol (2.5 μg/mL)[147]. We even found no inhibition of complexes I and II at the range of propofol concentrations[147] and complex III and IV were significantly affected only at high concentrations of propofol (10 μg/mL; see **Table 2** in Results)[147]. Yet, even very low concentrations of propofol decreased spare ETC capacity, which reflects cellular ability to increase respiration when ATP demands are high[147]. Because activities of individual respiratory complexes were unaffected by low propofol concentrations, we exploited propofol effects on electron flow between individual ETC complexes or upstream metabolic pathways, which feed electrons into ETC (see **Figure 27**)[147].

To obtain more information about electron flow between complexes in ETC, we looked specifically at our experiment testing both complexes I+II- and complex III-linked respiration (see **Figure 16** in Methods). According to the results, it seemed that low concentrations of propofol (1 and 2.5 μg/mL) inhibited respiration linked to complex I+II (see **Figure 24** in Results), but at higher concentrations there was a trend of propofol-induced direct inhibition of complex III.

In conclusion, although the results of comparison between respiration linked to complex I+II and between complex-III linked respiration were not statistically significant, this trend suggested propofol disturbation of electron flow in upstream pathway of Complex III, when tested lower concentrations. At higher concentrations propofol seemed to start inhibiting of complex III. Of note, we used the artificial substrate duroquinol to measure capacity of complex III[147], which donates electrons directly to respiratory complex III and bypasses Coenzyme Q, so its inhibition cannot be explained by propofol interference with coenzyme Q.

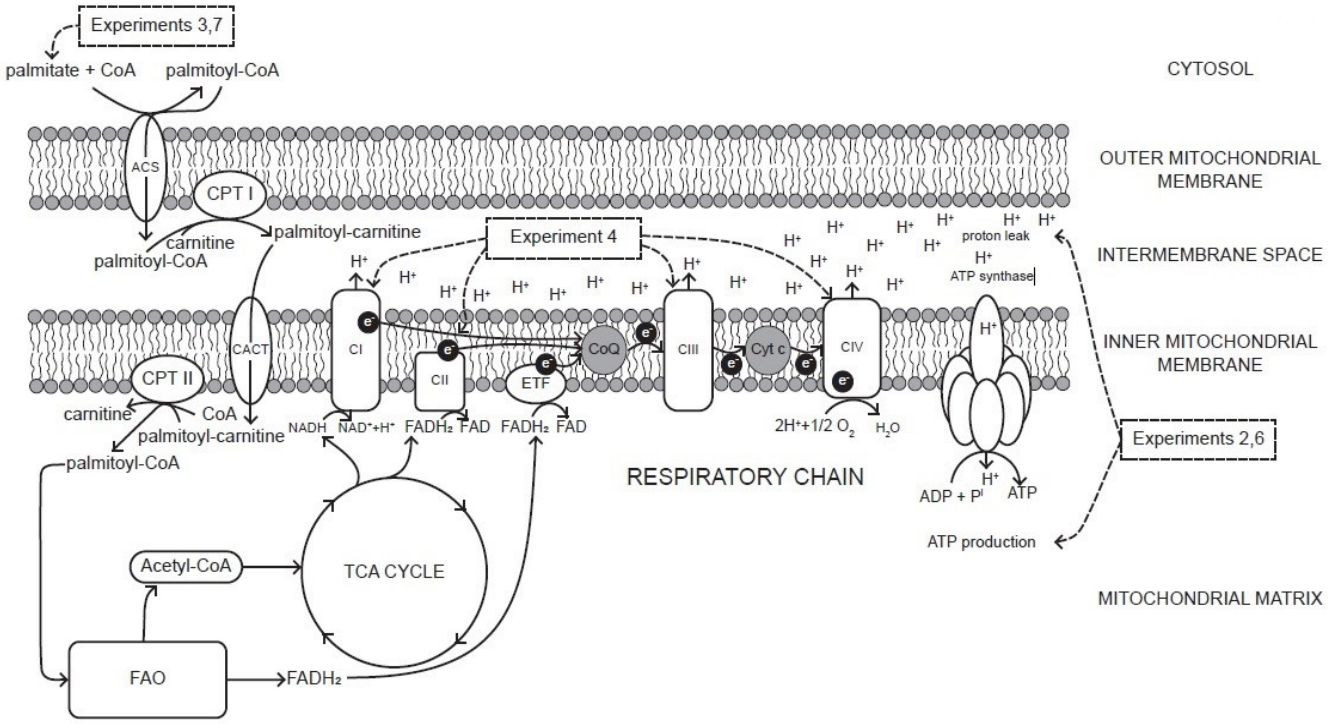

Figure 27. Electron transfer chain and major energy metabolism pathways. Note: ACS = Acyl-CoA Synthetase; CI = Complex I; CII = Complex II; CIII = Complex III; CIV = Complex IV; CPT = Carnitine Palmitoyl Transferase; CACT = Carnitine Acyl CoA Transferase; CoA = Coenzyme A; CoQ = Coenzyme Q; Cyt c = Cytochrome C; e^- = electron; ETF = Electron Transfer Flavoprotein; FAD = Flavin adenine dinucleotide; FAO = Fatty acid oxidation; NAD = Nicotinamide adenine dinucleotide; TCA cycle = Tricarboxylic Acid (Krebs) Cycle. Krajčová et al., 2017[147].

Looking at upstream metabolic pathways, which feed electrons into ETC, we focused also on fatty acid oxidation[147]. We found a profound inhibition of fatty acid oxidation by Extracellular Flux Analysis and confirmed this finding by the use of the [1-^{14}C] palmitate tracer method (see **Figure 22** in Results)[147]. Furthermore, abundant NEFA in the media abolished the inhibitory effects of propofol on the spare ETC capacity[147]. Taken together, these data suggest that propofol exposure limits spare ETC capacity by inhibiting FAO, rather than by inhibiting respiratory complexes or electron transfer within ETC. Data from our *in vitro* experiments firstly brought direct evidence of propofol inhibitory effect on FAO in human cells[147]. On the other hand, apart from measuring the activity of one of FAO enzymes (ACAD) that was unaffected by propofol, we have not studied the mechanism of FAO inhibition any further[147]. Propofol (or its intracellular metabolites) may inhibit enzyme involved in fatty acids transport, fatty acid oxidation process or electron transfer flavoprotein dehydrogenase (see **Figure 27**). We think it is less likely that

propofol-induced inhibition of FAO is secondary to an inhibition within ETC itself, as we have observed that any spare ETC capacity was unaffected if propofol-treated cells were cultured in fatty acid rich environment[147]. However, it should be noted that although the range of total propofol concentration we exposed our cells to was in the range of that seen in propofol-sedated patients, free propofol concentrations might have been higher due to decreased protein binding in culture media as compared to plasma[212]. In addition, added substances (BSA, palmitate) might have influenced propofol activity and confound the results[147].

Supplementation of CoQ may become a promising therapeutic strategy (a propofol "antidote") in the near future[133]. In our pilot experiments (data not shown), we co-exposed human myotubes to propofol and various concentrations of coenzyme Q_{10} for 4 days. The difficulties were observed with dissolvement of this strongly hydrophobic molecule. CoQ_{10} is only sparingly soluble in aqueous solutions and is recommended to dilute it rather in organic solvents such as ethanol and dimethyl formamide (DMF)[213]. These organic solvents themselves can have effects on cells and is needed to avoid too high concentrations because of risk of toxicity. The solubility of CoQ_{10} in ethanol and DMF is approximately 0.3 and 10 mg/mL, respectively[213]. With increasing concentrations of CoQ_{10} raises also the amount of solvent, which becomes harmful for cells. According to our first results, only lesser concentration of CoQ_{10} were thoroughly dissolved in small amount of DMF but had no preventable effect on respiration in cells co-exposed to both propofol and CoQ_{10}. When testing higher concentrations of CoQ_{10} (~50 µM prepared in DMF), respiration was lower in cells exposed to CoQ_{10} (without propofol) than in control group incubated in fresh "Differentiation medium" alone suggesting toxic effect of solvent. In addition, it is well-known that CoQ_{10}, as a lipophilic molecule, accumulates in membranes and only its small proportion reaches the mitochondria. In addition, much of the CoQ_{10} in mitochondria is likely to be trapped in the outer membrane and doesn't achieve the respiratory chain located in the mitochondrial inner membrane[214]. One of our aims in future is to expose the cells to analogues of CoQ_{10} with reduced hydrophobicity: e.g. short-chain analogue CoQ_2 or synthetic compound idebenone[214] (see **Figure 28**). We also considered to try incubation in medium supplemented by MitoQ, which is a novel orally bioavailable molecule conjugated to the lipophilic triphenyl phosphonium (TPP^+) cation[215]. The lipophilic cations are accumulated several hundred-fold by the large membrane potential (negative inside) generated by mitochondria during oxidative phosphorylation[216,217] and easily get into the cell and then further into mitochondria[215]. However, previous studies showed that MitoQ cannot restore respiration in mitochondria lacking coenzyme Q, possibly because the reduced

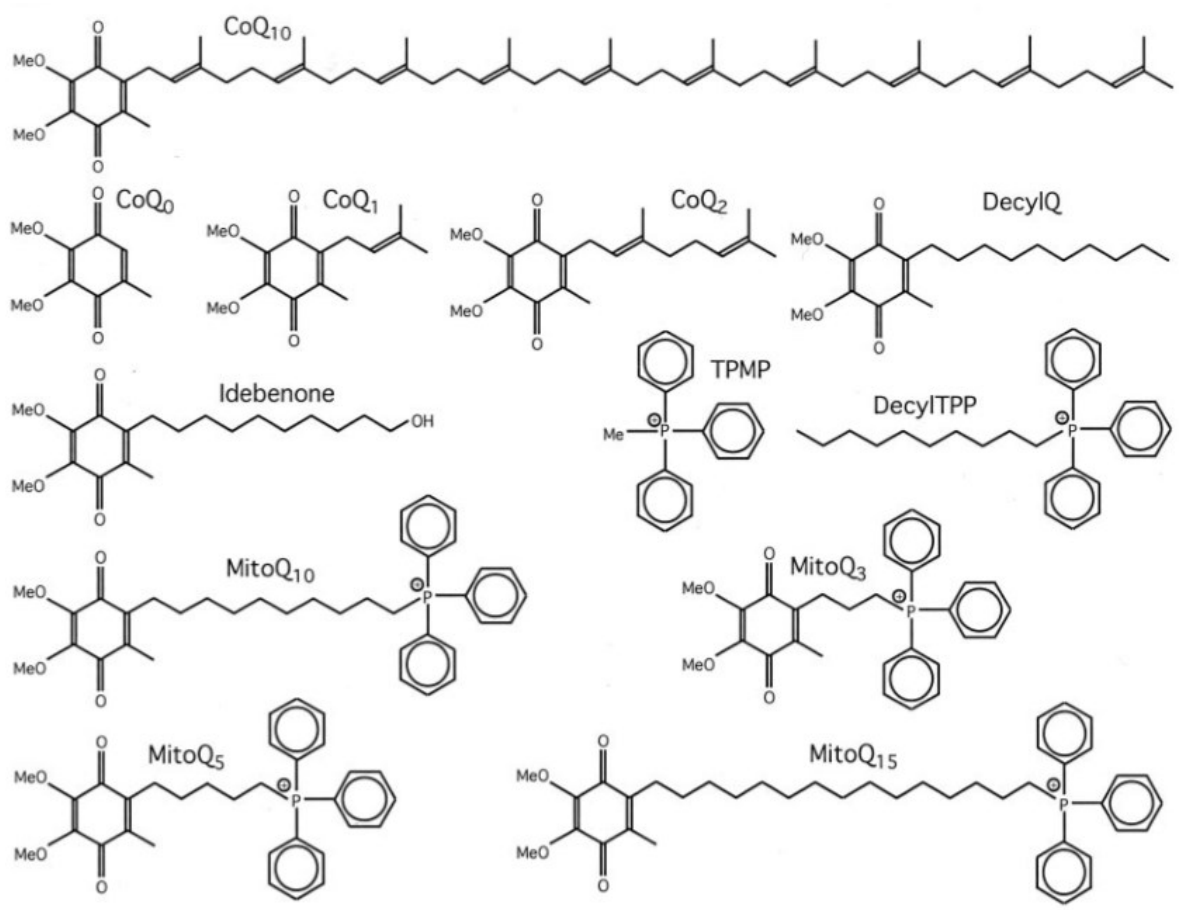

Figure 28. Mitochondria-targeted and untargeted ubiquinones. James et al., 2005[218].

form of MitoQ is poorly oxidized by complex III[218]. MitoQ acts as an effective antioxidant but has no effect on respiration[218].

In other sets of out pilot experiments, we started to deal with fatty acid oxidation in detail and focused on fatty acid metabolism and co-exposed myotubes to both propofol and carnitine (data not shown). Long-term carnitine supplementation (at range of 0.1 to 10 mM) didn't show any impact on respiration. However, we performed only initial set of experiments and effect of propofol on both fatty acid transport and oxidation still needs to be examined as we tested only the activity of one of FAO (ACAD). The palmitate as the substrate for FAO is at the beginning of the metabolic pathway including enzymes of fatty acid transport through outer and inner mitochondrial membrane, fatty acid oxidation and ETF dehydrogenase (see **Figure 27**). In future, we plan to test individual enzymes using different substrates for fatty acid transport (e.g. palmitate to test Acyl-CoA Synthetase, palmitoyl-CoA to test Carnitine Palmitoyl Transferase 1, palmitoyl-carnitine and acetyl-carnitine to test Carnitine Acyl CoA Translocase) and fatty acid

oxidation itself (by supplementation of butyrate, hexanoate or octanoate). The comparison between respiration using different substrates could reveal a defect in one of the enzymes. In addition, we would like to assess spectrophotometrically the activities of individual enzymes. We also tried to analyse the activity of ETF dehydrogenase, but it is needed to use a purified enzyme. We discussed the method with the colleagues abroad who eventually used bacterium *Paracoccus denitrificans* rather than human, because the human form proved difficult to work with. Generally, in case of ETF dehydrogenase, the purification process is extremely difficult and not routinely performed.

Finally, we have recently started with cultivation of human cardiomyocytes isolated from left ventricular myocardium obtained at Transplantation Centre of Institute of Clinical and Experimental Medicine in Prague from brain-dead donors without cardiac disease, whose hearts were not suitable for transplantation due to donor age. We believe that the model of human cardiac muscle cells could be the best for *in vitro* studying PRIS as arrhythmias and cardiac failure remain one of the most common signs of PRIS. In future, we would like to expose cardiomyocytes to a range of propofol concentrations and looked at all above mentioned possible propofol-induced changes of mitochondrial metabolism preferentially in these cells. We are also performing a set of experiments comparing propofol effect on human and rat skeletal and heart muscle homogenates using high resolution respirometry (the method is based on monitoring oxygen consumption in the closed chamber). We adapted the technique to measurement of human skeletal[146] and heart[5] muscle tissue homogenates to acquire a simple model for testing drug-induced mitochondrial defects in future.

18 Conclusions

We firstly analysed all the case reports and case series about PRIS (published between 1990-2014)[81]. PRIS may occur even after short duration of infusion and with moderate doses (<4 mg/kg per hour) and its diagnosis may be challenging as most typical symptoms are missing[81]. Overall mortality in reported cases of PRIS is 51 % and is decreasing over time[81]. Propofol infusion rate and duration, the presence of trauma brain injury and fever are risk factors independently associated with mortality in reported cases of patients with PRIS[81]. Metabolic acidosis and heart failure occur early and depend on the dose of propofol, whilst rhabdomyolysis, arrhythmia and other ECG changes are rather dependent on the duration of propofol infusion[81]. Experimental data suggest that early, dose-dependent signs may be caused by inhibition or uncoupling of respiratory chain, whilst late, time-dependent signs by inhibition of fatty acid oxidation[81].

In an *in vitro* study, we were the first, who exposed human cells to propofol for a long-term period reflecting the conditions when PRIS occurs most likely[72,76] and after that we assessed the bioenergetic profile[147]. We not only measured activities of individual ETC complexes but also studied effects of propofol on bioenergetics in a culture of intact or permeabilized cells by extracellular flux analysis, which we had previously adapted for the use in human myotubes[149]. 96-hours of exposure of human skeletal muscle cells to a range of propofol concentrations reduced the spare capacity of electron transfer chain and caused a significant inhibition of fatty acid oxidation, which was found by two independent methods (Extracellular Flux Analysis and [1-^{14}C] palmitate tracer technique)[147].

We chose skeletal muscle being a large body compartment comprising around 40% of total body mass and because it is directly affected in PRIS[147]. It remains unclear how propofol affects bioenergetics in other human tissues and organs and whether any metabolic effects would be detectable at a whole-body level[147].

19 References

1. Pagliarini D, Rutter J. Hallmarks of a new era in mitochondrial biochemistry. *Genes Dev*. 2013;27:2615-2627.

2. Meyer JN, Leung MCK, Rooney JP, et al. Mitochondria as a target of environmental toxicants. *Toxicol Sci*. 2013;134(1):1-17.

3. Scheffler IE. *Mitochondria*.; the second edition, 2008.

4. Junior HM. *Milestones in the History of Empirical Sciences.*; 2012.

5. Krajčová A, Megvinet D, Urban T, et al. High resolution respirometry to assess function of mitochondria in native homogenates of human heart muscle. *Circ Res (under Rev).* 2018.

6. Vuda M, Kamath A. Drug induced mitochondrial dysfunction: Mechanisms and adverse clinical consequences. *Mitochondrion*. 2016;31:63-74.

7. Szewczyk A, Wojtczak L. Mitochondria as a pharmacological target. *Pharmacol Rev*. 2002;54(1):101–127.

8. Wallace K. Adriamycin-induced interference with cardiac mitochondrial calcium homeostasis. *Cardiovasc Toxicol*. 2007;7:101–107.

9. Kudin AP, Mawasi H, Eisenkraft A, Elger CE, Bialer M, Kunz WS. Mitochondrial liver toxicity of valproic acid and its acid derivatives is related to inhibition of α-lipoamide dehydrogenase. *Int J Mol Sci*. 2017;18(9):1-11.

10. Komulainen T, Lodge T, Hinttala R, et al. Sodium valproate induces mitochondrial respiration dysfunction in HepG2 in vitro cell model. *Toxicology*. 2015;331:47-56.

11. Tiwari A, Bansal V, Chugh A, Mookhtiar K. Statins and myotoxicity: a therapeutic limitation. *Expert Opin Drug Saf*. 2006;5(5):651-666.

12. Schirris TJJ, Renkema GH, Ritschel T, et al. Statin-induced myopathy is associated with mitochondrial complex III inhibition. *Cell Metab*. 2015;22(3):399-407.

13. Deichmann R, Lavie C, Andrews S. Coenzyme q10 and statin-induced mitochondrial dysfunction. *Ochsner J*. 2010;10(1):16-21.

14. Nawarskas J. HMG-CoA reductase inhibitors and coenzyme Q10. *Cardiol Rev*. 2005;13(2):76-79.

15. Fromenty B, Fisch C, Labbe G, et al. Amiodarone inhibits the mitochondrial beta-oxidation of fatty acids and produces microvesicular steatosis of the liver in mice. *J Pharmacol Exp Ther*. 1990;255(3):1371-1376.

16. Kennedy J, Unger S, Horowitz J. Inhibition of carnitine palmitoyltransferase-1 in rat heart and liver by perhexiline and amiodarone. *Biochem Pharmacol*. 1996;52(2):273-280.

17. Chatzispyrou I, Held N, Mouchiroud L, Auwerx J, Houtkooper R. Tetracycline antibiotics impair mitochondrial function and its experimental use confounds research. *Cancer Res*. 2015;75(21):4446-4449.

18. Fromenty B, Pessayre D. Inhibition of mitochondrial beta-oxidation as a mechanism of hepatotoxicity. *Pharmacol Ther*. 1995;67(1):101-154.

19. Li C, Cheng Y, Liao P, Yang Y, Kang J. Chloramphenicol causes mitochondrial stress, decreases

ATP biosynthesis, induces matrix metalloproteinase-13 expression, and solid-tumor cell invasion. *Toxicol Sci*. 2010;116(1):140-150.

20. Glasgow JFT, Y BM, Moore R, Gray A, Hill J. The mechanism of inhibition of L -oxidation by aspirin metabolites in skin broblasts from Reye's syndrome patients and controls. *Biochim Biophys Acta*. 1999;1454:115-125.

21. Owen MR, Doran E, Halestrap AP. Evidence that metformin exerts its anti-diabetic effects through inhibition of complex 1 of the mitochondrial respiratory chain. *Biochem J*. 2000;614:607-614.

22. Fong JJ, Sylvia L, Ruthazer R, Schumaker G, Kcomt M, Devlin JW. Predictors of mortality in patients with suspected propofol infusion syndrome. *Crit Care Med*. 2008;36(8):2281-2287.

23. Rogers KM, Dewar KM, McCubbin TD, Spence a a. Preliminary experience with ICI 35 868 as an i.v. induction agent: comparison with althesin. *Br J Anaesth*. 1980;52(8):807-810.

24. Rutter D V, Morgan M, Lumley J, Owen R. ICI 35 868 (Diprivan): A new intravenous induction agent—A comparison with methohexitone. *Anaesthesia*. 1980;35:1188-1192.

25. Yip GMS, Chen Z-W, Edge CJ, et al. A propofol binding site on mammalian GABAA receptors identified by photolabeling. *Nat Chem Biol*. 2013;9(11):715-720.

26. Lalwani K, Michel M. Pediatric sedation in North American children's hospitals: A survey of anesthesia providers. *Paediatr Anaesth*. 2005;15(3):209-213.

27. Edelist G. A comparison of propofol and thiopentone as induction agents in outpatient surgery. *Can J Anaesth*. 1987;34(2):110-116.

28. Bahar M, Dundee JW, O'Neill MP, Briggs LP, Moore J, Merrett JD. Recovery from intravenous anaesthesia. Comparison of disoprofol with thiopentone and methohexitone. *Anaesthesia*. 1982;37(12):1171-1175.

29. Grounds RM, Lalor JM, Lumley J, Royston D, Morgan M. Propofol infusion for sedation in the intensive care unit: preliminary report. *Br Med J (Clin Res Ed)*. 1987;294(6569):397-400.

30. Kelly D, Goodale D, Williams J, et al. Propofol in the treatment of moderate and severe head injury: a randomized, prospective double-blinded pilot trial. *J Neurosurg*. 1999;90(6):1042-1052.

31. Ronan KP, Gallagher TJ, George B, Hamby B. Comparison of propofol and midazolam for sedation in intensive care unit patients. *Crit Care Med*. 1995;23(2):286-293.

32. Notis fra Bivirkningsnaenet. Propofol (Diprivan) bivirkninger. *Ugeskr Laeger*. 152:1176.

33. Parke TJ, Stevens JE, Rice a S, et al. Metabolic acidosis and fatal myocardial failure after propofol infusion in children: five case reports. *BMJ*. 1992;305(6854):613-616.

34. Chidambaran V, Costandi A, D'Mello A. Propofol: a review of its role in pediatric anesthesia and sedation. *CNS Drugs*. 2016;29(7):543-563.

35. Baker MT, Naguib M. Propofol: the challenges of formulation. *Anesthesiology*. 2005;103(4):860-876.

36. Briggs LP, Clarke RSJ, Watkins J. An adverse reaction to the administration of disoprofol (Diprivan). *Anaesthesia*. 1982;37:1099-1101.

37. http://www.medsafe.govt.nz/profs/Datasheet/d/Diprivaninj.pdf.

38. Langevin PB, Gravenstein N, Doyle TJ, et al. Growth of Staphylococcus aureus in Diprivan and Intralipid. *Anesthesiology*. 1999;(5):1394-1400.

39. Fukada T, Ozaki M. Microbial growth in propofol formulations with disodium edetate and the influence of venous access system dead space. *Anaesthesia*. 2007;62(6):575-580.

40. Kanto J, Gepts E. Pharmacokinetic Implications for the Clinical Use of Propofol. *Clin Pharmacokinet*. 1989;17(5):308-326.

41. Thompson KA, Goodale DB. The recent development of propofol (DIPRIVAN). *Intensive Care Med*. 2000;26(Suppl 4):S400-4.

42. James R, Glen J. Synthesis, biological evaluation, and preliminary structure-activity considerations of a series of alkylphenols as intravenous anesthetic agents. *J Med Chem*. 1980;23(12):1350-1357.

43. Kay B, Rolly G. Dosage of ici 35 868. *Br J Anaesth*. 1981;53(2):192-193.

44. Schnider T, Minto C, Shafer S, et al. The influence of age on propofol pharmacodynamics. *Anesthesiology*. 1999;90(6):1502-1516.

45. Khan KS, Hayes I, Buggy DJ. Pharmacology of anaesthetic agents I: intravenous anaesthetic agents. *Anaesthesia, Crit Care Pain*. 2014;14(3):100-105.

46. Duke T. A new intravenous anesthetic agent: Propofol. *Can Vet J*. 1995;36(3):181-183.

47. Glen JB. Animal Studies of the Anaesthetic Activity of Diprivan (Ici 35, 868). *Vet Anaesth Analg*. 1978;8(1):138-140.

48. Smith S, Scarth E, Sasada M. *Drug in Anaesthesia and Intensive Care*.; 2011.

49. Hardman JG, Hopkins PM, Struys MMR. *Oxford Textbook of Anaesthesia*.; 2017.

50. Shaw I, Kumar C, Dodds C. *Oxford Textbook of Anaesthesia for Oral and Maxillofacial Surgery*.; 2010.

51. Shafer SL. Advances in propofol pharmacokinetics and pharmacodynamics. *J Clin Anesth*. 1993;(suppl 1):14S-21S.

52. Sigel E, Steinmann ME. Structure, function, and modulation of GABAA receptors. *J Biol Chem*. 2012;287(48):40224-40231.

53. Ito H, Watanabe Y, Isshiki A, Uchino H. Suppression of parasympathetic reflex vasodilatation in the lower lip of the cat by isoflurane, propofol, ketamine and pentobarbital: implications for mechanisms underlying the production of anaesthesia. *Br J Anaesth*. 1998;81:563–568.

54. Zhan R, Qi S, Wu C, Fujihara H, Taga K, Shimoji K. Intravenous anesthetics differentially reduce neurotransmission damage caused by oxygen-glucose deprivation in rat hippocampal slices in correlation with N-methyl-D-aspartate receptor inhibition. *Crit Care Med*. 2001;29:808–813.

55. Sitar S, Hanifi-Moghaddam P, Gelb A, Cechetto D, Siushansian R, Wilson J. Propofol prevents peroxide-induced inhibition of glutamate transport in cultured astrocytes. *Anesthesiology*. 1999;90:1446-1453.

56. MCA/CSM. Serious adverse effects and fatalities in children associated with the use of propofol (Diprivan) for sedation. *Curr Probl Pharmacovilance*. 34:4.

57. Rosen DJ, Nicoara A, Koshy N, Wedderburn R V. Too much of a good thing? Tracing the history of the propofol infusion syndrome. *J Trauma*. 2007;63(2):443-447.

58. Ahlen K, Buckley CJ, Goodale DB, Pulsford AH. The "propofol infusion syndrome": The facts, their interpretation and implications for patient care. *Eur J Anaesthesiol*. 2006;23(12):990-998.

59. US Food and Drug Administration, Center for Drug Evaluation and Research (Anesthetic and Life Support Committee). ICI's Diprivan® (propofol) anesthetic has no link to pediatric deaths in ICUs. FDC Reports 1992, Sep 7;54: *FDC Reports*. 1992;Sep 7;(54:):14.

60. Barclay K, Williams AJ, Major E. Propofol infusion in children. *BMJ*. 1992;305(6859):953-954.

61. Bodd E, Endresen L. Use of propofol for children. *Tidsskr Nor Laegeforen*. 1992;112:1636–7.

62. Kirkpatrick M, Cole G. Propofol infusion in children. *BMJ*. 1992;305(6863):1223.

63. Martin PH, Murthy B V, Petros a J. Metabolic, biochemical and haemodynamic effects of infusion of propofol for long-term sedation of children undergoing intensive care. *Br J Anaesth*. 1997;79(3):276-279.

64. Bray RJ. Fatal Myocardial Failure Associated With a Propofol Infusion in a Child. *Anaesthesia*. 1995;50(1):94.

65. Bray RJ. Propofol infusion syndrome in children. *Paediatr Anaesth*. 1998;8(6):491-499.

66. Hanna JP, Ramundo ML. Rhabdomyolysis and hypoxia associated with prolonged propofol infusion in children. *Neurology*. 1998;50(1):301-303.

67. Mehta N, DeMunter C, Habibi P, Nadel S, Britto J. Short-term propofol infusions in children. *Lancet*. 1999;354(9181):866-867.

68. Wolf A, Weir P, Segar P, Stone J. Impaired fatty acid oxidation in propofol infusion syndrome. *Lancet*. 2001;357:606-607.

69. FDA issues warning on propofol (Diprivan). *CMAJ*. 164(11):1608.

70. Kill C, Leonhardt A, Wulf H. Lactic acidosis after short-term infusion of propofol for anaesthesia in a child with osteogenesis imperfecta. *Paediatr Anaesth*. 2003;13(9):823-826.

71. Stelow EB, Johari VP, Smith SA, Crosson JT, Apple FS. Propofol-associated rhabdomyolysis with cardiac involvement in adults: Chemical and anatomic findings. *Clin Chem*. 2000;46(4):577-581.

72. Cremer OL, Moons KGM, Bouman E a C, Kruijswijk JE, Smet AMG a De, Kalkman CJ. Long-term propofol infusion and cardiac failure in adult head-injured patients. *Lancet*. 2001;357(9250):117-118.

73. Perrier ND, Baerga-Varela Y, Murray MJ. Death related to propofol use in an adult patient. *Crit Care Med*. 2000;28(8):3071-3074.

74. Marinella MA. Lactic acidosis associated with propofol. *Chest*. 1996;109(1):292.

75. Kang TM. Propofol infusion syndrome in critically ill patients. *Ann Pharmacother*. 2002;36(9):1453-1456.

76. Jacobi J, Fraser GL, Coursin DB, et al. Analgesics in the Critically Ill Adult. *Crit Care Med*. 2002;30(1):119-141.

77. U.S. Food and Drug Administration. MedWatch. Detailed view: safety labeling changes approved by FDA Center for Drug Evaluation and Research (CDER)—February 2007. Diprivan (propofol) injectable emulsion for IV administration. 2007.

78. Summary of Product Characteristics: PROPOFOL. https://www.medicines.org.uk/emc/medicine/2275#UNDESIRABLE_EFFECTS.

79. Vasile B, Rasulo F, Candiani A, Latronico N. The pathophysiology of propofol infusion syndrome: A simple name for a complex syndrome. *Intensive Care Med*. 2003;29(9):1417-1425.

80. Kam PCA, Cardone D. Propofol infusion syndrome. *Anaesthesia*. 2007;62(7):690-701.

81. Krajčová A, Waldauf P, Anděl M, Duška F. Propofol infusion syndrome: a structured review of experimental studies and 153 published case reports. *Crit Care*. 2015;19(1):398.

82. Chukwuemeka A, Ko R, Ralph-Edwards A. Short-term low-dose propofol anaesthesia associated with severe metabolic acidosis. *Anaesth Intensive Care*. 2006;34(5):651-655.

83. Roberts RJ, Barletta JF, Fong JJ, et al. Incidence of propofol-related infusion syndrome in critically ill adults: a prospective, multicenter study. *Crit Care*. 2009;13(5):R169.

84. Richter S, Brugada P. Propofol-induced coved-type electrocardiogram during catheter ablation of paroxysmal atrial fibrillation: A case of Brugada syndrome? *Herzschrittmachertherapie und Elektrophysiologie*. 2012;23(1):56-58.

85. Schroeppel TJ, Fabian TC, Clement LP, et al. Propofol infusion syndrome: A lethal condition in critically injured patients eliminated by a simple screening protocol. *Injury*. 2014;45(1):245-249.

86. Linko R, Laukkanen A, Koljonen V, Rapola J, Varpula T. Severe Heart Failure and Rhabdomyolysis Associated With Propofol Infusion in a Burn Patient. *J Burn Care Res*. 2014;35(5):E364-E367.

87. Cravens GT, Packer DL, Johnson ME. Incidence of propofol infusion syndrome during noninvasive radiofrequency ablation for atrial flutter or fibrillation. *Anesthesiology*. 2007;106(6):1134-1138.

88. Smith H, Sinson G, Varelas P. Vasopressors and propofol infusion syndrome in severe head trauma. *Neurocrit Care*. 2009;10(2):166-172.

89. Iyer VN, Hoel R, Rabinstein A a. Propofol infusion syndrome in patients with refractory status epilepticus: an 11-year clinical experience. *Crit Care Med*. 2009;37(12):3024-3030.

90. Plotz FB, Waalkens HJ, Verkade HJ, Strengers JL, Knoester H MJ. Fatal side-effects of continuous propofol infusion in children may be related to malignant hyperthermia. *Anaesth Intensive Care*. 1996;24(6):724.

91. Vernooy K, Delhaas T, Cremer OL, et al. Electrocardiographic changes predicting sudden death in propofol-related infusion syndrome. *Hear Rhythm*. 2006;3(2):131-137.

92. Weiner JB, Haddad E V., Raj SR. Recovery following propofol-associated brugada electrocardiogram. *PACE - Pacing Clin Electrophysiol*. 2010;33(4):1-7.

93. Robinson JDC, Melman Y, Walsh EP. Cardiac conduction disturbances and ventricular tachycardia after prolonged propofol infusion in an infant. *PACE - Pacing Clin Electrophysiol*. 2008;31(8):1070-1073.

94. Koch M, De Backer D, Vincent JL. Lactic acidosis: An early marker of propofol infusion syndrome? *Intensive Care Med*. 2004;30(3):522.

95. Holzki J, Aring C, Gillor A. Death after re-exposure to propofol in a 3-year-old child: A case report. *Paediatr Anaesth*. 2004;14(3):265-270.

96. Burow BK, Johnson ME, Packer DL. Metabolic acidosis associated with propofol in the absence of other causative factors. *Anesthesiology*. 2004;101(1):239-241.

97. Romero P C, Morales R M, Donaire R L, et al. Acidosis láctica severa asociada a infusión de propofol. Caso clínico. *Rev Med Chil*. 2008;136(1):88-92.

98. Laquay N, Prieur S, Greff B, Meyer P, Orliaguet G. Le syndrome de perfusion du propofol. *Ann Fr Anesth Reanim*. 2010;29(5):377-386.

99. Mali AR, Patil VP, Pramesh CS, Mistry RC. Hyperkalemia during surgery: Is it an early warning of propofol infusion syndrome? *J Anesth*. 2009;23(3):421-423.

100. Aloizos S, Gourgiotis S, Oikonomou K, Stakia P. Acute renal failure and rhabdomyolysis in a patient with infectious mononucleosis: a case report. *Cases J*. 2008;1(1):222.

101. Fudickar A, Tonner PH, Mihaljovic Z, et al. Suggested beginning of propofol infusion syndrome in an adult patient without lactacidosis: a case report. *Eur J Anaesthesiol*. 2008;25(9):777-778.

102. Vokes DE, Linskey ME AW. Propofol lipemia mimicking chyle leak during neck dissection. *Head Neck*. 2006;28(12):1147-9.

103. Otterspoor LC, Kalkman CJ, Cremer OL. Update on the propofol infusion syndrome in ICU management of patients with head injury. *Curr Opin Anaesthesiol*. 2008;21(5):544-551.

104. Gottschling S, Meyer S, Krenn T, Kleinschmidt S, Reinhard H, Graf N SG. Effects of short-term propofol administration on pancreatic enzymes and triglyceride levels in children. *Anaesthesia*. 2005;60(7):660-3.

105. Cray S. Fat metabolism during propofol infusion. *Br J Anaesth*. 1999;82(3):473.

106. Orsini J, Nadkarni A, Chen J, Cohen N. Propofol infusion syndrome: Case report and literature review. *Am J Heal Pharm*. 2009;66(10):908-915.

107. Cray SH, Robinson BH CP. Lactic acidemia and bradyarrhythmia in a child sedated with propofol. *Crit Care Med*. 1998;26:2087–2092.

108. Sammartino M, Garra R, Sbaraglia F, Papacci P. Propofol overdose in a preterm baby: May propofol infusion syndrome arise in two hours? *Paediatr Anaesth*. 2010;20(10):973-974.

109. Sabsovich BI, Rehman Z, Yunen J, Coritsidis G, Surgical F. Propofol Infusion Syndrome: a Case of Incresing Morbidity With Traumatic Brain Injury. *Am J Crit care*. 2007;16(1):82-85.

110. Guitton C, Gabillet L, Latour P, et al. Propofol infusion syndrome during refractory status epilepticus in a young adult: Successful ECMO resuscitation. *Neurocrit Care*. 2011;15(1):139-145.

111. Fodale V, Monaca E La. Propofol infusion syndrome: an overview of a perplexing disease. Fodale V, La Monaca E. *Drug Saf.* 2008; 31(4):293-303.

112. Zarovnaya EL, Jobst BC, Harris BT. Propofol-associated fatal myocardial failure and rhabdomyolysis in an adult with status epilepticus. *Epilepsia*. 2007;48(5):1002-1006.

113. Jorens PG, Van den Eynden GG. Propofol Infusion Syndrome With Arrhythmia, Myocardial Fat Accumulation and Cardiac Failure. *Am J Cardiol*. 2009;104(8):1160-1162.

114. Shimony A, Almog Y, Zahger D. Propofol infusion syndrome: A rare cause of multi-organ failure in a man with complicated myocardial infarction. *Isr Med Assoc J*. 2008;10(4):316-317.

115. Ernest D, French C. Propofol infusion syndrome--report of an adult fatality. *Anaesth Intensive Care*. 2003;31(3):316-319.

116. Withington DE, Decell MK, Al Ayed T. A case of propofol toxicity: Further evidence for a causal mechanism. *Paediatr Anaesth*. 2004;14(6):505-508.

117. Casserly B, O'Mahony E, Timm EG, Haqqie S, Eisele G, Urizar R. Propofol infusion syndrome: an

unusual cause of renal failure. *Am J Kidney Dis*. 2004;44(6):e98-e101.

118. Liolios A, Guérit JM, Scholtes JL, Raftopoulos C, Hantson P. Propofol infusion syndrome associated with short-term large-dose infusion during surgical anesthesia in an adult. *Anesth Analg*. 2005;100(6):1804-1806.

119. Corbett SM, Moore J, Rebuck J a, Rogers FB, Greene CM. Survival of propofol infusion syndrome in a head-injured patient. *Crit Care Med*. 2006;34(9):2479-2483.

120. Karakitsos D, Poularas J, Kalogeromitros A, Karabinis A. The propofol infusion syndrome treated with haemofiltration. Is there a time for genetic screening? *Acta Anaesthesiol Scand*. 2007;51(5):644-645.

121. Pisapia JM, Wendell LC, Kumar MA, Zager EL, Levine JM. Lactate-to-pyruvate ratio as a marker of propofol infusion syndrome after subarachnoid hemorrhage. *Neurocrit Care*. 2011;15(1):134-138.

122. Poretti A, Bosemani T, Huisman TAGM. Neuroimaging findings in pediatric propofol infusion syndrome. *Pediatr Neurol*. 2014;50(4):431-432.

123. Imam TH. Propofol-related infusion syndrome: role of propofol in medical complications of sedated critical care patients. *Perm J*. 2013;17(2):85-87.

124. Menon DK, Matta BF, Gupta AK SA. Propofol use in head-injury patients. *Lancet*. 2001;357(9269):1708-9;

125. Machata a M, Gonano C, B??rsan T, Zimpfer M, Spiss CK. Rare but Dangerous Adverse Effects of Propofol and Thiopental in Intensive Care. *J Trauma Inj Infect Crit Care*. 2005;58(3):643-645.

126. Barbara DW WFJ. Propofol induction resulting in green urine discoloration. *Anesthesiology*. 2012. 116(4):924. 116AD;(4):924.

127. Da-Silva SS, Wong R, Coquillon P, Gavrilita C, Asuncion A. Partial-exchange blood transfusion: an effective method for preventing mortality in a child with propofol infusion syndrome. *Pediatrics*. 2010;125(6):e1493-e1499.

128. Branca D, Roberti MS, Lorenzin P, Vincenti E SG. Influence of the anesthetic 2,6-diisopropylphenol on the oxidative phosphorylation of isolated rat liver mitochondria. *Biochem Pharmacol*. 1991;42(1):87-90.

129. Branca D, Vincenti E SG. Influence of the anesthetic 2,6-diisopropylphenol (propofol) on isolated rat heart mitochondria. *Comp Biochem Physiol C Pharmacol Toxicol Endocrinol*. 1995;110(1):41-5.

130. Rigoulet M, Devin A, Avéret N, Vandais B, Guérin B. Mechanisms of inhibition and uncoupling of respiration in isolated rat liver mitochondria by the general anesthetic 2,6-diisopropylphenol. *Eur J Biochem*. 1996;241(1):280-285.

131. Schenkman KA, Yan S. Propofol impairment of mitochondrial respiration in isolated perfused guinea pig hearts determined by reflectance spectroscopy. *Crit Care Med*. 200;28(1):172-7.

132. Branca D, Roberti MS, Vincenti E SG. Uncoupling effect of the general anesthetic 2,6-diisopropylphenol in isolated rat liver mitochondria. *Arch Biochem Biophys*. 1991;290(2):517-21.

133. Vanlander AV, Okun JG, de Jaeger A, Smet J, De Latter E, De Paepe B, Dacremont G, Wuyts B, Vanheel B, De Paepe P, Jorens PG, Van Regenmortel N VCR. Possible pathogenic mechanism of propofol infusion syndrome involves coenzyme q. *Anesthesiol.* 2015;122(2)343-52.

134. Wolf AR, Potter F. Propofol infusion in children: When does an anesthetic tool become an intensive care liability? *Paediatr Anaesth*. 2004;14(6):435-438.

135. Rinaldo P, Cowan TM MD. Acylcarnitine profile analysis. *Genet Med*. 2008;(10(2):):151-6.

136. Tong XX, Kang Y, Liu FZ, Zhang WS LJ. [Effect of prolonged infusion of propofol on the liver mitochondria respiratory function in rabbits]. *Sichuan Da Xue Xue Bao Yi Xue Ban*. 2010;41(6):1021-3.

137. Jiang W, Yang ZB, Zhou QH, Huan X, Wang L. Lipid metabolism disturbances and AMPK activation in prolonged propofol-sedated rabbits under mechanical ventilation. *Acta Pharmacol Sin*. 2012;33(1):27-33.

138. Baumeister F, Oberhoffer R, Liebhaber G, et al. Fatal propofol infusion syndrome in association with ketogenic diet. *Neuropediatrics*. 2004;(35(4):):250-2.

139. Herregods L, Rolly G, Versichelen L, Rosseel MT. Propofol combined with nitrous oxide-oxygen for induction and maintenance of anaesthesia. *Anaesthesia*. 1987;42(4):360-365.

140. Casati A, Fanelli G, Casaletti E, Colnaghi E, Cedrati V, Torri G. Clinical assessment of target-controlled infusion of propofol during monitored anesthesia care. *Can J Anaesth*. 1999;46(3):235-239.

141. Gong Y, Li E, Xu G, et al. Investigation of propofol concentrations in human breath by solid-phase microextraction gas chromatography-mass spectrometry. *J Int Med Res*. 2009;37(5):1465-1471.

142. Kumar M, Urrutia V, Thomas C, Abou-Khaled K, Schwartzman R. The syndrome of irreversible acidosis after prolonged propofol infusion. *Neurocrit Care*. 2005;3(3):257-259.

143. Merz TM, Regli B, Rothen HU FP. Propofol infusion syndrome--a fatal case at a low infusion rate. *Anesth Analg*. 2006;103(4):1050.

144. Culp KE, Augoustides JG, Ochroch AE, Milas BL. Clinical Management of Cardiogenic Shock Associated with Prolonged Propofol Infusion. *Anesth Analg*. 2004;99(1):221-226.

145. Bergstrom J. Percutaneous needle biopsy of skeletal muscle in physiological and clinical research. *Scand J Clin Lab Invest*. 1975;35(7):609-616.

146. Ziak J, Krajcova A, Jiroutkova K, Nemcova V, Dzupa V, Duska F. Assessing the function of mitochondria in cytosolic context in human skeletal muscle: Adopting high-resolution respirometry to homogenate of needle biopsy tissue samples. *Mitochondrion*. 2015;21:106-112.

147. Krajčová A, Løvsletten NG, Waldauf P, et al. Effects of Propofol on Cellular Bioenergetics in Human Skeletal Muscle Cells. *Crit Care Med*. 2018;46(3):e206-e212.

148. Thompson D, Pratley R, Ossowski V. Human primary myoblast cell cultures from non-diabetic insulin resistant subjects retain defects in insulin action. *J Clin Invest*. 1996;98(10):2346-2350.

149. Krajcova A, Ziak J, Jiroutkova K, et al. Normalizing glutamine concentration causes mitochondrial uncoupling in an in vitro model of human skeletal muscle. *JPEN J Parenter Enteral Nutr*. 2015;39(2):180-189.

150. http://www.zen-bio.com/pdf/ZBM0044.pdf.

151. Reitzer L, Wice B, Kennell D. Evidence that glutamine, not sugar, is the major energy source for cultured HeLa cells. *J Biol Chem*. 1979;254:2669-2676.

152. Hou Y, Chiu W, Yeh C, Yeh S. Glutamine modulates lipopolysaccharide-induced activation of NF-κB via the Akt/mTOR pathway in lung epithelial cells. *Am J Physiol Lung Cell Mol Physiol*. 2012;302(1):L174-L183.

153. Yuneva M, Zamboni N, Oefner P, Sachidanandam, R Lazebnik Y. Deficiency in glutamine but not glucose induces MYC-dependent apoptosis in human cells. *J Cell Biol*. 2007;178:93-105.

154. Labitzke R, Friedl P. A serum-free medium formulation supporting growth of human umbilical cord vein endothelial cells in long-term cultivation. *Cytotechnology*. 2001;35:87-92.

155. Aguer C, Foretz M, Lantier L, et al. Increased FAT/CD36 cycling and lipid accumulation in myotubes derived from obese type 2 diabetic patients. *PLoS One*. 2011;6(12).

156. Fisher H, Yeh J. Contact inhibition in colony formation. *Science*. 1967;155(3762):581-582.

157. Pappas D. *Practical Cell Analysis*.; 2010.

158. http://catalog.takara-bio.co.jp/PDFFiles/AA-1039-7_0411(inst)_j.pdf.

159. http://www.medsafe.govt.nz/profs/datasheet/i/Intralipidinf.pdf.

160. Warltier DC, Ph D. VI review articles. 2016;(4):860-876.

161. Edwards LM, Lawler NG, Nikolic SB, et al. Metabolomics reveals increased isoleukotoxin diol (12 , 13-DHOME) in human plasma after acute Intralipid infusion. *J Lipid Res.* 2012; 53(9):1979-86

162. Lou P, Lucchinetti E, Zhang L, et al. The Mechanism of Intralipid H -Mediated Cardioprotection Complex IV Inhibition by the Active Metabolite , Palmitoylcarnitine , Generates Reactive Oxygen Species and Activates Reperfusion Injury Salvage Kinases. *PLoS One.* 2014; Jan 30;9(1):e87205.

163. Patková J, Anděl M, Trnka J. Palmitate-induced cell death and mitochondrial respiratory dysfunction in myoblasts are not prevented by mitochondria-targeted antioxidants. *Cell Physiol Biochem*. 2014;33(5):1439-1451.

164. http://www.seahorsebio.com/resources/tech-writing/protocol-bsa-palmitate.pdf.

165. Trounce IA, Kim YL, Jun AS, Wallace DC. Assessment of Mitochondrial Oxidative Phosphorylation in Patient Muscle Biopsies, Lymphoblasts, and Transmitochondrial Cell Lines. *Methods Enzymol.* 1996;264(1992):484-509.

166. Cory AH, Owen TC, Barltrop JA CJ. Use of an aqueous soluble tetrazolium/formazan assay for cell growth assays in culture. *Cancer Commun*. 1991;3(7):207-212.

167. Brand MD, Nicholls DG. Assessing mitochondrial dysfunction in cells. *Biochem J*. 2011;435(2):297-312.

168. Wu M, Neilson A, Swift A, et al. Multiparameter metabolic analysis reveals a close link between attenuated mitochondrial bioenergetic function and enhanced glycolysis dependency in human tumor cells. *Am J Physiol Cell Physiol*. 2007;292(1):125-136.

169. Gerencser AA, Neilson A, Choi SW, et al. Quantitative microplate-based respirometry with correction for oxygen diffusion. *Anal Chem*. 2009;81(16):6868-6878.

170. Choi S, Gerencser A, Nicholls D. Bioenergetic analysis of isolated cerebrocortical nerve terminals on a microgram scale: spare respiratory capacity and stochastic mitochondrial failure. *J Neurochem*. 2009;109(4):1179-1191.

171. Wikstrom JD, Sereda SB, Stiles L, et al. A novel high-throughput assay for islet respiration reveals

uncoupling of rodent and human islets. *PLoS One*. 2012;7(5):1-7.

172. https://www.agilent.com/cs/library/usermanuals/public/Hydrating%20an%20XFp%20Sensor%20Cartridge.pdf.

173. http://www.bioblast.at/index.php/State_1.

174. http://www.bioblast.at/index.php/Residual_oxygen_consumption.

175. http://www.bioblast.at/index.php/Proton_leak.

176. http://www.bioblast.at/index.php/LEAK_respiration.

177. http://www.bioblast.at/index.php/ET-capacity.

178. Overview T. Using PMP to Measure Substrate Specific ETC / OxPhos Activity in Permeabilized Cells. :1-6.

179. Shourie A. *Bioanalytical Techniques*.; 2005.

180. Jamur M, Oliver C. Permeabilization of cell membranes. *Methods Mol Biol*. 2010;588:63-66.

181. McCarthy D, Macey M. *Cytometric Analysis of Cell Phenotype and Function*.; 2001.

182. Salabei JK, Gibb AA, Hill BG. Comprehensive measurement of respiratory activity in permeabilized cells using extracellular flux analysis. *Nat Protoc*. 2014;9:421–438.

183. https://www.agilent.com/cs/library/technicaloverviews/public/5991-7157EN.pdf

184. https://www.agilent.com/cs/library/usermanuals/public/insert-xf-pmp-reagent-web.pdf.

185. Mookerjee SA, Divakaruni AS, Jastroch M, Brand MD. Mitochondrial uncoupling and lifespan. *Mech Ageing Dev*. 2010;131(7-8):463-472.

186. http://www.bioblast.at/index.php/Oxidative_phosphorylation.

187. Terada H. Uncouplers of Oxidative Phosphorylation. *Environ Health Perspect*. 1990;87:213-218.

188. Chance B, Williams G. A simple and rapid assay of oxidative phosphorylation. *Nature*. 1955;25(175(4469)):1120-1121.

189. http://www.bioblast.at/index.php/State_3u.

190. Hajri T, Abumrad NA. Fatty Acid Transport Across Membranes: Relevance to Nutrition and Metabolic Pathology. *Annu Rev Nutr*. 2002;22:383-415.

191. https://www.agilent.com/cs/library/usermanuals/Public/XF_Palmitate_BSA_Substrate_Quick start_Guide.pdf.

192. Zhang J, Nuebel E, Wisidagama DRR, et al. Measuring energy metabolism in cultured cells, including human pluripotent stem cells and differentiated cells. *Nat Protoc*. 2012;7(6).

193. Srere PA. Citrate Synthase. *Methods Enzym*. 1969;13:3-11.

194. http://www.sigmaaldrich.com/content/dam/sigma-aldrich/docs/Sigma/Bulletin/cs0720bul.pdf.

195. Bradford MM. A rapid and sensitive method for the quantitation of microgram quantities of protein utilizing the principle of protein-dye binding. *Anal Biochem*. 1976;72(1-2):248-254.

196. Trnka J, Elkalaf M, Andel M. Lipophilic Triphenylphosphonium Cations Inhibit Mitochondrial Electron Transport Chain and Induce Mitochondrial Proton Leak. *PLoS One*. 2015;10:e0121837-14.

197. Ijlst L. A simple spectrophotometric assay for long-chain acyl-CoA dehydrogenase activity measurements in human skin fibroblasts. *Ann Clin Biochem.* 1993;30:293-297.

198. Neubauer S. The failing heart--an engine out of fuel. *N Engl J Med*. 2007;356(11):1140-1151.

199. Jouven X, Charles M, Desnos M, Ducimetière P. Circulating nonesterified fatty acid level as a predictive risk factor for sudden death in the population. *Circulation*. 2001;104(7):756–61.

200. Stanley C, Bennett M, Mayatepek E. *Inborn Metabolic Diseases. Berlin: Springer Berlin Heidelberg; Disorders of Mitochondrial Fatty Acid Oxidation and Related Metabolic Pathways*.; 2006.

201. Terrone G, Ruoppolo M, Brunetti-Pierri, N Cozzolino C, et al. Child neurology: recurrent rhabdomyolysis due to a fatty acid oxidation disorder. *Neurology*. 2014;82(1):1-4.

202. Heyman M, Storch S, Ament M. The fat overload syndrome. Report of a case and literature review. *Am J Dis Child*. 1981;135(7):628–30.

203. Adolph M, Heller A, Koch T, et al. Lipid emulsions—Guidelines on Parenteral Nutrition, Chapter 6. *Ger Med Sci*. 2009;7.

204. Gura K, Puder M. Rapid infusion of fish oil-based emulsion in infants does not appear to be associated with fat overload syndrome. *Nutr Clin Pr*. 2010;25(4):399–402.

205. Ypsilantis P, Politou M, Mikroulis D, et al. Attenuation of propofol tolerance conferred by remifentanil co-administration does not reduce propofol toxicity in rabbits under prolonged mechanical ventilation. *J Surg Res*. 2011;168(2):253-261.

206. Quinzii C, Hirano M. Coenzyme Q and Mitochondrial Disease. *Dev Disabil Res*. 2010;16(2):183-188.

207. López-Martín JM, Salviati L, Trevisson E, et al. Missense mutation of the COQ2 gene causes defects of bioenergetics and de novo pyrimidine synthesis. *Hum Mol Genet.* 2007;16(9):1091-7

208. Turunen M, Olsson J, Dallner G. Metabolism and function of coenzyme Q. *Biochim Biophys Acta - Biomembr*. 2004;1660(1-2):171-199.

209. Darras BT, Friedman NR. Metabolic Myopathies : A Clinical Approach ; Part I. 2000;22(2):87-97.

210. Lee S, Lee J, Kim J, et al. Coenzyme Q10 increases the fatty acid oxidation through AMPK-mediated PPARα induction in 3 T3-L1 preadipocytes. *Cell Signal*. 2012;24(12):2329–36.

211. Jiang W1, Yang ZB, Zhou QH, Huan X WL. Lipid metabolism disturbances and AMPK activation in prolonged propofol-sedated rabbits under mechanical ventilation. *Acta Pharmacol Sin*. 2012;33(1):27-33.

212. Dawidowicz A, Kalitynski R, Kobielski M, Pieniadz J. Influence of propofol concentration in human plasma on free fraction of the drug. *Chem Biol Interact*. 2006;159(2):149-155.

213. https://www.caymanchem.com/pdfs/11506.pdf.

214. Geromel V, Darin N, Chrétien D, et al. Coenzyme Q10 and idebenone in the therapy of respiratory chain diseases: Rationale and comparative benefits. *Mol Genet Metab*. 2002;77(1-2):21-30.

215. Cochemé HM, Kelso GF, James AM, et al. Mitochondrial targeting of quinones: Therapeutic implications. *Mitochondrion*. 2007;7:94-102.

216. Murphy M, Smith R. Drug delivery to mitochondria: the key to mitochondrial medicine. *Adv Drug Deliv Rev*. 2000;41(2):235-250.

217. Smith R, Porteous C, Gane A, Murphy M. Delivery of bioactive molecules to mitochondria in vivo. *Proc Natl Acad Sci USA*. 2003;100(9):5407-5412.

218. James AM, Cochemé HM, Smith RAJ, Murphy MP. Interactions of mitochondria-targeted and untargeted ubiquinones with the mitochondrial respiratory chain and reactive oxygen species: Implications for the use of exogenous ubiquinones as therapies and experimental tools. *J Biol Chem*. 2005;280(22):21295-21312.

20 Annexes

20.1 List of publications

20.1.1 Publications with IF related to the thesis

Krajčová A, Waldauf P, Anděl M, Duška F. Propofol infusion syndrome: a structured review of experimental studies and 153 published case reports. *Crit Care.* 2015 Nov 12;19:398. *(IF = 4.476)*

Krajčová A, Løvsletten NG, Waldauf P, Frič V, Elkalaf M, Urban T, Anděl M, Trnka J, Thoresen GH, Duška F. Effects of Propofol on Cellular Bioenergetics in Human Skeletal Muscle Cells. *Crit Care Med.* 2018 Mar;46(3):e206-e212 *(IF = 7.05)*

20.1.2 Abstracts related to the thesis

Krajcova A, Waldauf P, Andel M, Duska F. Mitochondrial pathogenesis of propofol infusion syndrome in an *in vitro* model of human skeletal muscle. MitoFit Science Camp, Kuehtai, Austria, 2016 Jul 07-13.

Krajčová A, Waldauf P, Duška F. Mitochondrial pathogenesis of propofol infusion syndrome in an *in vitro* model of human skeletal muscle. 29th Annual Congress of the European Society of Intensive Care Medicine, Milan, Italy, 1 - 5 October 2016.

Krajčová A, Løvsletten NG, Waldauf P, Frič V, Elkalaf M, Urban T, Anděl M, Trnka J, Thoresen GH, Duška F. Mitochondrial pathogenesis of propofol infusion syndrome in an *in vitro* model of human skeletal muscle. Emerging Concepts in Mitochondrial Biology, Weizmann Institute of Science, Rehovot, Israel, February 4-8, 2018.

Krajčová A, Waldauf P, Urban U, Džupa V, Duška F. Mitochondriální patogeneze *syndromu propofolové infuze* v *in vitro* modelu lidského kosterního svalu. XXIV. Kongres České společnosti anesteziologie, resuscitace a intenzivní medicíny, Brno, *7. - 9. září, 2017.*

20.1.3 Publications with IF non-related to the thesis

Krajčová A, Megvinet D, Urban T, Waldauf P, Hlavička J, Budera P, Janoušek L, Pokorná E, Duška F. High resolution respirometry to assess function of mitochondria in native homogenates of human heart muscle. *Circ Res (under review)*

Jiroutková K, Krajčová A, Žiak J, Fric M, Gojda J, Džupa V, Kalous M, Tůmová J, Trnka J, Duška F. Mitochondrial Function in an In Vitro Model of Skeletal Muscle of Patients With Protracted Critical Illness and Intensive Care Unit-Acquired Weakness. *J Parenter Enteral Nutr.* 2016 Jun 29.

Jiroutková K, Krajčová A, Ziak J, Fric M, Waldauf P, Džupa V, Gojda J, Němcova-Fürstová V, Kovář J, Elkalaf M, Trnka J, Duška F. Mitochondrial function in skeletal muscle of patients with protracted critical illness and ICU-acquired weakness. *Crit Care.* 24;19(1):*448. (IF = 4.476)*

Ziak J, Krajcova A, Jiroutkova K, Nemcova V, Dzupa V, Duska F. Assessing the function of mitochondria in cytosolic context in human skeletal muscle: adopting high-resolution respirometry to homogenate of needle biopsy tissue samples. *Mitochondrion.* 2015 Mar;21:106-12. *(IF = 3.52)*

Krajcova A, Ziak J, Jiroutkova K, Patkova J, Elkalaf M, Dzupa V, Trnka J, Duska F. Normalizing glutamine concentration causes mitochondrial uncoupling in an in vitro model of human skeletal muscle. *J Parenter Enteral Nutr.* 2015 Feb;39(2):180-9. *(IF = 3.14)*

Krajčová A, Matoušek V, Duška F. Mechanism of paracetamol-induced hypotension in critically ill patients: a prospective observational cross-over study. *Aust Crit Care.* 2013 Aug;26(3):136-41. *(IF = 1.2)*

20.1.4 Publications without IF non-related to the thesis

Gojda, Jan; Rossmeislová, Lenka; Tůmová, Jana; Krajčová, Adéla; Elkalaf, Moustafa; Žiak, Jakub; Jaček, Martin; Balušíková, Kamila; Duška, František; Trnka, Jan; Anděl, Michal. Postavení perkutánní biopsie kosterního svalu v diabetologickém výzkumu. Metodologický přehled. *Diabetologie, metabolismus, endokrinologie, výživa.* 2015, 18(4), 167-176.

Krajčová Adéla, Matoušek Vojtěch, Duška František. Mechanismus vzniku hypotenze po i. v. paracetamolu u kriticky nemocných. *Anesteziologie a intenzivní medicína*, 22, 2011, č. 5, s. 266-271.

20.1.5 Abstracts non-related to the thesis

Krajcova A, Megvinet D, Waldauf P, Urban T, Budera P, Hlavicka J, Duska F, Drahota Z. Developing a method of assessing mitochondrial functions in homogenates of human heart muscle. 10th MitoEAGLE Workshop WG1-4, Obergurgl, Rakousko; 2017, Jul 27-30.

Krajčová A, Žiak J, Jiroutková K, Patková J, Elkalaf M, Džupa V, Trnka J, Duška F. Vliv glutaminu na proliferaci myoblastů a energetický metabolismus v in vitro modelu lidského kosterního svalu. 51. diabetologické dny, Luhačovice, 16. - 18. dubna 2015.

Krajcova A, Ziak J, Jiroutkova K, Patkova J, Elkalaf M, Dzupa V, Trnka J, Duska F. Normalizing glutamine concentration causes mitochondrial uncoupling in an in vitro model of human skeletal muscle. Mitochondrial Disease: Translating biology into new treatments, Hinxton, Velká Británie, 2–4 October 2013.

Krajčová A, Matoušek V, Duška F. Mechanism of paracetamol-induced hypotension in critically ill patients International Student Congress of (bio)Medical Studies in Groningen, Netherlands, Jun 2013.